Molecular mechanisms of ARF regulation in response to DNA damage

A thesis presented for the degree of Doctor of Philosophy

By

Giulia Orlando

Supervisors:
Prof. Grigory Dianov
Dr. Svetlana Khoronenkova

Brasenose College
CRUK/MRC Oxford Institute for Radiation Oncology,
Department of Oncology,
University of Oxford

Trinity Term 2014

Dedication

Ai miei genitori

“Ci sono due cose durature che possiamo sperare di lasciare in eredità ai nostri figli:

le radici e le ali.”

- Hodding Carter -

To my parents

“There are only two lasting bequests we can hope to give our children.

One of these is roots; the other, wings.”

- Hodding Carter -

Acknowledgments

I was coming back from my distress Zumba class tonight, thinking about all the people I met during this incredible time here in Oxford and, since I am about to submit my thesis in a couple of weeks, I felt it had come the time to write the last bit of it. So let's take a big breath, put some music on and let's do it.
First of all I would like to thank the University of Oxford, the Oxford Institute for Radiation Oncology and the funding bodies, MRC and CR-UK, for having given me the financial support to do my DPhil degree here. Also, a thank you for having been awarded the Scatcherd European Scholarship to cover my stipend. A thank you to Brasenose College and to all the staff, for having financially supported me to go to conferences and to my college advisor, Professor Elspeth Garman, for the lovely chats over dinner.
A big big thank you to my Supervisor, Grigory. Thank you Grigory for all the things you taught me, for the advice, for the opportunity to be involved in an interesting and scientifically rewarding project and for the help in advising me in the next step of my career. To Sveta for her help, for the advice, for the chat between experiments in the lab, for the support and for having corrected this thesis. To Jason for his endless patience, for the helpful chat and for his mentoring support. To Irina for having been such a lovely and kind presence in the lab, for having given me a hug every time I needed it and for the philosophical chat about life. To Conny who taught me what it is to be a DPhil, for all the laughs, for the singing over the radio – in particular "Fast car" by Tracy Chapman – between incubation time, for being a friend and for the help during hard times. To the new members of the Dianov's Lab, Enni for her endless and inspiring energy, Arnaud, Mattia and Sally (you will see this ChIP ChOP will work ☺). To Shivons, for being a friend when I need to have a laugh, and for having gone through this thesis to correct my English. Thank you so much, the sofa bed will be there for you.
To the Kilties, my lunch buddies, Alexa, Judith, Helen, Naomi, Eva; to Sarah for all the after lunch walks that kept me sane during the winter, for her support and for the dancing in Maxwell's together with Katalin – let's do it one more time! Thank you to Martin and Blaz, Cip&Ciop, thank you for all the fun, the jokes, the laughs, oh my God, you made me laugh so much. To the people who work in the department, thank you for having made this place so special and so familiar to me. To the Hammonds, Monica, Kasha, Joana, Cindy, to the Oneills, Angelo, Nikola, Garth, Dafni and all the others. To Eric, for the helpful chat about science and for his mentoring support. To the DGS, Niki and Ester, to Sarah Norman and to Larry. Thank you to my examiners Andy Ryan and Keith Caldecott.
To Carly Rae Jepsen and her "Call me Maybe" song which became the soundtrack of my DPhil and the first – and possibly last song – I will ever sing at the Karaoke. To Bon Iver for having been the soundtrack of my thesis's writing. To the Zumba teacher, Rihanna, for her amazing classes.
To my former flatmates, Clare, Olga and Alison for having shared with me one of the most difficult year of my life, for having been my first ever flatmates. To Alison, who has been more than a flatmate, a friend, a good listener, for the energy she gave me when I was low. To my current flatmates, to Aswin for his endless kindness and to Iosifina for the political chat.

To Selva, thank you my friend, for all the lunches in the hospital over the weekend while I was writing my thesis, for his endless support, for his amazing food, in particular the chicken soup that cures every cold. To Sofia, my flatmate, my lab bench buddy and my friend for life; for having listened to my worries, for all the dinners at home, for all the movies, for the unforgettable Oscar night, for having put me together when I am in pieces, for all the hugs and the laughs, thank you. To Serena for the long chat about the future over lunches and Saturdays walks, for the support she is still giving me from Barcelona; to Alessandro for the philosophical conversations and for his amazing advice about life, for being such a wise friend.
To the Portuguese gang, to Bruno for having been a great support, to Carina for her endless patience in trying to teach me some Portuguese (I promise, next year I am going to learn it ☺), to Henrique and Patricia for their amazing cooking skills over numerous dinners and for their support over difficult and stressful times.
To Chiara, for all the help, the support, the patience she had with me while I was low, for having been always present, for having been the elder sister I have never had, for having taught me that family is not only about having biological relationship, but there is also a family that you can choose. You have been my family here and for this I can never thank you enough. To Roberto for his amazing dinners and for having made me feel home every time I would visit.
To my long-term friend Marianna, ten years of friendship have flown. I still remember that day, me and you in my car, talking about the future, where we would be, what we would have done with our life. I am so looking forward to see where the next ten years will take us. Thank you Mari for the support during dark and uncertain times, for having taught me that a friendship does not end because of the distance, but it can instead grow and flourish.
To Daniel, I don't even know where to start to thank you. I wouldn't have made it without you. Writing the thesis in the Radcliffe Camera has been bearable just because of you. When waking up and keep writing was not easy, you were my strength, always ready to give me a warm hug. Thank you for all the love, the support, the kind words, the constant reassuring, the constant presence, for having made me laugh and for having dried my tears over these difficult months. For the patience you had in handling my terrible moods, my stressful days, my insecurity, for completing me and for understanding me as no one else could. You are my home, the safe port where I feel always secure to come back. For all of these, thank you.
Un grazie alla mia professoressa del Liceo di Biologia, Prof. Ponzi, per avermi indirizzato su questo cammino di ricerca. Un grazie alla mia famiglia. Ai miei nonni, purtroppo non piu' qui tra noi, a mio Zio Guido, mia Zia Luisella e mia cugina Monia. A mio fratello, quanto mi manchi, Lori. Grazie per tutti i bei momenti che riusciamo a passare insieme, per le chiacchierate al telefono a parlare di cinema e altro. Mi dispiace di non poter essere piu' presente, ma spero che tu sappia quanto tu sia importante per me. Sono cosi' orgogliosa di te e di come tu stia proseguendo il tuo cammino. Ti voglio un gran bene, Picci – anche se tanto picci non sei piu'. Ai miei genitori, per avermi dato delle solide radici dalle quali partire, per i valori e i principi che mi hanno insegnato, per i sacrifici e gli sforzi che hanno fatto negli anni per permettermi di studiare. Per avermi donato un paio di ali con le quali sono riuscita piano piano a spiccare il volo per inseguire i miei sogni e per costruire il mio percorso. Grazie, non sarei qua se non fosse stato per voi. Non sarei quella che sono oggi senza i vostri preziosi insegnamenti che porto con me ogni giorno dal sorgere del sole fino al suo tramontare. Grazie per il vostro sostegno, per la pazienza, per l' infinita dose di fiducia, per avermi insegnato a credere in me stessa e per avermi consentito di trovare me stessa. Questo dottorato lo dedico a voi, in attesa dell'eventuale Premio Nobel ☺. Grazie, grazie, grazie, grazie.

Declaration

I declare that this thesis is wholly my own work, aside from the comet assay presented in **figure 2.2**, which was performed by Dr. Svetlana Khoronenkova.

Abstract

Giulia Orlando
Doctor of Philosophy
University of Oxford
Brasenose College, Trinity Term 2014

DNA is a highly unstable molecule. Endogenous souces of DNA damage, such as reactive oxygen species (ROS), can cause DNA damage and it has been estimated that 20000 lesions occur in a cell per day. BER is the major pathway for the repair of these lesions and therefore maintains genome stability, thus preventing the development of human diseases such as neurodegenerative diseases and cancer. Therefore, if BER cannot accomplish the repair, accumulation of DNA damage occurs, triggering different cellular responses, such as cell cycle delay and senescence.

The ARF tumour suppressor protein, the gene of which is frequently mutated in many human cancers, plays an important role in the cellular stress response by orchestrating upregulation of p53 protein. Moreover, ARF expression is upregulated in senescent cells, suggesting that ARF induction might be triggerred in response to persistent DNA damage. Although ARF has been reported to be important in the regulation of proteins involved in the DNA damage response, its role is still controversial.

Here, it has been shown that *ARF* gene transcription is induced by DNA strand breaks (SBs) and that ARF protein accumulates in response to persistent DNA damage generated by disabling BER. These data suggest that PARP1-dependent poly(ADP-ribose) synthesis at the sites of SBs initiates DNA damage signal transduction by reducing the cellular concentration of NAD^+, thus inhibiting SIRT1 activity and consequently activating E2F1-dependent *ARF* transcription. These findings suggest a vital role for ARF in DNA damage signalling, and furthermore explain the critical requirement for ARF inactivation in cancer cells, which are frequently deficient in DNA repair and accumulate DNA damage.

Table of contents

List of figures

List of tables

List of abbreviations

3’-OH	3’-hydroxyl
3meA	3-methyladenine
5’-dRP	5'-deoxyribose-phosphate
5’-P	5’-phosphate
7meG	7-methylguanine
8oxoG	8-Oxoguanine
A	Adenine
AIF	Apoptosis inducing factor
AMP	Adenosine monophosphate
AOA	Ataxia-oculomotor apraxia syndrome
AP	apurinic/apyrimidinic
APE1	AP endonuclease 1
APTX	Aprataxin
ARF	Alternative reading frame
ARF/BP1	ARF/binding protein 1
Arg	Arginine
ATCC	American Type Culture Collection
ATM	Ataxia telangiectasia mutated
ATR	Ataxia telangiectasia and Rad3-related
BER	Base excision repair
BRCT	BRCA1 C Terminus
BSA	Bovine serum albumin
C	Cytosine
CDC	Cell division cycle
CDK	Cyclin-dependent kinase
CHIP	Carboxyl terminus of Hsc70 interacting protein
CHK1/2	Checkpoin kinase ½
CHX	Cycloheximide
CK2	Casein kinase
CKI	Cyclin-dependent kinase inhibitor
CMV	Cytomegalovirus
CPD	cyclobutane pyrimidine dimer
CPT	Camptothecin
DBD	DNA binding domain
DDR	DNA damage response
DEPC	Diethylpyrocarbonate
DMEM	Dulbecco's Modified Eagle's medium

DMSO	Dimethyl sulfoxide
DNA	Deoxyribonucleic acid
dNTPs	Deoxynucleotides
ds	Double strand
DSBs	Double strand breaks
DTT	Dithiothreitol
EDTA	Ethylenediaminetetraacetic acid
EGFR	Epidermal growth factor receptor
FACS	Fluorescence-activated cell sorting
FBS	Fetal bovine serum
FEN1	Flap endonuclease 1
FHIT	Fragile histidine triad
FOXO3	Forkhead box O3
G	Guanine
H_2O_2	Hydrogen peroxide
H3	Histone 3
H3AcK9	Histone 3 acetylated lysine 9
H3K9	Histone 3 lysine 9
HIPK2	Homeodomain-interacting protein kinase 2
HIT	histidine triad motif
HR	Homologous recombination
HU	Hydroxyurea
IR	Ionising radiation
JNK	Jun N-terminal kinase
LD	Loading dye
LIGI/III	Ligase I/III
Lys	Lysine
MAPK	Mitogen-activated protein kinase
MBD4	Methyl-binding domain glycosylase 4
MDM2	Mouse double minute 2
MEFs	Mouse embryonic fibroblasts
MLS	Mitochondriallocalisation signal
MMS	Methyl methanesulfonate
MPG	Methyl purine glycosylase
mRNA	Messanger RNA
MYH	MutY homolog DNA glycosylase
NAD^+	Nicotinamide adenine dinucleotide
NAM	Nicotinamide
NAMPT	Nicotinamide phosphoribosyltransferase
NEIL1	Endonuclease VIII-like 1

NEIL2	Endonuclease VIII-like 2
NEIL3	Endonuclease VIII-like 3
NEM	N-Ethylmaleimide
NF-κB	Nuclear factor kappa beta
NHEJ	Non-homologous end joining
NLS	Nuclear localisation signal
NMI	N-myc (and STAT) interactor
NMNAT2	Nicotinamide mononucleotide adenylyltransferase 2
NMR	Nuclear magnetic resonance
nt	Nucleotide
NTHL1	Endonuclease III-like 1
O^6meG	O^6-methylguanine
OGG1	8oxoG DNA glycosylase 1
OH	Hydroxyl radical
PAGE	Polyacrylamide gel electrophoresis
PAR	Poly-(ADP)-ribose
PARP1	Poly-(ADP)-ribose polymerase 1
PBS	Phosphate buffered saline
PCNA	Proliferating cell nuclear antigen
PCVs	Packed cell volumes
PI	Propidium iodide
PI3K	Phosphatidylinositol 3-kinase
PMSF	Phenylmethanesulfonylfluoride
PNPK	Polynucleotide kinase phosphatase
POLβ	Polymerase beta
POLλ	Polymerase lambda
PRMT6	Protein arginine methyltransferase 6
PTMs	Post-translational modifications
PVDF	Polyvinylidene fluoride
qPCR	quantitative polymerase chain reaction
RNA	Ribonucleic acid
RNAi	RNA interference
RNAi-R	RNAi-resistant
RNR	Ribonucleoside reductase
ROS	Reactive oxygen species
RPA	Replication factor A
rRNA	Ribosomal RNA
RT	Room temperature
SAM	S-Adenosylmethionine
SBs	Strand breaks

SCEs	sister-chromatid exchanges
SDS	Sodium dodecyl sulfate
SDS	Sodium Dodecyl Sulphate
Ser	Serine
SIRT1	Sirtuin 1
SMUG1	Single-strand-specific monofunctional uracil DNA glycosylase 1
ss	Single strand
SSBR	Single strand break repair
SSBs	Single strand breaks
T	Thymine
TCA	Tricarboxylic acid cycle
TDG	Thymine DNA glycosylase
TDP1	Tyrosyl-DNA phosphodiesterase 1
TOP1	Topoisomerase 1
TOP2	Topoisomerase 2
TRADD	TNFR-associated death domain
tRNA	Transfer RNA
Tyr	Tyrosine
UBR3	Ubiquitin protein ligase E3 component n-recognin 3
UNG	Uracil-N glycosylase
USP47	Ubiquitin specific peptidase 47
UV	Ultraviolet
WCEs	Whole cell extracts
WT	Wild type
XRCC1	X-ray repair cross-complementing protein 1
β-ME	β-mercaptethanol

1. Introduction

1.1 Cancer and genome instability

Cancer is a human disease characterised by the abnormal proliferation of a group of cells that form a cellular mass which acquires the ability to invade and metastasise in other tissues. Cancer refers to a family of diseases with different degrees of malignancies, most of which share a core of biological characteristics that are acquired during the tumour development.

Cancer biology has been extensively studied with the aim to address the molecular mechanisms leading to its development and maintenance. In fact, a better understanding of the biological process generates a spectrum of new therapeutic approaches to cure the disease. In 2000 Hanahan and Weinberg reviewed and identified six hallmarks of cancer: the aberrant mitogen stimulation, the resistance to cell death mechanisms, the inactivation of the growth control pathways, the achievement of infinitive duplication capability, the acquisition of tissue invasion abilities and the induction of angiogenesis (Hanahan et al., 2000). These characteristics are essential for allowing the onset of the disease and in the last ten years other hallmarks have been identified to complete the pattern of biological changes that occur during cancer development. Among the emerging hallmarks, the ability to avoid the immune system response and the reprogramming of the cellular metabolism have been described (Hanahan and Weinberg, 2011). Moreover, two enabling characteristics have been identified to allow the development of all the previously mentioned hallmarks of cancer: the tumour microenvironment and genome instability. The latter one is an intrinsic feature that promotes the formation of sporadic mutations allowing cancer development via a heterogeneous clonal selection mechanism. Genome instability

is indeed a fundamental factor that correlates with tumour formation. Therefore studying the molecular basis of DNA damage formation and the cellular mechanisms involved in DNA repair would enhance the knowledge of cancer biology.

DNA damaging agents have been used extensively in cancer therapy, highlighting the importance of studying DNA repair mechanisms in order to acquire the necessary knowledge to improve cancer treatments (Helleday et al., 2008; Lord and Ashworth, 2012). For instance, the use of alkylating agents, platinum compounds (such as cisplatin) and radiotherapy in combination with the inhibition of specific proteins involved in DNA repair is one of the strategies to treat cancer. Monotherapy approaches have also been tried in combination with specific genetic backgrounds (Helleday et al., 2008). Breast cancers carrying mutations in the *BRCA1/2* genes have been found to be sensitive to treatment with Poly-(ADP)-ribose polymerase (PARP) inhibitors (Bryant et al., 2005). Although the synthetic lethality mechanism is not truly understood, it is thought that PARP inhibition enhances the number of double strand breaks (DSBs) which in turn cannot be repaired as a consequence of a defective homologous recombination (HR) pathway, thus leading to cell death (Helleday, 2011). However, other strategies are used in the treatment of cancer. For instance, the combination of radiotherapy and gefitinib, an inhibitor of the epidermal growth factor receptor (EGFR) tyrosine kinase, has been shown to have an additive effect compared to gefitinib treatment alone in *in vivo* xenografts mouse models (Bokobza et al., 2014).

Finally, studying the DNA damage response (DDR) will improve knowledge of cancer biology, with an ultimate goal being to improve cancer therapy. The aim of this chapter is to give a comprehensive overview on the sources of genome instability (DNA damage formation) and on DDR. Particular attention will be given to the base excision repair (BER) pathway because of its relevance in repairing the majority of the spontaneous DNA lesions. Lastly, the alternative reading frame (ARF) tumour suppressor gene will be

introduced and relevant knowledge on the mechanisms of regulation of ARF will be summarised.

1.2 DNA damage and repair

1.2.1 Instability of DNA

In living cells, the genetic information is conserved and encoded by the DNA, a macromolecule composed of nucleotides. Each nucleotide consists of a deoxyribose sugar molecule, bound by a glycosidic bond to a nitrogenous base and by a phosphodiester bond to a phosphate group. The formation of the phosphodiester bond between the 3'-hydroxyl group (3'-OH) and 5'-phosphate (5'-P) of consecutive nucleotides allows the polymerisation of the DNA backbone, giving a 5'-3' orientation to each single strand fibre. Two opposite oriented chains of DNA are positioned to form the three-dimensional double helix structure (Watson, J. D., Crick, 1953). The bases constituting the DNA are adenine (A), guanine (G), cytosine (C) and thymidine (T). The nitrogenous ring of a purine (A or G) positioned on one strand forms non-covalent hydrogen bonds with a pyrimidine (C and T) on the opposite strand. Moreover, the interstrand base pairing always follows the same pattern, A with T and G with C (Watson and Crick, 1953).

The whole content of DNA in a living cell constitutes the genome. For instance, the human genome has been recently sequenced and it has reported to contain 2.85 billion nucleotides, encoding for 20,000 – 25,000 proteins (CONSURTIUM, 2005). In eukaryotic cells the genomic DNA is situated in the nucleus and it is wound around the nucleosome, a structure composed of histone proteins. Together, DNA and histone proteins form chromatin (Li, 2002).

DNA is more stable than RNA because of its double stranded structure and chromatin packaging. However, like other biological macromolecules, DNA is susceptible to spontaneous decomposition due to the instability of the bonds (Lindahl, 1993). Moreover, endogenous and exogenous DNA damaging factors can further affect the stability of these bonds. The following sections aim to describe the type of DNA lesions that can arise in more detail.

1.2.2 Endogenous DNA damage

1.2.2.1 DNA hydrolysis

The loss of a base and the consequent formation of an abasic site occur very frequently in a cell. The hydrolysis of the glycosidic bond leads to either depurination or depyrimidination, with different rates between the two processes (Lindahl, 1993). It has been estimated that ~ 10,000 of purines can be spontaneously hydrolysed compared to 500 pyrimidines in a cell per day (Lindahl and Karlström, 1973; Lindahl and Nyberg, 1972). Abasic sites should be removed from DNA since if left unrepaired they can cause DNA mutations during replication and may also block transcription (Lindahl and Barnes, 2000).

Deamination can also influence the stability of DNA by removing an amino group from the nitrogenous ring. In the case of purines, deamination converts guanine and adenine into xanthine and hypoxanthine, respectively. The deamination of cytosine leads to the formation of uracil which can be easily recognised and substituted by specific DNA repair mechanisms. However, deamination of 5-methylcytosine leads to thymidine, thus causing the formation of mismatch base pairs that can potentially create a point mutation (GC → AT). Cytosine deamination has been estimated to produce 100-500 lesions in a cell per day (Lindahl and Nyberg, 1974).

1.2.2.2 DNA oxidation

Cellular metabolism produces reactive oxygen species (ROS) which can potentially damage intracellular components. Mitochondria are responsible for the endogenous production of ROS (Murphy, 2009). Among ROS, the most reactive is the hydroxyl radical ($^{\bullet}OH$). One of the most dangerous DNA lesions generated by oxidation is 8-hydroxyguanine (8oxoG). 8oxoG generates a mutation because of its ability to mispair with adenine instead of cytosine, thus leading to a base change during replication (Lindahl, 1993; Lindahl and Barnes, 2000).

ROS attack also leads to the formation of single strand breaks (SSBs) by directly disrupting the sugar backbone, thus creating a 3'-phosphate or 3'-phosphoglycolate ends (Caldecott, 2008). Unrepaired SSBs can affect cellular processes, such as DNA transcription and replication, and can be even converted into deleterious DSBs during DNA replication (Kuzminov, 2001; Ryan et al., 1994; Saleh-gohari et al., 2005).

1.2.2.3 Spontaneous DNA methylation

The monofunctional alkylating agent S-adenosyl methionine (SAM), a co-factor used by DNA methylase enzymes, is another endogenous metabolite which can generate DNA lesions. The purine ring is affected by this compound through the reaction with the nitrogen atom, leading to the conversion of guanine and adenine into 7-methylguanine (7meG) and 3-methyladenine (3meA), respectively. Whereas 7meG does not create any mispairing, the 600 3meA residues produced in a cell per day can block replication, creating a potentially harmful situation (Lindahl, 1993).

1.2.2.4 Topoisomerase-generated strand breaks

DNA replication and transcription can lead to the formation of supercoiled DNA structures as a consequence of the double-helix-like topology of the DNA. Overwound DNA can pose problems to DNA replication and transcription. The activity of a specific class of enzymes named Topoisomerases is responsible for resolving supecoiled DNA (Wang, 2002). The first step of the reaction leads to a transient break with a tyrosine (Tyr) residue of the enzyme bound to the 5'-phosphate of the DNA, followed by a second step in which the supercoiled is unwound and the break is sealed. Topoisomerase 1 (TOP1) catalytic activity leads to the formation of an intermediate SSB, whereas the activity of Topoisomerase 2 (TOP2) generates a DSB. Therefore, abortive activities of these enzymes can lead to either TOP1-linked SSBs or TOP2-linked DSBs, which require appropriate repair to ensure correct DNA replication and transcription (Wang, 2002).

1.2.3 Exogenous DNA damage

1.2.3.1 DNA alkylation

Exogenous sources of alkylating agents are food, such as smoked meat and fish, and human-made products, such as tobacco smoke and pollutants. As mentioned above, alkylating compounds are chemical species that can react with DNA by transferring an alkyl group onto the nitrogenous ring of the base. Monofunctional and bifunctional alkylating agents can create different types of DNA lesions. Monofunctional alkylating agents can create 7meG, 3meA and O6-methylguanine (O^6meG). The latter has been reported to have a strong mutagenic potential by mispairing with thymine (Fu et al., 2012). Bifunctional alkylating agents can not only create the lesions mentioned above, but also contribute to the appearance of more complex DNA lesions, such as base adducts, creating an interstrand crosslink (Fu et al., 2012). This type of damage severely impairs cellular processes that require the opening of the double helix, such as DNA replication and transcription.

1.2.3.2 Ultraviolet (UV) lesions

UV light is the most dangerous exogenous source of DNA damage, causing the formation of 100,000 DNA lesions in a cell for a day of sunlight exposure (Hoeijmakers, 2009). The DNA lesions produced by UV light are cyclobutane pyrimidine dimers (CPD) and 6-4 pyrimidine-pyrimidone photoproducts. If those lesions are not repaired before DNA replication, they can lead to stalled replication forks which can eventually collapse forming a DSB. Moreover, UV light can also produce ROS through photo-oxidation, resulting in DNA oxidation (Hoeijmakers, 2009; Scharffetter-Kochanek et al., 1997).

1.2.3.3 Ionising radiation (IR)

The types of DNA lesions generated directly by IR include base damages, SSBs and DSBs. These lesions are created either by the direct ionisation of the DNA or by the formation of free radicals, such as ROS (Riley, 1994; Ward, 1990). It has been estimated

that the amount of SSBs produced per cell after a dose of 1 Gy is 1000, whilst the amount of DSBs is 40-60 (Riley, 1994; Ward, 1990). Moreover, the production of high amount of free radicals in a defined space leads to the production of clustered lesions, defined as two or more lesions within one to two helical turns of the DNA. These lesions are particularly complex to repair and the appropriate repair pathways have to be activated depending on the type of DNA damage produced (Sage and Harrison, 2011).

1.3 The Base Excision Repair pathway

It has been estimated that 10000-20000 lesions can spontaneously occur per day in a cell and the majority of these can be repaired by BER. Therefore this pathway is essential in maintaining genome instability, thus avoiding the onset of cancer and neurodegenerative diseases.

BER targets the repair of single base lesions which occur as a consequence of the instability of the DNA molecule. For instance, the loss, oxidation and the alkylation of the DNA bases can be caused by endogenous and exogenous sources of damage. Moreover, the repair of SSBs also involves BER proteins, broadening the spectrum of lesions which are repaired by this pathway.

The recognition of base lesions by DNA glycosylases is the initial step, followed by the incision of the sugar backbone, end processing, synthesis of the complementary nucleotide and ligation of the sugar backbone. In order to give a detailed overview of this pathway, the canonical short-patch repair mechanism will be presented first and then the long-patch repair pathway will be introduced (**figure 1.1**). Finally, single strand break repair (SSBR) will be described (**figure 1.2**).

1.3.1 BER pathway

1.3.1.1 DNA base damage recognition and removal by DNA glycosylases

The BER pathway was identified in 1974 with the discovery of uracil-DNA glycosylase (UNG), the enzyme responsible for the removal of uracil resulting in cytosine deamination (Lindahl, 1974). Since then, 11 human glycosylases have been identified (Jacobs and Schär, 2012). Several studies have shown substrate specificity for each glycosylase, although some overlap in substrate recognition has been shown by knock out (KO) studies in mice. Classification of DNA glycosylases based on the types of lesions recognised is summarised in **table 1.1**.

	NAME	MONO/BIFUNCTONAL ACTIVITY	TYPE OF BASE LESION
UNG	Uracil-N glycosylase	Monofunctional	Uracil bases
SMUG1	Single-strand-specific monofunctional uracil DNA glycosylase 1	Monofunctional	
MBD4	Methyl-binding domain glycosylase 4	Monofunctional	Pyrimidines
TDG	Thymine DNA glycosylase	Monofunctional	
OGG1	8-oxoG DNA glycosylase 1	Bifunctional	Oxidised bases
MYH	MutY homolog DNA glycosylase	Monofunctional	
MPG	Methyl purine glycosylase	Monofunctional	Alkylated purines
NTHL1	Endonuclease III-like 1	Bifunctional	
NEIL1	Endonuclease VIII-like 1	Bifunctional	Oxidised, ring-fragmented or saturated pyrimidines
NEIL2	Endonuclease VIII-like 2	Bifunctional	
NEIL3	Endonuclease VIII-like 3	Bifunctional	

Table 1.1: Mammalian DNA glycosylases.
[Adapted from (Jacobs and Schär, 2012)]

Even though, each DNA glycosylase recognises a specific base, the mode of action for detection of the damaged base is common. The recognition step occurs by rotating the base out of the DNA helix so to accommodate the base into the catalytic pocket. Specificity for the DNA lesions is obtained by steric exclusion depending on the active site of the enzyme. However, it is still not very clear how the detection of the damaged bases occurs considering the size of the whole genome and the fact that most of these lesions do not cause any distortion to the DNA helix. The current hypothesis is that DNA glycosylases are associated with undamaged DNA and they scan the DNA sequence to find base lesions (Jacobs and Schär, 2012). Studies on UNG and oxoguanine glycosylase 1 (OGG1) suggest the presence of a pre-selection step to establish initially a superficial contact between the base and the catalytic site to avoid each base of the DNA sequence to be fully accommodate in the catalytic pocket (Banerjee et al., 2005; Jacobs and Schär, 2012; Parker et al., 2007). Moreover, nuclear magnetic resonance (NMR) studies on the UNG protein suggest that a conformational change from an open to a closed form allows pre-examination of the bases (Friedman et al., 2009; Jacobs and Schär, 2012). However, the damaged base can be recognised only by inserting it fully inside the catalytic pocket and in order to do so the base has to be rotated out of the double helix. For instance, UNG uses a leucine (Leu) residue to drive the uracil inside the active site while the other bases are excluded from the catalytic site by either steric effects (purines) or by the presence of a conserved tyrosine (Tyr) residue in the catalytic pocket (other pyrimidines) (Jacobs and Schär, 2012; Kavli et al., 1996; Mol et al., 1995).

After the recognition of a damaged base, the removal of the base occurs by different catalytic reactions, depending on the type of DNA glycosylases involved. In fact, DNA glycosylases can be divided in two subgroups: monofunctional or bifunctional. The monofunctional glycosylases catalyse the base removal by performing a hydrolytic cleavage at the glycosidic bond between the nitrogenous base and the sugar. As a result of this reaction an apurinic/apyrimidinic (AP) site is generated, leaving the phosphodiester

backbone intact. The bifunctional glycosylases have a 3'-AP lyase activity and they process the lesions by creating a gap in the DNA backbone, thus leaving a SSB flanked by a 3'-unsaturated aldehyde and 5'-phosphate (Jacobs and Schär, 2012).

1.3.1.2 Incision

The removal of the base by the DNA glycosylase generates an AP site that can be recognised and processed by the apurinic/apyrimidinic endonuclease 1 (APE1). APE1 is a 35 kDa monomeric protein which has two catalytic domains with separate functions; the N-terminal portion is involved in the regulation of the activity of transcription factors, while the C-terminus harbours the endonuclease activity domain which is involved in DNA repair (Tell et al., 2009). It has been found that the glycosylase remains bound to the DNA, probably to protect the AP site, until APE1 displaces it from the site (Hill et al., 2001; Parikh et al., 1998). APE1 recognises the AP lesion and catalyses the formation of a DNA nick, leaving a 3'-OH and 5'-deoxyribosephosphate (5'-dRP) (Barzilay et al., 1995; Demple et al., 1991). AP sites can also spontaneously occur following hydrolysis of the glycosidic bond. APE1 is also able to recognise these sites independently of DNA glycosylase (Almeida and Sobol, 2007; Dianov et al., 2003; Fung and Demple, 2005).

Finally, APE1 is also able to tailor the 3'-ends of several lesions having 3'-diesterase and 3'-phosphatase activities (Chen et al., 1991). For instance, the activity of bifunctional DNA glycosylases leaves a 3'-unsaturated aldehyde that can be removed by APE1. Moreover, ROS can generate SSB lesions with 3'-phosphate or 3'-phosphoglycolate end groups which can be processed by APE1 to give 3'-OH ends (Izumi et al., 2000; Parsons et al., 2004; Winters et al., 1994).

1.3.1.3 Gap filling

DNA polymerase β (POLβ) is the major human polymerase involved in BER (Chan et al., 2006). POLβ is a 39 kDa protein made up of an 8 kDa N-terminal domain with a 5′-deoxyribose phosphate (5'-dRP) lyase activity and a 31 kDa C-terminal domain with DNA

polymerase activity. The dRP lyase activity is essential for processing the 5'-ends left by APE1 incision. POLβ does not have any of the proofreading activities, lacking exonuclease activity typical of replicative DNA polymerases (Beard and Wilson, 2006). However, the incorporation of the right nucleotide is enhanced when the enzyme is processing a 1 nucleotide (nt) gap with a 5'-phosphorylated end (Chagovetz et al., 1997; Chan et al., 2006).

Even though, POLβ plays a major role in the BER pathway, a backup role for DNA polymerase (POLλ) in BER has also been suggested (García-Díaz et al., 2001). POLλ like POLβ has the usual catalytic polymerase domain and the additional dRPase domain which allows the processing of 5'-dRP ends. POLλ has been reported to be important when cells are exposed to ROS, indicating a role for the polymerase in fixing oxidative lesions (Tano et al., 2007). Recently it has been reported that POLλ cooperates with long-patch BER in the correction of mispaired 8oxoG:A. These findings highlight the importance of POLλ in BER, especially in repairing oxidative base lesions (van Loon and Hübscher, 2009).

1.3.1.4 Ligation

The ligation process requires the activity of a DNA ligase to seal the nick positioned on the sugar backbone. DNA ligase III (LIG III) has been identified as the enzyme involved in this step during BER. The two isoforms, α and β, have the same catalytic domain with a different C-terminus. LIG IIIα has a BRCA1 C- terminus (BRCT) domain, whereas LIG IIIβ has a nuclear localisation signal (NLS) sequence. The LIG IIIα (for simplicity will be called, LIG III) isoform is a 103 kDa monomeric protein which has a mitochondrial leader sequence (MLS), important for the localisation of the protein within the mitochondria (Tomkinson and Sallmyr, 2013). However, the interaction with the nuclear scaffold X-ray repair cross-complementing protein 1 (XRCC1) via the BRCT motif allows it to be imported into the nucleus, enabling ligation to proceed. Moreover, XRCC1 is also required for the stabilisation of LIG III as shown by the fact that LIG III is absent in cells lacking

XRCC1 (Caldecott et al., 1995). XRCC1 does not have any catalytic domain, but it has two BRCT motifs, important for the interaction and the recruitment of proteins involved in BER, such as POLβ (Kubota et al., 1996; Marintchev et al., 2000) and APE1 (Vidal et al., 2001), suggesting a dominant role for this protein in BER (Horton et al., 2008). Even though LIG III is the major ligase reported to be involved in nuclear BER, it has been shown that LIG I can efficiently substitute for the XRCC1-LIG III complex during BER *in vitro* (Sleeth et al., 2004).

1.3.2 BER sub-pathway: long-patch BER

The long-patch and short-patch BER pathways share initial steps, such as the recognition of the base by the appropriate DNA glycosylases and the creation of a DNA nick in the sugar backbone. The type of 5'-end generated seems to be the deciding factor which triggers the switch between the two pathways. For instance, when the 5'-end cannot be processed by the dRP lyase activity of POLβ, strand displacement takes place (Fortini et al., 1999). Firstly, POLβ synthetises and adds the first nucleotide (Dianov et al., 1999; Prasad et al., 2000), followed by the synthesis of a 2-13 nt chain by the DNA replicative polymerases ε and δ (Fortini et al., 1998; Stucki et al., 1998). The recruitment of the replicative polymerases is dependent on the proliferating cell nuclear antigen (PCNA) (Gary et al., 1999), while the flap structure-specific endonuclease 1 (FEN1) is responsible for the removal of the displaced strand (Tom et al., 2000). Finally, ligation of the DNA nicks occurs via the activity of LIG I (Pascucci et al., 1999).

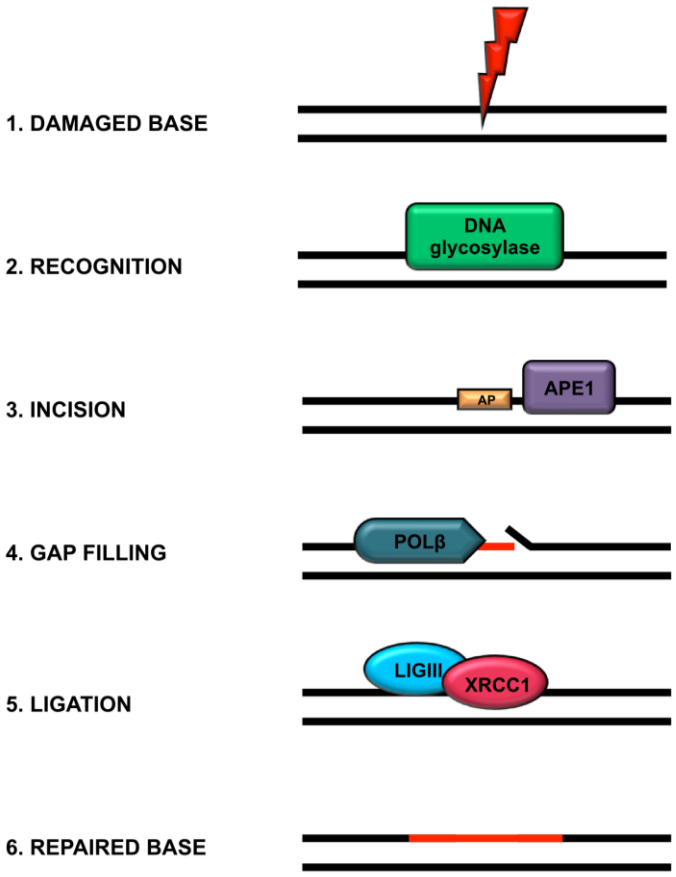

Figure 1.1: Simplified overview of the base excision repair (BER) pathway.
(1) Endogenous or exogenous sources of damage generate base lesions on the DNA. DNA glycosylases scan the genome to find base lesions. **(2)** Depending on the type of lesions, a different DNA glycosylase is able to recognise the lesion. After recognition, DNA glycosylases process cleavage of the glycosidic bond, leaving an apyrimidinic/apurinic site (AP). **(3)** Following the formation of an AP site, APE1 endonuclease catalyses the formation of a DNA nick flanked by 3'-OH and 5'-dRP ends. **(4)** POLβ fills the gap by synthesising the complementary nucleotide and by processing the 5'dRP ends leaving a 5'-phosphate. **(5)** Finally, the XRCC1-LIG III complex completes repair by sealing the DNA nick, thus leaving a repaired base (6).

1.3.3 BER sub-pathway: single-strand break repair (SSBR)

During BER a SSB is generated by APE1 as an intermediate of the repair process. However, SSBs can also arise spontaneously. BER proteins have been identified in the repair of SSBs and consequently SSBR is considered to be a sub-pathway of BER. The purpose of this section is to give a detailed overview of this pathway and of the players involved.

1.3.3.1 SSB formation

The formation of SSBs in the DNA sugar backbone occur mainly via the attack of ROS produced either endogenously by cellular metabolism or exogenously as a consequence, for instance, of exposure to IR. Moreover, SSBs are also created during BER. For instance, APE1 endonuclease generates a DNA nick to allow replacement of the damaged base. Also, DNA topoisomerase 1 (TOP1) creates a SSB to unwind the DNA double helix which is then immediately resealed by TOP1 itself. When the latter step is not achieved, the enzyme cannot be released from the DNA and a SSB is created (Caldecott, 2008; Wang, 2002). If either the DNA replication or transcription machinery encounter an unrepaired SSB, a DSB can occur which is far more complex lesion to repair (Kuzminov, 2001; Saleh-gohari et al., 2005). Therefore, it is crucial that SSBs are repaired correctly to avoid the appearance of DSBs (Caldecott, 2008).

1.3.3.2 SSB detection

The detection of SSB lesions is mainly achieved by PARP1, a 116 kDa protein which acts as a nick-sensor. All seventeen PARP proteins contain a PARP motif domain, situated in the catalytic region at the C-terminus. Not all the PARP proteins can synthesise poly-(ADP)-ribose (PAR), despite the presence of a PARP catalytic domain. For instance, mono-ADP transferase and oligo-ADP transferase activities have been found in PARP5 and PARP10, respectively (Gibson and Kraus, 2012). However, only PARP1, PARP2 and PARP3 have been found to be activated in response to DNA breaks, with PARP1

activation 5-fold higher than PARP2 (Ame et al., 1999), and PARP3 being activated in response to DSBs during non-homologous end joining (NHEJ) (Rulten et al., 2011). PARP1 is also characterised by the presence of a DNA-binding domain (DBD) and a NLS, both situated at the N-terminus (Woodhouse and Dianov, 2008). The BRCT domains, situated in the central portion of the protein, have been shown to be important for the interaction with proteins involved in BER such as XRCC1 (Okano et al., 2003), LIG III (Leppard et al., 2003) and POLβ (Dantzer et al., 2000).

PARP1 binds to DNA strand breaks (SBs), leading to a 500-fold increase in its enzymatic activity (Gradwohl et al., 1990). It functions as a homodimer and has the ability to synthesise PAR, a multi-branched polymer using the nicotinamide adenine dinucleotide (NAD^+) molecule as a co-factor (Singh et al., 1985). The PAR polymer binds to the acceptor proteins at lysine (Lys), aspartic (Asp) or glutamic (Glu) acid residues. PARP1 automodification establishes a turnover of the protein between a DNA-bound and a DNA-free status. In fact, automodification leads to the release of PARP1, allowing the repair of the DNA nick by the DNA repair enzymes (Ferro AM and Olivera, 1982; Woodhouse and Dianov, 2008). PAR is then hydrolysed by poly-(ADP)-ribose glycohydrolase (PARG), thus allowing PARP1 to bind to the DNA nick again (Davidovic et al., 2001; Fisher et al., 2007).

1.3.3.3 SSB end tailoring and gap filling

In order for ligation to occur, a DNA nick flanked by a 3'-OH and a 5'-P group is necessary. End tailoring is required, for instance, following ROS induced breaks, following the activity of bifunctional DNA glycosylases and in resolving TOP1-linked SSBs. The modification of the DNA ends induced by APE1 and POLβ has been discussed in previous sections. However, other proteins are also involved in this step. For instance, the polynucleotide phosphatase/kinase (PNKP) protein has both phosphatase and kinase activity and is required for the conversion of the 3'-phosphate end to 3'-OH (Jilani et al., 1999; Whitehouse et al., 2001). The tyrosyl-DNA phosphodiesterase 1 (TDP1) is essential to solve the SSBs generated by incomplete TOP1 activity (Pouliot et al., 1999; Yang et al.,

1996). Finally, aprataxin (APTX) is important to remove 5'-adenosine monophosphate (AMP) which results from unsuccessful DNA ligase activity (Ahel et al., 2006).

Once the processing of the ends has finished, the gap filling step occurs. The polymerases involved in short- and long-patch BER, such as POLβ, POLλ and POLδ, are required for this step. Finally, the DNA nicks are sealed by either the XRCC1-LIG III complex or LIG I.

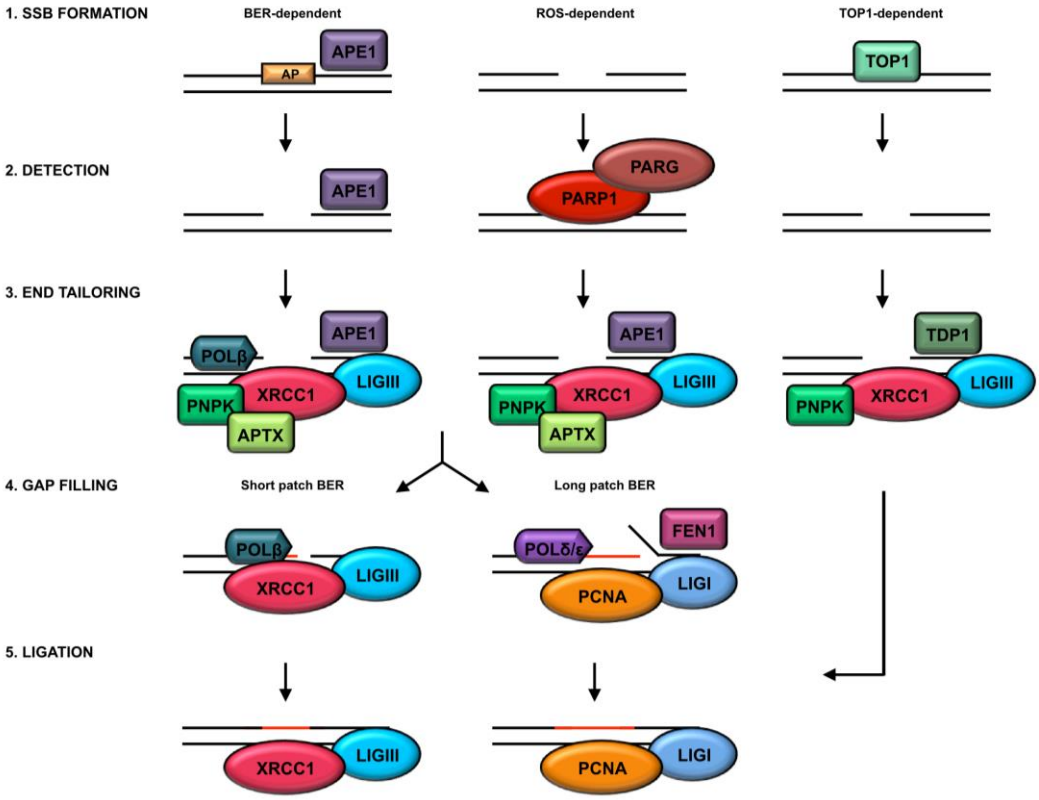

Figure 1.2: Overview of the single-strand break repair (SSBR) pathway.
(1) SSBs can arise in three different way: i) as an intermediate of the BER pathway as a consequence of the catalytic activity of APE1 endonuclease enzyme (or of bifunctional DNA glycosylases); ii) by the direct attack of ROS on the sugar backbone; iii) by unsuccessful TOP1 activity leading to TOP1-linked SSBs. **(2)** ROS-dependent SSBs are detected by PARP1, whereas a protein-protein interaction mechanism helps the right enzyme to localise to the site of damage in the other two situations. PARP1 detection of SSBs stimulates the autoparylation of the enzyme, PARG catabolises PAR bound to PARP1, thus leading to the release of PARP1 from the SSBs to allow repair. **(3)** At this stage, the activity of POLβ, PNPK, APTX and APE1 is required for tailoring 5' and 3' ends. In TOP1-linked SSBs, TDP1 is required first to remove TOP1. **(4-5)** The synthesis of the nucleotides can occur by using either short-patch BER or long-patch BER. The former pathway employs POLβ for the gap-filling stage and the XRCC1-LIG III complex for the ligation stage; the latter one employs PCNA for the recruitment of replicative POLδ/ε, FEN1 endonuclease and LIG I. [Adapted from (Caldecott, 2008)]

1.3.4 Coordination of BER mechanism

Several studies have focused on trying to address how the proteins required for repair of single base lesions and SSBs are co-ordinated to the site of damage. In fact, the recruitment of the proteins depends on the specificity of each lesion.

The amount of protein-protein interactions described among BER components suggests that the formation of a multi-protein complex is one of the possible mechanisms to implement the protein-substrate interaction (Almeida and Sobol, 2007; Caldecott, 2003a). Immunoprecipitation studies confirmed the interaction between BER proteins, but did not investigate the existence of stable multi-protein complexes *in vivo* (Dianov and Parsons, 2007).

However, these studies have helped to establish another model, the “passing the baton” model. In this, the intermediate is passed from one protein to the next for being quickly processed. In this way, the possibility that the intermediates can stimulate the activation of a DDR is avoided. Several studies support this “passing the baton” model. For instance, APE1 has been suggested to displace DNA glycosylases after the formation of an AP site (Hill et al., 2001; Parikh et al., 1998). The interaction between APE1 and POLβ indicates a possible mechanism for recruitment of the polymerase (Bennett et al., 1997), whereas the affinity of POLβ for XRCC1 explains the recruitment of the XRCC1-LIG III complex (Caldecott et al., 1996; Kubota et al., 1996).

Although the preliminary steps of the pathway require the activity of a very specific set of proteins, resolving of the SSB intermediates is the common denominator which determines each round of repair in BER; moreover, this is the initial step of SSBR. Several studies have indicated that the coordination of this step depends on the cooperation between PARP1 and XRCC1. SSB lesions, which are generated either as an intermediate during BER or directly by ROS attack, are detected by PARP1. The role of PARP1 in both pathways has been discussed in several studies. It has been shown that the presence of the protein is not necessary for BER repair, but it is important to protect the degradation of

the DNA ends to avoid DSB formation (Parsons et al., 2005; Woodhouse et al., 2008). However, it has also been shown that PARP1 is essential for accelerating the repair of SSBs by stimulating the recruitment of XRCC1/POLβ/LIG III proteins, thus indicating a possible role for PARP1 in the coordination of the final steps of BER (El-Khamisy et al., 2003). Indeed, the interaction between PARP1 and XRCC1 is not constitutive, but it is promoted by automodified PARP1 (Dantzer et al., 2000; Masson et al., 1998). Recently, it has been suggested that PARP1 is required for XRCC1 recruitment during SSB repair, whereas XRCC1 recruitment can occur independently of PARP1 during BER *in vivo*. These findings indicate that the interaction between XRCC1 and BER proteins, such as the DNA glycosylase OGG1, APE1 or POLβ, might drive XRCC1 localisation to the sites of damage during BER (Campalans et al., 2013).

Finally, two different models have been proposed for describing the role of PARP1, the nick-protection and the protein-recruiter models. The former describes PARP1 to be necessary for avoiding the formation of DSBs when the number of SB lesions is higher than the repair capacity. In this model, PARP1 is not important for the repair itself. The latter gives PARP1 a central role in resolving SSB lesions based on the findings that show the importance of PARP1 in the recruitment of the XRCC1 protein at the site of damage.

XRCC1 itself is important in creating a platform for proteins required during SSBR. Indeed, XRCC1 directly interacts with APE1 (Vidal et al., 2001), POLβ (Caldecott et al., 1996; Kubota et al., 1996; Marintchev et al., 2000), PNKP (Whitehouse et al., 2001) and indirectly through LIG III with TDP1 (Plo et al., 2003). The central role of XRCC1 in SSBR has been shown by the fact that XRCC1 depletion leads to SSBR-deficiency and accumulation of unrepaired SBs (Brem and Hall, 2005; Fan et al., 2007).

1.3.5 BER in human diseases

BER is essential for the repair of a vast range of lesions to both avoid DNA damage accumulation and the appearance of more harmful lesions, such as DSBs. Indeed, deficiency in BER has been associated with human diseases, such as cancer and

neurological disorders. The next section aims to summarise this by highlighting the importance of maintaining intact BER genes.

1.3.5.1 BER and cancer

BER is important in correcting a high number of DNA lesions in order to avoid genome instability, one of the contributing factors for cancer development (Hanahan and Weinberg, 2011). Studies in mice have revealed that the recognition of base lesions by DNA glycosylases is not always specific. Knockout mice for each of the 11 glycosylases have been created and except for the thymine DNA glycosylase (*Tdg*) KO, which has been shown to be embryonic lethal, all are viable without a severe phenotype (Fortini et al., 2003; Jacobs and Schär, 2012). Therefore, impairment of a single glycosylase does not affect development of the organism, suggesting the existence of compensatory mechanisms amongst DNA glycosylases. However, a higher accumulation of mutations and, in some cases, development of a tumour indicates that DNA glycosylases are necessary for maintaining genome stability. Indeed, mutations in *OGG1* gene have been found in lung and kidney tumours (Chevillard et al., 1998), whereas homozygote mutations of *MYH* can lead to colorectal cancer (Jones et al., 2002). More recently, a polymorphism in the *OGG1* gene has been identified in non-small cell lung cancer (Fortini et al., 2003; Sugimura et al., 1999).

Even though, there is some functional overlap between DNA glycosylases, the other BER proteins have a unique function during development. Indeed, *Ape1* (Xanthoudakis et al., 1996), *Xrcc1* (Tebbs et al., 1999) and *Lig III* (Puebla-osorio et al., 2006) KO mice are embryonic lethal, whereas *Polβ* KO mice shows defective neurogenesis, thus leading to neonatal death (Sugo et al., 2000). Moreover, misregulation of the level of these proteins has been found in several human cancers, suggesting that a tight control of the expression is required to maintain genome stability.

Indeed, the *POLβ* gene has been sequenced in order to identify mutations which correlate with the onset of cancer. *POLβ* mutations have been found in colorectal, lung, bladder, breast, gastric and prostate cancers (Chan et al., 2006).

Regarding XRCC1, an extensive evaluation of the *XRCC1* gene polymorphisms has been carried out to correlate those variants with a cancer-associated risk. 37 single nucleotide polymorphisms have been detected. Among the most frequent polymorphisms, are Arg399Gln (27%), Arg194Trp (13%) and Arg180His (7%) (Ladiges et al., 2003). In the Asiatic population individuals with an Arg399Gln polymorphism have shown an increased risk in developing lung cancer (Sykora et al., 2013). Studies on other polymorphisms, such as Arg194Trp and Arg180His, do not show a correlation with an increased risk of lung cancer (Maynard et al., 2009).

Regarding a role for APE1 in cancer development, the protein has been found to localise mainly in the cytoplasm of epithelial ovarian cancers (Moore et al., 2000) and in hepatocellular carcinoma (Maso et al., 2007), suggesting an inability to repair genomic DNA.

1.3.5.2 BER and neurodegenerative disorders

In the brain, high levels of oxygen are required to maintain the neuronal transmissions and cellular metabolism. Therefore, the generation of ROS during these processes requires the intervention of DNA repair mechanisms to avoid an accumulation of DNA lesions. For instance, accumulation of unrepaired base lesions can lead to SSB formation, which impairs DNA transcription. Moreover, SSB are detected by PARP1 and prolonged activation of this enzyme leads to neuronal death (Alano et al., 2010; Andrabi et al., 2006; Wang et al., 2011).

As neurons are post-mitotic cells, they lack HR, and mainly rely on BER and NHEJ pathways for DNA repair. Therefore, the correlation between the activity of BER proteins and the onset of neurodegenerative diseases has been investigated using mouse models.

For instance, *Polβ* KO mice show extensive apoptosis in the cortex and the hindbrain, indicating that the enzyme is important in neural differentiation (Sugo et al., 2000).

The studies in mice indicate a role for BER in brain development. However, a correlation between neurodegenerative diseases and BER protein in human diseases has also been investigated. For instance, analysis of neuronal tissues from patients affected by Alzheimer's Disease (AD) correlates with higher levels of APE1 (Marcon et al., 2009; Weissman et al., 2007) and POLβ (Copani et al., 2006). Indeed, the overexpression of these proteins also leads to genomic instability, thus explaining a possible mechanism for the onset of AD. For instance, hyperactivation of APE1 can lead to an increase in the production of SSBs which are detected by PARP1. In fact, a correlation between PARP1 and AD pathogenesis has been described, indicating that PARP1 activation triggers neuronal cell death via PAR accumulation and NAD^+ depletion (Strosznajder et al., 2012). Also, an association between AD and *OGG1*, *PARP1*, *APE1* and *XRCC1* gene polymorphisms has been found (Mantha et al., 2013).

More interestingly, three hereditary genetic diseases have been linked to defects in SSBR, through a deficit in the activity of PNKP, APTX and TDP1 proteins. The *PNKP* gene has been found to be mutated in individuals who are affected by a neurological disorder, characterised by microcephaly and defects in brain development (Shen et al., 2010). Studies on lymphocytes from patients and *in vitro* studies on PNKP mutants have shown that the repair of DNA lesions following both H_2O_2 and CPT treatment is slower, as a consequence of a decrease in PNKP protein stability (Reynolds et al., 2012; Shen et al., 2010).

Mutations in the *APTX* gene have been identified to be the cause for the onset of ataxia-oculomotor apraxia 1 (AOA1) (Moreira et al., 2001), an autosomal recessive neurological disorder characterised by cerebellar atrophy. This leads to difficulties in coordinating movement (ataxia) and also results in limited movement of the eye (apraxia). The histidine traid domain (HIT) carries most of the detected mutations in the *APTX* gene, thus leading

to a decrease in the stability of the protein and consequently to a deficit in SSBR (Clements et al., 2004; Hirano et al., 2007). Therefore, an accumulation of unrepaired SSBs might be the cause for the onset of the neurological disorder (Caldecott, 2008).

Regarding the *TDP1* gene, a missense mutation (H493R) in the second catalytic domain (HKD2) has been identified in patients affected by spinocerebellar ataxia with axonal neuropathy 1 (SCAN1) (Takashima et al., 2002). SCAN1 is an autosomal recessive neurological disorder characterised by cerebellar atrophy. The decrease in the catalytic activity of the TDP1 mutant has been suggested as the cause for the development of this neurological disorder leading to SSBR-deficiency (El-khamisy et al., 2005). Indeed, *Tdp1* KO mice show a decrease in cerebellar size, indicating that Tdp1 might be necessary for maintaining cerebellar function (Caldecott, 2008; Katyal et al., 2007).

1.4 Regulation of BER and genome instability

Correct and prompt regulation of BER proteins is fundamental to avoid accumulation of unrepaired lesions, thus preventing genome instability and the onset of human diseases, such as cancer and neurological disorders.

In general, the function of cellular proteins is controlled at different levels by: i) regulating the protein activity; ii) regulating the protein turn-over; iii) regulating the protein localisation; iv) inducing or repressing the protein expression at transcriptional level; v) regulating the chromatin status of the gene. Post translational modifications (PTMs) influence protein activity and stability to obtain a quick response, whilst modification of the protein expression is a slower and possibly more long-term response.

BER activity has been shown to be regulated by several PTMs such as phosphorylation, acetylation, ubiquitination and sumoylation. Despite the fact that the overall levels of BER proteins do not change radically in response to genotoxic treatment, some recent data suggest that the steady-state level of BER proteins is adjusted based on the level of DNA damage which needs to be repaired. For the scope of this thesis, the regulation of the BER proteins involved in the SSBR sub-pathway will be discussed focussing on the consequences of their misregulation in terms of genomic instability.

1.4.1 APE1

The cellular level of APE1 has to be regulated to ensure that the amount of SSB lesions generated can be efficiently repaired by the downstream effectors of the BER pathway. As mentioned in the previous section, *Ape1* KO mice is embryonically lethal, showing the importance of APE1 during development (Xanthoudakis et al., 1996). *In vitro* studies have outlined that the level of APE1 needs to be regulated properly to avoid genomic instability. For instance, the downregulation of the enzyme sensitises the cells to treatments with DNA damaging compounds and leads to the accumulation of unprocessed AP sites (Fung and Demple, 2005; Izumi et al., 2005).

It has been shown that APE1 downregulation triggers apoptosis as a consequence of an accumulation of AP sites, which cannot be repaired. The cell death mechanism is activated to avoid genomic instability (Fung and Demple, 2005). As well as downregulation leading to unrepaired lesions, the upregulation leads to an elevated amount of SSBs, thus overloading BER capacity. Indeed, in the XRCC1-deficient Chinese hamster ovary (CHO) EM9 cell line, the overexpression of APE1 generates an increase in the amount of sister chromatid exchanges (SCEs), leading to genomic instability (Sossou et al., 2005).

In terms of PTMs, it has been reported that in response to H_2O_2 treatment APE1 gets polyubiquitinated by the E3 ubiquitin ligase mouse double minute 2 homolog (MDM2) protein *in vivo*. The authors suggest that the reduction of APE1 was necessary for triggering apoptosis due to the amount of unrepaired lesions (Busso et al., 2009).

The phosphorylation of tyrosine 232 (T232) by the cyclin-dependent kinase 5 (CDK5) has been reported to decrease the activity of APE1, leading to an increase in the amount of AP sites and consequently triggering neuronal cell death (Huang et al., 2010). Moreover, the CDK5-dependent phosphorylation of APE1 increases APE1-recognition by MDM2, thus reducing the level of APE1 and therefore triggering apoptosis (Busso et al., 2011).

More recently, the E3 ubiquitin ligase component n-recognin 3 (UBR3) has been identified as the main E3 ubiquitin ligase involved in controlling the state-steady levels of APE1. In this work, E3 ubiquitin ligase was purified from HeLa WCEs and the activity of UBR3 on APE1 was confirmed by an *in vitro* ubiquitination assay. More interestingly, it has been shown that the *Ubr3* KO mouse cells have elevated levels of Ape1 protein. As a consequence of increasing levels of Ape1, *Ubr3* KO cells show an increase in both γH2AX and 53BP1 foci formation, which are known markers of DSB formation (Meisenberg et al., 2012).

Lastly, the deacetylation of APE1 by SIRT1 has been reported to promote the binding of APE1 to XRCC1, enhancing the repair of an AP site in response to methyl methanesulfonate (MMS) treatment (Yamamori et al., 2010).

1.4.2 POLβ

POLβ is the main polymerase involved in the gap-filling step during BER; moreover, its dRPase activity is essential for preparing the 5'-end for the ligation step. Polβ has an essential role in the development of the brain as shown by the fact that KO mice show defective neurogenesis and die shortly after birth (Sugo et al., 2000). To study the consequences of a reduction in POLβ levels, a *Polβ* haploinsufficient mouse has been generated. These mice show elevated levels of SSBs and chromosomal aberrations. Moreover, an increase in the mutagenesis rate has been described in response to exposure to alkylating agents (Cabelof et al., 2003). *Polβ* null mouse embryonic fibroblasts (MEFs) show a similar phenotype with an increase in apoptosis, higher levels of SCEs and chromosomal breaks in response to MMS (Sobol et al., 2000, 2002).

It has been reported that upregulation of POLβ increases the frequencies of spontaneously formed mutations, with an increase in the mutation rate by 2-4 fold (Canitrot et al., 1998). Cells overexpressing POLβ lead to the development of a larger tumour compared to control cells (Bergoglio et al., 2002).

Together these results show the importance of tightly regulating the amount of POLβ within the cell. Recently, a role for the E3 ubiquitin ligase ARF-binding protein 1 (ARF-BP1)/MULE in the regulation of the steady-state levels of POLβ has been described. MULE has been found to monoubiquitylate POLβ. The interaction between POLβ and MULE has been shown to be regulated by the tumour suppressor protein ARF, which is known to inhibit the activity of MULE. Indeed, ARF downregulation leads to an increasing amount of monoubiquitylated POLβ, thus impairing DNA repair. The monoubiquitination catalysed by MULE allows the E3 ubiquitin ligase C-terminus of hsc70 interacting protein (CHIP) to recognise POLβ, leading to POLβ polyubiquitination and consequently

proteasome degradation (Parsons et al., 2009). Additionally, the ubiquitin-specific protease 47 (USP47) has been identified to be responsible for the deubiquitylation of POLβ, thus allowing POLβ recruitment for DNA repair. Indeed, the downregulation of USP47 leads to activation of PARP1 as a consequence of deficiency in DNA repair due to a low level of POLβ (Parsons et al., 2011).

Lastly, the p300 histone acetylase has been reported to acetylate POLβ, although the consequences of this modification still remain unclear (Hasan et al., 2002). Moreover, arginine methylation of POLβ by protein arginine N-methyltransferase (PRMT6) has been found to enhance the binding of the polymerase to the DNA, thus increasing the repair of MMS-induced lesions (El-Andaloussi et al., 2006).

1.4.3 XRCC1

The XRCC1 scaffold protein has been found to form a stable complex with the LIG III protein, thus maintaining the stability of LIG III. The XRCC1-LIG III complex is recruited to SSBs in order to seal the DNA nicks. Moreover, XRCC1 has been reported to interact with APE1, POLβ and PNKP to promote the recruitment of these proteins at damage sites (Caldecott et al., 1996; Kubota et al., 1996; Marintchev et al., 2000; Vidal et al., 2001; Whitehouse et al., 2001).

In vivo studies have demonstrated the importance of correctly maintaining XRCC1 protein levels; in fact, *Xrcc1* KO in mice is embryonic lethal and these embryos were reported to accumulate unrepaired SSBs. Moreover, an elevated level of SCEs was also identified (Tebbs et al., 1999), suggesting that unsealed SSBs can be converted to DSBs during DNA replication, requiring the intervention of DSB repair pathways, such as NHEJ or HR.

To get a better understanding of the consequences of low levels of XRCC1, the CHO EM9 cell line, which is deficient in XRCC1, has been used. These cells are highly sensitive to MMS and they show moderate sensitivity to H_2O_2 and camptothecin (CPT) treatments (Caldecott, 2003b). Moreover, they show a severe deficiency in the repair of SSBs, which leads to a great accumulation of SCEs (Shen et al., 1998; Thompson et al., 1982). These

cells also exhibit a ~ 5-fold reduction in LIG III levels, as demonstrated by a reduction in the repair of DNA nicks (Caldecott et al., 1995). The transient depletion of XRCC1 using RNAi has shown similar results with elevated sensitivity to MMS treatment and an increase in the amount of spontaneously formed SCEs, confirming an impairment in the repair of SSBs (Fan et al., 2007). Besides a deficiency in DNA repair, the hyperactivation of PARP1 has been detected in both XRCC1-deficient and XRCC1-depleted cells. Indeed, activation of PARP1 has been monitored measuring the level of NAD(P)H. CHO EM9 cells exhibit a dramatic decrease in the metabolite in response to treatment with MMS when compared to the CHO EM9 cell line complemented with XRCC1 (Nakamura et al., 2003). Moreover, the silencing of XRCC1 has also been shown to trigger PAR synthesis and therefore NAD^+ consumption (Brem and Hall, 2005). Overall these findings show that a decrease in the level of XRCC1 has severe consequences in terms of accumulation of unrepaired SSBs, thus leading to genomic instability.

In terms of PTMs, casein kinase 2 (CK2) has been reported to phosphorylate XRCC1 at 8 different sites on the XRCC1 C-terminus, thus enhancing the repair of SSB lesions, by preventing the ubiquitination of XRCC1 (Loizou et al., 2004). Indeed, cells depleted of CK2 show a decrease in XRCC1 protein levels. Consequently, *in vitro* studies using oligonucleotides have demonstrated defected repair in SSBs whereas an increase in PAR synthesis was identified *in vivo* (Parsons et al., 2010). The steady-state level of the protein, XRCC1 has been found to be polyubiquitinated by the E3 ubiquitin ligase CHIP, which also is responsible for the degradation of POLβ and LIG III, conferring a central role for CHIP in the regulation of BER capacity (Parsons et al., 2008).

1.4.4 PARP1

In contrast to other proteins involved in the SSBR, PARP1 does not have a direct role in the DNA repair. However, PARP1 activation occurs after the detection of SSB nicks, stimulating the synthesis of PAR through the consumption of NAD^+(Singh et al., 1985).

Although PARP1 activity has been reported to stimulate the recruitment of the XRCC1-LIG III complex at the site of damage (El-Khamisy et al., 2003; Okano et al., 2003), KO mice model have shown that the presence of the protein is not essential during BER. Indeed, these mice are viable and they do not show any abnormalities during development (Masutani et al., 2000; de Murcia et al., 1997). These results have also been confirmed by *in vitro* studies, suggesting that PARP1 is dispensable during BER (Parsons et al., 2005). However, the excessive production of DNA lesions in the intestine and in the stomach of *Parp1* KO mice in response to genotoxic treatments, such as 1-methyl-1-nitrosourea (MNU) and IR treatment, has been shown, suggesting that cells lacking PARP1 are highly sensitive to DNA damage (Masutani et al., 2000; de Murcia et al., 1997). Moreover, histological sections of these tissues exhibit an increase in the amount of both SCEs and chromatid breaks, suggesting a fundamental role for Parp1 in maintaining genomic instability. Similar results have been obtained when comparing WT MEFs with *Parp1* KO MEFs: a 2-fold increase in the amount of micronuclei was observed without any supplementary treatments, suggesting that the lack of Parp1 promotes chromosomal aberrations (Trucco et al., 1998). *In vivo* studies in human cell lines have shown that PARP1 depletion increases the amount of γH2AX foci formation (a marker for DSBs) in cells treated with H_2O_2, suggesting that, when BER is overloaded, PARP1 is essential in preventing the formation of DSBs (Fisher et al., 2007; Woodhouse et al., 2008). From the studies presented here, it appears clear that the regulation of PARP1 levels is essential to avoid genomic instability.

1.5 DNA damage response (DDR)

Even though, DNA repair mechanisms and DNA damage signalling pathways have been presented as two different entities, they both contribute to DDR. Indeed, while DNA repair proteins are involved in directly resolving DNA lesions, other players are activated for enhancing the efficiency of the repair and for reporting DNA damage. Depending on the amount and the type of lesions, the DNA signalling transducers lead to different cellular responses, such as cell cycle arrest and cell death. As described in the previous section, prompt and correct regulation of BER is essential to avoid the persistence of unrepaired DNA lesions. Thus, misregulation of BER protein levels leads to persistent SSBs and potentially to DSBs, one of the most powerful trigger of the DNA damage signalling pathway. The following sections give an overview on the proteins involved in DNA damage signalling and consequent cellular responses. A section describing the role of PARP1 in the DNA damage signalling pathway is included to give a comprehensive view on the role of PARP1 in DDR.

1.5.1 PARP1 activation at the cross-road between repair and DNA damage signalling

PARP1 activation has been found to be part of several signalling pathways, such as the nuclear factor kappa-light-chain-enhancer (NF-κB)-dependent inflammatory response, the heat shock response and the c-Jun N-terminal kinase (JNK)-dependent pathway (Luo and Kraus, 2012). For the purpose on this work, the role of PARP1 as a signalling molecule in DDR will be presented in more detail.

As described previously, PARP1 senses SSB accumulation and prevents the formation of DSBs, thus recruiting SSB repair proteins to the site of damage. However, the function of PARP1 is not only limited to facilitate repair, but several studies have also outlined the importance of PARP1 in modulating cellular responses to DNA damage.

Firstly, a link has been reported between PARP1 and other proteins involved in DDR, such as ataxia telangiectasia mutated (ATM) protein kinase. ATM kinase is activated in response to DNA damage, mainly after the formation of DSBs. It has been shown that ATM binds to PAR *in vivo*, suggesting a possible mechanism in the recruitment of the kinase to the site of damage. Moreover, the downstream signalling activated by ATM in response to DNA damage is impaired in cells lacking PARP1, suggesting an indispensable role for PARP1 in activating ATM (Haince et al., 2007). Other evidence that PARP1 activity is important for signalling DNA damage is supported by the findings that link PARP1 to the regulation of the tumour suppressor protein p53. Both PARP1 inhibition (Wieler et al., 2003) and *PARP1* KO (Valenzuela et al., 2002) have been shown to impair the accumulation of p53 protein and, consequently, to lead to a defective G1 arrest after treatment with IR. Recently, the direct parylation of p53 by PARP1 has been shown to regulate the activity of the transcription factor (Lee et al., 2012).

The activation of PARP1 has been found to be important for the regulation of cell fate. Indeed, high levels of DNA damage correlate with the accumulation of PAR polymers and this has been shown to trigger neuronal cell-death by stimulating the release of the apoptosis-inducing factor (AIF) from the mitochondria after the treatment with methyl-nitro-nitroso-guanidine (MNNG) (Andrabi et al., 2006; Wang et al., 2011). Also, PARP1-dependent depletion of NAD^+ following DNA damage has been suggested to cause neuronal cell-death (Alano et al., 2010). This type of cell-death is called parthanatos, a caspase-independent mechanism. Parthanatos requires PARP1 activation and the release of AIF from the mitochondrial membrane (Wang et al., 2011). However, PARP1 has also been shown to trigger apoptosis and necrosis. For instance, it has been shown that following H_2O_2 treatment PARP1 triggers necrosis in MEFs and in the human HCT116 cell line in a p53-dependent manner (Montero et al., 2013).

Therefore, PARP1 activity reports the presence of DNA damage to the cytoplasm either via PAR polymer synthesis or via the consumption of NAD^+, suggesting a role for PARP1 in signalling the amount of DNA lesions, ultimately determining cell fate.

Then, hyperactivation of PARP1 can have dramatic consequences for the survival of the cells, suggesting the existence of antagonistic mechanisms to regulate cell survival. For instance, PARylated PARP1 protein is ubiquitinated by the E3 ubiquitin ligase IDUNA in response to DNA damage. These findings indicates the presence of a mechanism that promotes cell survival, avoiding both excessive PAR accumulation and NAD^+ depletion (Kang et al., 2011). Indeed, MCF7 cells are more sensitive to MNNG treatment when IDUNA is depleted and, conversely, cells are more resistant to cell death when the protein is overexpressed.

SIRT1 is also important for restraining PARP1-dependent cell death activation. SIRT1 is part of the class III deacetylase family and it uses NAD^+ as a co-factor for the catalytic reaction. SIRT1 activity has been reported to have a role in directly regulating gene expression through the targeting of the histone tails, thus promoting chromatin condensation and supressing gene transcription (Fatoba and Okorokov, 2011; He et al., 2011; Vaquero et al., 2004). However, SIRT1 can also indirectly affect gene transcription through the deacetylation of its non-histone substrates, such as p53 (Kim et al., 2007; Langley et al., 2002; Peck et al., 2010; Thakur et al., 2012), the forkhead box 3 (FOXO3) protein (Brunet et al., 2004; Wang et al., 2012) and E2F1 (Wang et al., 2006). Indeed, the deacetylation decreases the binding of the transcription factors to their specific promoter sequences, subsequently reducing the transcription of the gene (Ozaki et al., 2009). SIRT1 localises in the nucleus and it is therefore likely to share the nuclear NAD^+ pool with PARP1 protein. SIRT1 and PARP1 have been reported to regulate each other's activity throughout the consumption of the NAD^+ available (Bai et al., 2011; Caito et al., 2010; Kolthur-seetharam et al., 2006). The functional interplay between SIRT1 and PARP1 in regulating cell death mechanisms has been previously shown. In fact, it has

been reported that *SIRT1* KO 293 cells show an increase of PAR synthesis in response to H_2O_2 treatment, suggesting a role for SIRT1 in balancing PARP1 activity. Moreover, a 2-fold increase of apoptotic cells has been detected between WT and *SIRT1* KO cells after H_2O_2 treatment. These results indicate that SIRT1 limits the amount of PAR synthesis possibly by competing with PARP1 for the consumption of NAD^+ (Kolthur-seetharam et al., 2006). Additionally SIRT1 directly modulates PARP1 activity by deacetylating the protein *in vitro* and *in vivo* (Rajamohan et al., 2009). Moreover, SIRT1 overexpression reduces the amount of dead cells in response to MNNG treatment (Rajamohan et al., 2009).

Overall these findings describe PARP1 as a multifunctional protein and its role is not only related to DNA repair. Indeed, PARP1 acts more as DNA damage stress-sensor. The biological consequences of PARP1 activation depend on the amount of DNA damage and on the capacity of the DNA repair machinery. Hence, small amount of lesions lead to moderate PARP1 activation in order to prevent the formation of more complicated lesions, such as DSBs, by stimulating the recruitment of DNA repair enzymes and/or protecting the lesions. In the presence of high amounts of lesions, PARP1-dependent synthesis of PAR and consumption of NAD^+ signal the activation of cell death mechanisms, to avoid genomic instability.

1.5.2 DNA damage signalling

In the event that a SSB does not get repaired, it is likely that a DSB arises either via the formation of another SSB in close proximity or by an encounter between the DNA replication/transcription machinery and the unrepaired lesions (Kuzminov, 2001). Endogenous DSBs do not occur very frequently, however, this type of lesions is very dangerous because of the high possibility of genomic instability. Aside from the proteins involved in directly sensing and repairing these lesions (NHEJ and HR repair pathways), a complicated cascade of signalling is mediated by ATM and the ataxia telangiectasia and Rad3-related (ATR) protein kinases (Maréchal and Zou, 2013). The aim of these powerful transducers is to: i) enhance the efficiency of DSB repair pathways (NHEJ and HR), ii)

promote cell cycle delay via checkpoint activation (Jackson and Bartek, 2009; Maréchal and Zou, 2013).

ATM and ATR are both part of the phosphoinositide 3-kinase (PI3K) family and they have a similar domain organisation. Even though there are similarities between these two proteins, the mechanisms of recruitment and of activation are different. For instance, the activation of ATM and ATR is dependent on the recognition of the DNA damage by different sensing proteins. The MRE11-RAD50-NBS1 (MRN) complex has been reported to induce the activation of ATM (Lee and Paull, 2005; Uziel et al., 2003), while the replication protein A (RPA) mediates the activation of ATR (Zou and Elledge, 2003).

The MRN complex detects double-strand (ds) DNA ends *in vitro* and is required for the localisation of ATM at the site of damage (Lee and Paull, 2005; Uziel et al., 2003). ATM autophosphorylates and is activated following an interaction with the MRN complex, although the mechanism of activation by MRN is not clear (Bakkenist and Kastan, 2003). Consequently, a cascade of phosphorylation occurs to identify the DNA region that has to be repaired. Indeed, ATM phosphorylates H2AX, thus flagging the chromatin and stimulating the recruitment of proteins involved in the repair (Burma et al., 2001). Alternatively to ATM, ATR localises at the site of damage through the interaction with RPA, a protein that interacts with single-strand (ss) DNA during DNA replication. Indeed, ATR is induced during S-phase when a replication fork is stalled by the presence of DSBs (Zou and Elledge, 2003). Thus, ATR seems to have a role during DNA replication in monitoring the status of replication forks (Flynn and Zou, 2011).

One of the consequences of the activation of ATM/ATR is cell cycle arrest, thus enabling DNA repair to occur (**figure 1.3**). ATR and ATM phosphorylate and activate checkpoint kinases 1 (CHK1) and 2 (CHK2) proteins, which are responsible for regulating the activity of several downstream effectors which delay the cell cycle (Liu et al., 2000; Matsuoka et al., 1998). CHK2 has been reported to be mainly involved in the G1 arrest, whereas CHK1 is responsible for the activation of the intra-S and G2/M arrest.

Cell cycle progression is regulated by cyclin-dependent kinases (CDKs) which are activated by the interaction with phase-specific cyclins. CDK inhibition occurs via phosphorylation at Tyr sites by WEE1 kinase and by the direct interaction with the CDK inhibitor (CKI) proteins (Zilfou and Lowe, 2009). G1 arrest is stimulated by the direct phosphorylation of p53 by CHK2. The phosphorylation of p53 at serine (Ser) 20 prevents the degradation of the protein by the E3 ubiquitin ligase MDM2, thus promoting accumulation of p53. P53 promotes G1 arrest stimulating the expression of the *CDKN1A* gene, which encodes for the CKI p21. P21 blocks the action of the CDK2-cyclin E complex, thus preventing the G1/S transition until the damage is repaired (Bartek and Lukas, 2003).

Inhibition of the cell division cycle 25 (CDC25) phosphatases is necessary for the activation of the intra-S and G2/M checkpoints. CDC25 proteins promote cell-cycle progression by removing the WEE1-dependent inhibitory phosphorylation situated on the CDK complexes. Both CHK1 and CHK2 are responsible for the phosphorylation of CDC25C, which stimulates its sequestration by 14-3-3 proteins, thus promoting G2/M cell cycle arrest (Bartek & Lukas, 2003; Matsuoka et al.,1998b). CDC25A phosphorylation by CHK1 promotes the interaction with the E3 ubiquitin ligase Skp/Cullin/F-box (SCF) protein complex, thus increasing CDC25A proteasome degradation and consequently promoting the intra-S phase checkpoint activation (Busino et al., 2003; Falck, Mailand et al., 2001). The p53-p21 axis is also responsible for the inhibition of the activity of CDK1-cyclin B1, thus preventing the G2/M transition (Agarwal et al., 1995; Bunz et al., 1998).

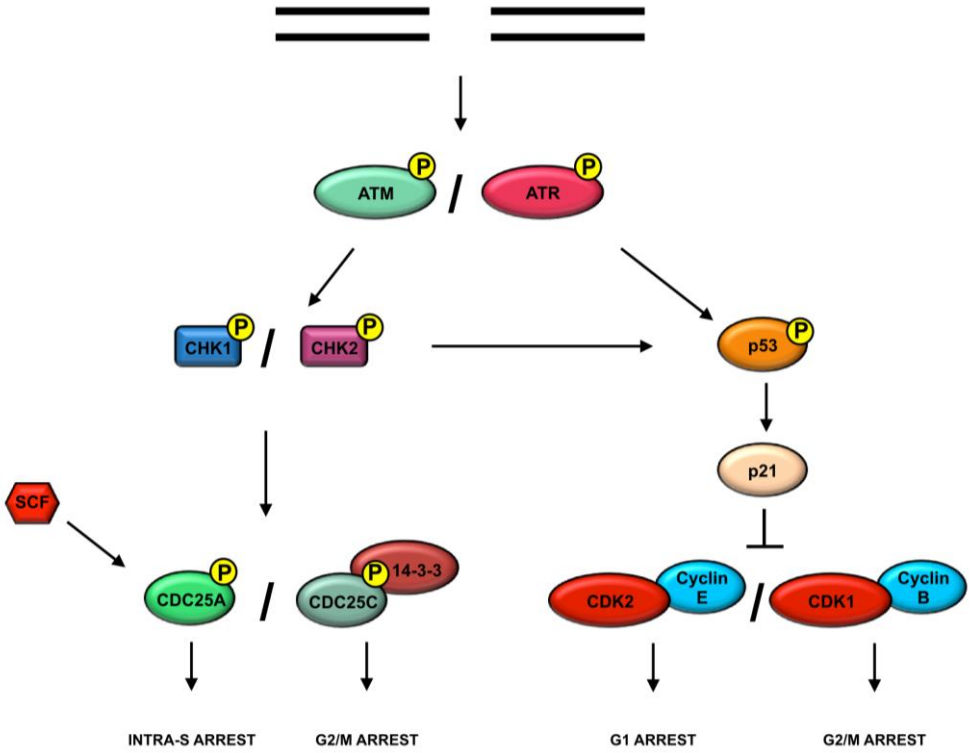

Figure 1.3: Overview of the ATM/ATR checkpoint regulation.
DSB formation leads to the activation of ATM and ATR kinases. Both kinases can autophosphorylate themselves and then phosphorylate their downstream targets. CHK1 and CHK2 are directly phosphorylated by ATM/ATR, thus becoming active. CHK1 phosphorylates CDC25A, thus allowing the E3 ubiquitin ligase SCF to promote CDC25A degradation and the activation of the intra-S checkpoint. Both CHK1 and CHK2 can phosphorylate CDC25C, promoting the sequestration of CDC25C by 14-3-3, thus activating G2/M arrest. P53 is phosphorylated directly by ATM/ATR and by CHK1/CHK2. Phosphorylation of p53 promotes stabilisation of the protein, thus leading to an increase in p21 levels and therefore stimulating either G1 or G2/M arrest.

1.5.3 p53, “the guardian of the genome”

p53 activation in response to DNA damage has been extensively studied and it is essential in preserving genomic stability (Lane, 1992). In fact, p53 induces anti-proliferative and cell death mechanisms, thus preserving the integrity of the genome and avoiding accumulation of mutations that could lead to cancer development. Indeed, the loss of *TP53* gene through mutation or deletion has been found in 50% of tumours, highlighting the importance of the function of the encoded protein (Hollstein et al., 1991). The *TP53* gene encodes for a 53 kDa transcription factor which promotes or suppresses different panels of genes, thus inducing cell cycle arrest, apoptosis or senescence (Meek, 2009; Zilfou and Lowe, 2009).

The central role for p53 in promoting cell cycle arrest has been outlined in the previous section. p53 stimulates the expression of *CDKN1A* gene (which encodes for p21) and the transcription of *YWHAG* gene (which encodes for 14-3-3 protein) and supresses the expression of *CDC25C* gene in response to DNA damage (Clair and Manfredi, 2006; Hermeking et al., 1997).

P53 has also been found to promote apoptosis by stimulating the transcription of pro-apoptotic genes, such as *PUMA* and *BAX* (Koutsodontis et al., 2005; Riley et al., 2008; Thornborrow & Manfredi, 2001). Additionally to a transcriptional-related contribution in activating apoptosis, p53 has also been reported to translocate to the cytoplasm and to stimulate the release of pro-apoptotic proteins, such as BAX and BAK, from the mitochondrial membrane (Moll et al., 2005).

Since the activation of p53 can stimulate both cell cycle arrest and apoptosis, a mechanism for distinguishing between these cellular responses has been investigated. Although, the mechanism is not well understood, it has been speculated that it might depend on the cellular context, on the pattern of PTMs and on the affinity of p53 for the specific promoter (**figure 1.4**). For instance, ATM phosphorylation of p53 on multiple Ser residues as well as CHK2 kinase phosphorylation on Ser 15 and Ser 20 leads to p53-

dependent cell cycle arrest (Carvajal and Manfredi, 2013). The amount of DNA damage also determines the p53 response. Indeed, a high level of DNA damage induces phosphorylation on Ser 46 by p38 mitogen-activated protein kinase (MAPK) and homeodomain-interacting protein kinase 2 (HIPK2), stimulating the transcription of apoptosis-related genes (Bulavin et al., 1999; Hofmann et al., 2002). Another factor contributing to the choice between cell cycle arrest and apoptosis is the affinity of p53 for the DNA-binding sites. For instance, it shows a high-affinity for the promoters of cell cycle arrest-related genes, while a low-affinity for the apoptotic-related genes (Resnick-Silverman et al., 1998). Hence, the cooperation between upstream signalling and the different affinities for DNA binding sites gives a possible explanation on how p53 can trigger different cellular responses to DNA damage (Carvajal and Manfredi, 2013).

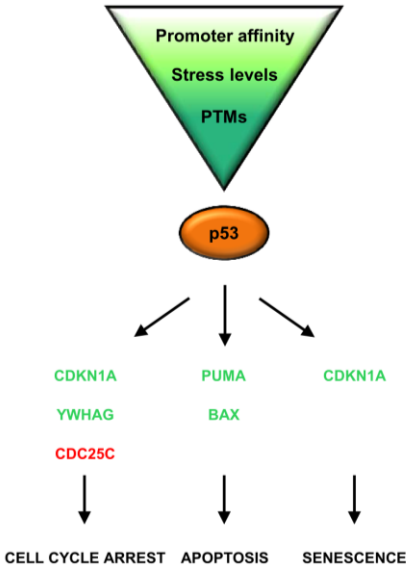

Figure 1.4: p53 response.
p53 response depends on the different p53-promoter affinities, on the level of cellular stress and on PTMs. Depending on these factors, p53 can promote cell cycle arrest, apoptosis and senescence. Examples of genes activated by p53 in response to different stimuli are represented in the above figure (the green colour represents positively activated genes, while red represents repressed genes).

1.5.4 DNA damage accumulation and cellular senescence

Cell cycle arrest and apoptosis are not the only cellular responses to DNA damage coordinated by p53. Indeed, cells can also undergo senescence when DNA damage is accumulated (Campisi & d'Adda di Fagagna, 2007; Collado et al., 2007).

Generally speaking, senescent cells are unable to proliferate and to re-enter the cell cycle, despite stimulation by growth factors in the medium (Hayflick, 1965). They are also resistant to apoptosis stimuli (Hampel et al., 2004) and the pattern of gene expression is altered. For instance, the expression of genes required for cell cycle progression such as, cyclins and PCNA, has been found to be repressed (Pang and Chen, 1994). Several senescence markers have been identified in order to characterise and identify senescent cells *in vivo*. The expression of β-galactosidase, encoded by the *GLB1* gene, is the most employed marker used for distinguishing between normal and senescent cells (Dimri et al., 1995). More interestingly, another marker of senescent cells is the presence of unrepaired DNA damage flagged by the persistence of γH2AX foci (Rodier et al., 2009; Sedelnikova et al., 2004).

Indeed, senescence can be triggered in response to several DNA damage-related cellular stresses such as telomere shortening, accumulation of DNA damage and elevated oncogene activation (Campisi, 2013). The common factor between them is prolonged DDR. Shortening of the telomeres and an accumulation of unrepaired DNA damage are signalled by ATM/ATR and their downstream partners CHK2/CHK1. The inhibition or depletion of these proteins has been reported to reduce the efficiency of activating cellular senescence mechanisms (d'Adda di Fagagna et al., 2003; Mallette et al., 2007a). Oncogene-stress has also been found to activate DDR. Indeed, hyperactivation of oncogenes increases the proliferation rate, thus enhancing the formation of replicative-associated DNA damage and consequently leading to activation of DDR (Bartkova et al., 2006; Mallette et al., 2007). Overexpression of activated RAS and E2F1 has been

reported to increase the occurrence of DNA damage following replication-stress, thus inducing senescence (Goberdhan et al., 2000; Serrano et al., 1997).

The p16-RB and the p53-p21 pathways have been identified as the molecular effectors for activation of senescence (Campisi and d'Adda di Fagagna, 2007; Collado et al., 2007). The p16-RB pathway has been shown to be activated in response to oncogenic-stress (Campisi and d'Adda di Fagagna, 2007; Collado et al., 2007). P16 is part of the CKI family which recognises and inhibits the CDK4 and CDK6 proteins, which are responsible for the G1/S transition. Inhibition of these kinases maintains the RB tumour suppressor protein in a hypophosphorylate status and bound to the E2F1 transcription factor. In this case, E2F1 cannot bind to the DNA and consequently abolishes the E2F1-dependent expression of genes involved in promoting cell cycle progression, such as cyclin E (Sherr and McCormick, 2002). *INK4*, which encodes for the p16 protein, and *ARF* gene expression are stimulated by RAS hyperactivation (Barradas et al., 2009; Lin and Lowe, 2001; Ohtani et al., 2001). Elevated levels of both p16 and ARF have been found in senescent cells (Krishnamurthy et al., 2004). ARF targets the E3 ubiquitin ligase MDM2, thus inhibiting its function and consequently allowing accumulation of p53 (Llanos et al., 2001; Zhang et al., 1998).

In contrast to the p16-RB axis, the p53-p21 pathway activation is also directly stimulated by DDR, via the ATM/ATR pathway (Bartek and Lukas, 2003). p53 stabilisation is essential for triggering senescence through the expression of p21 (Jackson and Pereira-Smith, 2006). As described in the previous section, p21 targets CDK-cyclin complexes, thus contributing in promoting the permanent cell cycle arrest (Brown et al., 1997). Additionally, p21 can directly contribute in establishing senescence by mediating p53-dependent repression of genes involved in cell cycle progression (Abbas and Dutta, 2009).

Therefore, at the cellular level, senescence is another cellular response employed in response to DNA damage. The main purpose for activating senescence is to avoid

abnormal proliferation and cancer development (Campisi, 2013). Indeed, *INK4*, *RB*, *TP53* and *ARF* genes have been found to be mutated or deleted in several cancers, confirming to have a crucial role in preventing the onset of cancer. On the other hand, senescence promotes aging tissue, thus reducing the pool of cells necessary to sustain tissue renewal (Campisi and d'Adda di Fagagna, 2007; Collado et al., 2007). Therefore, senescence has been selected during evolution as a beneficial mechanism which promotes the survival of young organisms, but it has negative consequences in older organisms – the "antagonistic pleiotropic" hypothesis on aging (Kirkwood and Austad, 2000).

1.6 The tumour suppressor gene *ARF*

1.6.1 The *INK4-ARF* locus

The ARF protein (also known as p14 in human and p19 in mouse) was identified as an alternative transcript for the *INK4 l*ocus which encodes for CKI p16 (Kamijo et al., 1997; Stott et al., 1998). The transcription of these two proteins is under the control of two separated promoters, thus allowing independent activation. The two mRNA transcripts share exon 2 and exon 3, but they have two separate exons 1, exon 1β encodes for ARF, exon 1α encodes for p16. The homology between ARF and p16 proteins is very low, explaining a difference in function. However, the primary sequence of ARF is highly conserved between species, suggesting an essential role for this protein (Gil and Peters, 2006).

1.6.2 ARF protein structure

ARF mRNA translation leads to a 14 kDa protein with a primary sequence of 132 amino acids. The amino acid composition is very unusual with more than 20% arginine (Arg) residues, therefore leading to a highly basic protein. Considering its primary sequence, ARF has to bind to other proteins to stabilise its charge. Indeed, ARF is defined as a "sticky" protein and it has been reported to form complexes with several proteins, thus affecting their biological functions (Sherr, 2006). The N-terminal domain, encoded by the exon 1β has been reported to be important for the binding of ARF to its targets, such as MDM2 (Honda and Yasuda, 1999; Pomerantz et al., 1998; Stott et al., 1998) and ARF-BP1/MULE (Chen et al., 2005), while the C-terminus seems to be essential for ARF localisation in the nucleolus (Zhang and Xiong, 1999).

Regarding the biological function of ARF, no catalytic domain has yet been identified, thus leading to the conclusion that its function merely depends on the binding with other proteins. Thus, the level of the protein and its localisation regulate the interaction with ARF binding targets. Similarly, PTMs have not been found, even though, there are

numerous potential sites for phosphorylation in the ARF sequence. Interestingly, ARF does not have any Lys residues, suggesting that acetylation and ubiquitination are also impaired. However, the N-terminal domain has been reported to be ubiquitinated probably through the N-terminal amino group (Kuo et al., 2004). Recently, the E3 ubiquitin ligase ULF (Chen et al., 2010) and SIVA1 (Wang et al., 2013) have been shown to ubiquitinate ARF, thus regulating the protein level.

1.6.3 ARF-dependent regulation of p53

One of the major consequences of ARF induction is the accumulation of the p53 protein, through the interaction and ultimately the inhibition of the E3 ubiquitin ligase MDM2 activity. ARF has been found to interact with MDM2 through its N-terminal region in order to inhibit the ubiquitinatation of p53 (Honda and Yasuda, 1999; Pomerantz et al., 1998; Stott et al., 1998). It has been shown that the mechanism of action of ARF on MDM2 occurs through the inhibition of the activity of the E3 ubiquitin ligase protein (Llanos et al., 2001).

MDM2 is not the only E3 ubiquitin ligase targeted by ARF. In fact, ARF can also regulate the activity of another E3 ubiquitin ligase protein, ARF-BP1/MULE. It has been shown that ARF induction leads to the inhibition of the ubiquitination activity of ARF-BP1/MULE on p53 (Chen et al., 2005). Again, the interaction between ARF and ARF-BP1/MULE occurs through the N-terminus, confirming that the N-terminal domain is fundamental for ARF function. A negative feedback loop between p53 and ARF has also been identified. P53 itself regulates the level of ARF expression through its transcriptional activity. In fact in cells lacking p53, ARF protein levels are elevated and the re-expression of p53 restores ARF levels (Kamijo et al., 1998; Stott et al., 1998; Zeng et al., 2011). Therefore, there is a negative feedback loop between ARF and p53: ARF stabilizes p53 and p53 suppresses the expression of the *ARF* gene.

Since ARF regulates p53, ARF induction has been revealed to modulate p53-dependent physiological functions (Sherr, 2006). For instance, ARF overexpression leads to cell

cycle arrest in p53-proficient HCT116 cells (Weber et al., 2002), whereas it does not affect the cell cycle in TP*53* and *CDKN1A* KO HCT116 cells (Hemmati et al., 2005). These results show that ARF-dependent cell cycle arrest requires the presence of a functional p53. Moreover, it has been shown that in response to IR treatment, an increase in ARF correlates with p53 induction in MEFs, suggesting that ARF has, indeed, a role in regulating the amount of p53 in response to DNA damage (Khan et al., 2004). Even though an ARF-dependent cell cycle arrest in the G1 phase has been shown to require p53, several studies report the ability of ARF to stimulate a G2 arrest in a p53-independent manner, although the molecular mechanism has not been clarified (Eymin et al., 2003; Hemmati et al., 2008; Normand et al., 2005).

ARF expression has also been shown to trigger apoptosis in both a p53-dependent (Hemmati et al., 2002; Radfar et al., 1998; Zindy et al., 1998) and a p53-independent manner (Eymin et al., 2003; Hemmati et al., 2002; Milojkovic et al., 2013), thus adding another physiological role for the ARF tumour suppressor protein. Recently, it has been reported that in response to DNA damage ARF is required to trigger apoptosis in a p53-dependent manner (Chen et al., 2013), implying that ARF is responsible for triggering cell death in response to DNA lesions.

1.6.4 Oncogenic-signalling induces *ARF* expression

Aberrant mitogenic signals have been found to increase ARF expression, thus blocking the cell cycle and eventually promoting either apoptosis or senescence via p53 accumulation. The induction of ARF has been linked to oncogenic hyperactivation, such as overexpression of Myc, E2F1 and Ras (Lomazzi et al., 2002; Palmero et al., 1998; Zindy et al., 1998). E2F1 has been reported to directly stimulate *ARF* mRNA transcription (Komori et al., 2005), thus binding the promoter in response to oncogenic-stress (Berkovich et al., 2003). Recently, it has been suggested that the induction of ARF in response to E2F1 and MYC overexpression may also occur via a transcription-independent mechanism. Indeed, the overexpression of a MYC mutant lacking the DBD

has been shown to impair the interaction between ARF and the E3 ubiquitin ligase ULF, thus leading to ARF accumulation in the human H1299 cancer cell line (Chen et al., 2010). Another group has shown that the interaction between ARF and the novel binding factor N-Myc interactor (NMI) in response to E2F1 and MYC overexpression leads to an increase in ARF protein levels, disrupting the interaction with ULF (Li et al., 2012).

Regarding the induction of ARF by RAS oncogene, there is discrepancy between the findings in mice which show that ARF is induced by the overexpression of activated Ras (Ferbeyre et al., 2002; Ha et al., 2007; Lin and Lowe, 2001), and the evidence from humans which show an induction of p16, but not of ARF (Wei et al., 2001). Indeed, overexpression of activated Ras leads to an induction in Arf, stimulating the synthesis of *Arf* mRNA levels through the activation of the histone demethylase protein Jmdm3 in MEFs. In the same study, it has been shown that RAS overexpression leads only to an increase of p16 and not of ARF levels in human diploid fibroblasts (HDFs) (Barradas et al., 2009). Furthermore, it has been recently reported that Ras-dependent induction of ARF also occurs in a transcriptional-independent fashion in MEFs. The molecular mechanism described requires the disruption of the interaction between Arf and Ulf by the tumour necrosis factor receptor (TNFR)-associated death domain (TRADD) protein (Chio et al., 2012).

1.6.5 ARF role in the DDR

A possible role for ARF in DDR is still controversial and unclear. In earlier studies, ARF has been reported to be induced in response to hyperproliferative stimuli due to aberrant oncogenic activation. However, the fact that oncogenic-stress activates DDR and that ARF regulates p53 levels suggests that ARF might have a role in DDR (Evan and d'Adda di Fagagna, 2009). Several studies have found a correlation between DNA damage and ARF activation. Lee and colleagues have shown that after UV irradiation, ARF protein delocalizes from the nucleoli to the nucleoplasm in DU145 cells. They have also shown that after UV irradiation there is an increase in the interaction between MDM2-ARF (Lee et

al., 2005). Moreover, ARF levels have been reported to be upregulated in response to IR exposure in MEFs (Khan et al., 2004) and to MMS treatment in human H358 and H1299 cells (Eymin et al., 2006; Li et al., 2012). Also, ARF has been recently reported to be transcriptionally induced by replicative stress caused by hydroxyurea (HU) treatment in MEFs (Monasor et al., 2013).

Furthermore, growing evidence has linked ARF protein levels to ATM (Bailey et al., 2008; Grønbaek et al., 2002; Li et al., 2004; Velimezi et al., 2013) and ATR kinases (Carlos et al., 2013; Eymin et al., 2006; Rocha et al., 2005). Li and colleagues have shown that the ectopic induction of ARF in NIH 3T3 cells enhanced ATM activity. Furthermore, ARF overexpressing cells show ATM localized nuclear foci (Li et al., 2004). Eymin and colleagues have also shown that in response to DNA damage, ARF is able to activate the ATM pathway in p53-deficient cells and to trigger apoptosis. Furthermore, the use of RNA interference (RNAi) against ARF prevents the activation of ATM (Eymin et al., 2006). Recently, a functional interplay between ARF and ATM has been suggested. The depletion and inhibition of ATM has been shown to upregulate ARF levels in the H1299 and HeLa cancer cell lines, indicating that when ATM function is abrogated, the ARF tumour suppressor protein is induced to avoid tumour development (Velimezi et al., 2013). Conversely, another study has shown that in response to a HR-deficiency (Brca2-deletion), ARF is upregulated and the ATM (and ATR) proteins are required for ARF induction (Carlos et al., 2013). Thus, the relationship between ATM activation and ARF is still unclear, but these recent findings suggest a role for ARF in the DDR.

Regarding ATR and ARF interplay, it has been reported by Rocha and colleagues that ARF interacts with ATR and activates the protein. Moreover, this interaction is responsible for the localization of ATR to the nucleolus. Although ATR is related to DDR, they propose that the interaction between ATR and ARF proteins is not triggered by DNA damage (Rocha et al., 2005). However, in the context of the DNA damage signalling, ATR activity

has also been shown to be indispensable for ARF upregulation in response to persistent DNA damage (Carlos et al., 2013).

Another study has recently reported a link between ARF, ARF-BP1/MULE and DNA repair. Following DNA damage ARF is able to inhibit the ubiquitination activity of ARF-BP1, allowing the accumulation of POLβ. Furthermore, ARF-depleted cells show slower DNA repair kinetics due to a decrease in the level of POLβ (Parsons et al., 2009).

Since it has been speculated that ARF is involved in DDR through the activation of ATM/ATR pathways, it is important to outline that the activation of these pathways and the biological outcomes do not strictly require ARF. For instance, the accumulation of p53 occurs independently of ARF both *in vivo* and in mouse models. Indeed, IR has been shown to induce p53 in ARF-null tumours, demonstrating that exogenous DNA damage can induce p53 in the absence of ARF (Kamijo et al., 1999a).

1.6.6 ARF role in senescence

Senescence is triggered in response to aberrant oncogenic signals through the activation of the DDR. Furthermore, unrepaired DNA damage, independently from oncogenic-stress, also leads to DDR activation and therefore to senescence, as shown by the findings of persistent DNA damage foci in senescent cells.

As discussed, the biological relevance of inducing ARF mainly depends on p53 downstream functions. Indeed, ARF has been reported to be required for triggering cell cycle arrest and apoptosis. Moreover, an elevated expression of ARF has been found to correlate with aging tissue (Collado et al., 2007). Indeed, it has been shown that there is a ~ 3.5-fold increase in Arf expression when comparing young and old mouse tissues, such as lung, liver and intestine. These results suggest that Arf upregulation occurs with aging (Krishnamurthy et al., 2004). Moreover, it has been shown that overexpression of activated Ras leads to senescence in a Arf-dependent manner in MEFs (Barradas et al., 2009; Chio et al., 2012; Ferbeyre et al., 2002) and in mouse melanocytes (Ha et al., 2007). In other studies, it has been shown that the induction of human ARF leads to

senescence, in a p53-dependent manner, in mouse epidermis (Tokarsky-Amiel et al., 2013) and in human WI-38 fibroblasts (Dimri et al., 2000; Wei et al., 2001). Moreover, Arf has been shown to be required for inducing senescence in response to HR-deficiency (Brca2 depletion) in MEFs, thus suggesting that Arf is important for triggering senescence in a DDR-activated context.

Although the molecular mechanism of ARF upregulation after DNA damage is still unclear, those results suggest that ARF induction might be linked to chronic activation of DDR as a consequence of accumulation of unrepaired DNA damage.

1.6.7 ARF in cancer progression

KO of the *Arf* gene in mice revealed that ARF is dispensable for development. However, Arf-null mice have been shown to develop spontaneous tumours by two months, thus revealing a fundamental role for Arf in preventing tumour formation *in vivo* (Kamijo et al., 1999b). It has been reported that 28 out of 39 Arf-null mice died within 1 year of birth as a consequence of tumour formation. Without any additional treatment, 43 of the Arf-null mice develop sarcomas, 29% develop lymphoma and interestingly, 3 mice develop gliomas which rarely occur in mice (Kamijo et al., 1999b). They have also shown that Arf-heterozygote animals develop tumours due to the loss of function of the second allele, through deletion or promoter methylation at the WT gene (Kamijo et al., 1999b). Immunostaining of papilloma derived from Arf-null mice has revealed an increase in γH2AX and a dramatic decrease in p53 levels, showing that the ARF protein is important in the regulation of p53 basal levels *in vivo* (Bailey et al., 2008). However, another study has shown that Arf-null mice still exhibit functional p53 accumulation after IR treatment, despite Arf being depleted (Kamijo et al., 1999a).

Several studies have assessed the ARF status in human cancers by either analysing mutations or deletions of the specific *ARF* 1β exon or by verifying promoter methylation (Ozenne et al., 2010). Methylation of the *ARF* promoter has been found in colorectal, bladder, oral and gastric carcinoma (Ozenne et al., 2010). Analysis of the level of *ARF*

mRNA has revealed that low levels correlate with lung and breast cancer (Ozenne et al., 2010). Analysis of 100 primary breast cancer samples has revealed that 26% have very low levels of *ARF* mRNA, whereas 17% expressed elevated levels of *ARF* mRNA (Silva et al., 2001). Of the 26% with decreased amount of *ARF* mRNA levels, 50% had an aberrant promoter hypermethylation, while in 37% of the samples the gene is either deleted in both the alleles or shows a loss of heterozygosis (LOH) (Silva et al., 2001). Homozygote deletion (HD) and LOH of the *ARF* gene have also been found in lung, hepatocellular and prostate carcinoma (Ozenne et al., 2010). Moreover, three germ line mutations have been found in patients affected by melanoma; these mutations generate an aberrant *ARF* mRNA transcript due to defects during the splicing process (Harland et al., 2005).

In conclusion, the expression of the *ARF* tumour suppressor gene is important to avoid tumour development since ARF has a fundamental role in regulating p53 levels, thus contributing to the activation of different cellular responses, such as cell cycle delay or senescence. Moreover, several studies have suggested a link between ARF induction and DNA damage. However, whether ARF is induced in response to DNA damage is still not clear.

1.7 Aims of the study

The aims of this study are:

1. To investigate whether the tumour suppressor gene *ARF* is induced in response to DNA damage.
2. To investigate the molecular mechanism of ARF induction in order to characterise the pathway that regulates ARF levels in response to DNA damage.
3. To characterise the physiological relevance of ARF induction in response to DNA damage.

2. Materials and Methods

2.1 Materials

2.1.1 Reagents

The materials and reagents used in this thesis are listed in **Appendix I**.

2.1.2 Plasmid

Human XRCC1 cDNA was previously cloned into the pCMV 3Tag3a mammalian vector containing C-terminal 3x Flag-tag (Agilent Technologies) in Grigory Dianov's lab. The plasmid was verified by sequencing.

2.1.3 Human cell lines

The HeLa human cervical cancer cell line was purchased from ATCC (American Type Culture Collection) and TIG-1 primary human foetal lung fibroblasts were obtained from Coriell Cell Repositories.

2.2 Cell culture, cell treatments and cell transfection

2.2.1 Basal cell culture handling

HeLa and TIG-1 cells were cultured in Dulbecco modified Eagle's medium (DMEM) supplemented with 10% and 15% foetal bovine serum (FBS), respectively. Cells were grown at 37°C in 5% CO_2 air in a humidified air incubator (Thermoscientific). After reaching 80-90% confluence, cells were split using a Trypsin-EDTA solution (0.025% trypsin, 0.01% EDTA) and re-seeded at either a 1:5 or 1:10 ratio.

When necessary, the cell number was determined using a Countess® Automated Cell Counter system (Invitrogen) according to the manufacturer's protocol. Briefly, cells were detached using Trypsin-EDTA solution, diluted 1:1 in trypan blue and counted.

For harvesting, cells were scraped into phosphate buffer saline (PBS) and pelleted by centrifugation at 350 rcf for 5 min at 4°C. Cell pellets were re-suspended, centrifuged at 250 rcf for 5 min at 4°C and pellets stored at -80°C.

2.2.2 Cell treatments

After counting, 5 X 10^5 cells were seeded in 10 cm^2 dishes and treated after 2 days. Following treatment, cells were harvested as described in **section 2.2.1** at different time points. Solutions for treatments were prepared fresh in full growth medium. For H_2O_2 treatment, a 8.8 M stock solution of H_2O_2 was diluted in medium to a final concentration of 150 µM (Fisher et al., 2007; Woodhouse et al., 2008). Cells were irradiated using a GSR-D1 137Cs γ-irradiator (RPS Services Limited) at a dose rate of 1.5 Gy/min (Godon et al., 2008). A 100 mM stock solution of NU1025 PARP1 inhibitor was prepared in dimethylsulfoxide (DMSO); the inhibitor was further used at a working concentration of 100-200 µM (Bowman et al., 1998; Sabisz et al., 2010; Woodhouse et al., 2008). FK866 was used at a 10-30 nM working concentration, prepared from a 1 mM stock solution in DMSO (Caito et al., 2010; Cantó et al., 2009). Cells were treated with cycloheximide

(CHX) at a concentration of 50 µg/ml (Korner, 1966) prepared from a 50 mg/ml stock solution.

2.2.3 Cell transfection

For overexpression studies, 5 x 10^5 cells were seeded in 10 cm^2 dishes and transfected after 24-36 h when 60-80% confluent. For each dish, a transfection mixture (1 mL) containing either 10 µl of lipofectamine transfection reagent alone or in combination with the indicated amount of plasmid (150-250 pmol) was prepared in FBS-free medium. Complete medium (5 ml) and transfection mixture were then mixed and added to the dishes. Cells were harvested according to **section 2.2.1** 18-24 h after transfection.

For knockdown studies RNA interference (RNAi) technology was used. Cells were counted, 2 x 10^5 cells were seeded in 10 cm^2 dishes and transfected at 30-50% confluence, 24-36 h after seeding. For each plate, a transfection mixture (1 ml) containing either 10 µl of lipofectamine alone or in combination with RNAi (40-80 nM RNAi final concentration) was prepared. Complete medium (5 ml) was combined with 1 ml of the transfection mixture and added to all dishes. Fresh medium was replaced 6 h after incubation and cells were harvested 24-72 h after transfection as described in **section 2.2.1**. The list of RNAi sequences used in this work is given in **table 2.1**.

For XRCC1 complementation studies, 2 x 10^5 cells were seeded in 10 cm^2 dishes for 24 h and XRCC1 knockdown was performed using RNAi (40-80 nM) as described above. Following 36 h of RNAi transfection, cells were transfected with 250 pmol of RNAi resistant XRCC1, expressing plasmid (XRCC1 RNAi-R), and harvested 24 h post-transfection as described in **section 2.2.1**.

GENE	SEQUENCE	REFERENCE
XRCC1	5'AGGGAAGAGGAAGUUGGAU3'	(Brem and Hall, 2005)
SIRT1	5'GAUGAAGUUGACCUCCUCA3'	(Lee et al., 2011)
p53	5'AAGACUCCAGUGGUAAUCUAC3'	(Zhu et al., 2004)
E2F1	5'CGCUAUGAGACCUCACUGA3'	(Goto et al., 2006)
PARP1	5'AAGAUAGAGCGUGAAGGCGAA3'	(Kameoka et al., 2004)
PARP1_2	5’GGGCAAGCACAGUGUCAAA3’	(Ying et al., 2012)
NAMPT	5'GAGUGUUACUGGCUUACAA3'	(Zhang et al., 2009)
APE1	5'AAUGACAAAGAGGCAGCAGG3'	(Fung and Demple, 2005)
APE1	5'AACCUGCCACACUCAAGAUC3'	(Fung and Demple, 2005)
ARF	5'GAACAUGGUGCGCAGGUUCTT3'	(Eymin et al., 2006)

Table 2.1: RNAi sequences.
RNAi sequences used for knockdown experiments. The chosen sequences have been previously employed in the indicated references.

2.3 Analysis of mRNA levels

2.3.1 Extraction of total RNA

Total RNA extraction was performed at room temperature (RT) according to the manufacturer's protocol (RNA extraction kit, Qiagen). Lysis RLT buffer (350 µl) supplemented with 1% β-mercaptethanol (β-ME) was added to each pellet and drawn through a 1.1 mm diameter needle at least 8-10 times. One volume of 70% ethanol was added to the lysate and mixed by pipetting. The lysate was then transferred to an RNeasy spin column, placed in a collection tube and centrifuged for 15-30 sec at 8000 rcf. The flow-through containing salts, proteins and cellular components was discarded. The pore size of the membrane significantly improves the recovery of the mRNAs since most of the RNAs shorter than 200 nucleotides (nt) in length, including 5S rRNA, 5.8S rRNA and tRNA, were discarded. To remove any remaining impurities and salts, several wash steps were applied. RW1 buffer (700 µl) was added and followed by two washes with 500 µl of RPE buffer. Samples were centrifuged at each wash step for 15-30 sec at 8000 rcf. To elute the RNA, the column was placed into a new 1.5 ml collection tube, 30-50 µl of RNase-free water were added onto the membrane and incubated at RT for 1 min. The columns were then centrifuged for 1 min at 8000 rcf. Following elution, total RNA samples were kept on ice, quantified as described in **section 2.3.2**, aliquoted and stored at -80°C until further processing.

2.3.2 RNA quantification and quality control

RNA quantification was performed using a NanoDrop 1000 (Thermoscientific) at a wavelength of 260 nm (A_{260}).

The quality of the RNA extracted was assessed according to the A_{260}/A_{280} and A_{260}/A_{230} ratios expected to be 1.8-2.0. Additionally, RNA samples were run on a 1% agarose gel in 1X TAE buffer, containing 40 mM Tris-HCl, 20 mM acetic acid, 1 mM EDTA, pH 8.3, and visualised using Sybr green. Prior to electrophoresis samples (1 µg) were prepared in 1X

loading dye (LD) containing 10 mM Tris-HCl pH 7.6, 0.03% bromophenol blue, 0.03% xylene cyanol FF, 60% glycerol and 60 mM EDTA. Samples were subsequently run at 60 V for 90 min. The gel was scanned using an FX molecular imager (Bio-Rad). RNA quality was determined by the 2:1 ratio between the 28S and 18S rRNA subunits.

2.3.3 Reverse transcription reaction

To obtain cDNAs, a retro transcriptase reaction was prepared using Superscript II First Strand Synthesis system (Invitrogen). To ensure the synthesis of cDNA from mRNA, oligo (dT) primers were used. Initially, an individual RNA/primer solution containing 1 µg of total RNA, 0.5 mM of dNTPs, 25 ng/µl of oligo(dT) in RNAse-free water was prepared and incubated at 65°C for 5 min using a thermo cycler (Eppendorf mastercycler personal). For each sample, a reaction master mix containing 1X First strand buffer, 5 mM $MgCl_2$, 10 µM DTT and 2 U/µl of RNaseOUT was prepared, added to the RNA/primer mix and pre-incubated for 2 min at 45°C. SuperScript II RT (2.5 U/µl) was added to each sample and incubated for 50 min at 45°C. To inactivate the SuperScript II RT enzyme, the samples were incubated at 70°C for 15 min and chilled on ice. Finally, 2 U/µl of RNase H enzyme was added following incubation at 37°C for 20 min. cDNA solutions were stored at -20°C until further processing.

2.3.4 Quantitative polymerase chain reaction (qPCR)

Roche software was used to design 18-21 mer oligonucleotides with a melting temperature (Tm) of 60 °C which produce 50-100 nt amplicons (Roche, 1996). The list of oligonucleotides is depicted in **table 2.2.** cDNAs of the control samples were used to optimise the concentration of both primers and cDNA. To optimise qPCR conditions, primer concentrations within a range of 40-80 nM were tested in combination with 1-10 ng of cDNA. Concentrations giving Ct values between 20-30 were chosen. For analysis of *ARF* and *p16* mRNA levels, 1 µM ARF, p16 primers and 10 ng of template were used, whereas 2 µM GAPDH primers in combination with 1 ng of template were employed to assess *GAPDH* mRNA levels.

Each reaction contained a mix of optimised amounts of both primers and cDNAs, 1 X ABsolute Blue SYBR Green ROX solution (Thermo-Start™ DNA Polymerase, 3 mM $MgCl_2$, dNTPs, SYBR® Green I fluorescent dye), and DEPC-treated H_2O to final volume of 25 µl. Reactions were performed in triplicate.

Reactions were run using a 7500 fast real-time PCR system (Applied Biosystem) using the following conditions: 15 min at 95 °C, following 40 cycles of 15 sec at 95 °C, 30 sec at 60 °C and 30 sec at 72 °C. A melting curve stage was added to check the PCR products obtained and the possible presence of unspecific products using the following conditions: 95°C 15 sec, 60°C 1 min, 95°C 30 sec, 60°C 15 s.

The $2^{\Delta\Delta Ct}$ method was used to calculate the fold change (FC) in gene expression between lipofectamine (L) and knockdown (KD) samples. Firstly, ΔCt for both L ($\Delta Ct_{(L)}$) and KD ($\Delta Ct_{(KD)}$) samples were calculated by normalising the Ct values of the target gene ($Ct_{(t)}$) against the Ct values of the housekeeping gene ($Ct_{(h)}$) as shown in **equation 2.1**.

2.1 $$\Delta Ct = Ct(t) - Ct(h)$$

In order to calculate the FC between L and KD **equation 2.2** was used.

2.2 $$FC = 2^{\Delta Ct(L) - \Delta Ct(KD)}$$

PRIMERS	SEQUENCES
ARF forward primer (qPCR)	5'CTACTGAGGAGCCAGCGTCTA3'
ARF reverse primer (qPCR)	5'CTGCCCATCATCATGACCT3'
P16INK4a forward primer (qPCR)	5'GCTGACTGGCTGGCCACGG3'
P16INK4a reverse primer (qPCR)	5'TCATGACCTGGATCGGCCTCCG3'
GAPDH forward primer (qPCR)	5'AGCCACATCGCTCAGACAC3'
GAPDH reverse primer (qPCR)	5'GCCCAATACGACCAAATCC3'

Table 2.2: qPCR primers.
Sequences of qPCR primers used for analysis of mRNA levels.

2.4 Analysis of protein levels

2.4.1 Preparation of whole cell extracts

Whole cell extracts (WCEs) were prepared according to Tanaka (Tanaka et al., 1992). Packed cell volumes (PCVs) were estimated and 1 volume of Tanaka buffer I (10mM Tris HCl, pH 7.8, 200 mM KCl) was used to re-suspend cells. To lyse the cells 2 volumes of Tanaka buffer II (10mM Tris HCl, pH 7.8, 600 mM KCl, 0.1 mM EDTA, 40% glycerol and 0.2% Nonidet P-40) were added. Both buffers were supplemented with 1mM phenylmethanesulfonylfluoride (PMSF), 1mM N-Ethylmaleimide (NEM), and 1 µg/ml each of aprotinin, pepstatin, chymostatin and leupeptin to prevent protein degradation. Cell lysates were incubated for 30 min at 4°C at 7 rpm on a tube rotor (Labinco) and then centrifuged at 98000 rcf for 20 min at 4°C. The supernatant was collected and stored at -80°C. Protein concentrations were measured using the colorimetric Bradford assay (Bradford, 1976).

2.4.2 Polyacrylamide gel electrophoresis (PAGE)

Both pre-cast tris-glycine 4-20% or in house Tris-HCl 4-16% gradient gels were used for protein electrophoresis. Laemmli Loading buffer, containing 60 mM Tris HCl, pH 6.8, 2% sodium dodecyl sulphate (SDS), 10% glycerol, 5% β-ME and 0.2% bromophenol blue, was added to each protein sample (25-40 µg) and the final volume adjusted to 30 µl with H_2O. Samples were boiled at 95°C for 5 min in a heating block (Eppendorf, thermomixer comfort), prior to loading. Electrophoresis was performed using tris/glycine/SDS 1X running buffer (25 mM Tris-HCl, pH 8.3, 192 mM glycine, 0.1% w/v SDS) at 125 V for 1.5 h.

2.4.3 Western blotting

Immobilon-FL polyvinylidene fluoride (PVDF) membranes were incubated for 15 s in 100% methanol, then rinsed in H_2O and equilibrated in chilled transfer buffer (1X Tris/glycine buffer containing 25 mM Tris-HCl, pH 8.3, 192 mM glycine, supplemented

with 20% Methanol). Sponges, gels and 3MM paper were all equilibrated in transfer buffer and placed with the membrane into the transfer apparatus. Proteins were transferred from the gel to the membrane at 25 V for 1.5 h.

Membranes were rinsed in 1X PBS, incubated for 1 h at RT in Odyssey Blocker buffer (LI-COR) diluted 1:1 in 1X PBS and incubated with primary antibodies overnight at 4°C on a roller (Stovall, low profile roller). The following day membranes were washed in 1X PBS supplemented with 0.1% Tween-20 three times for 5 min and incubated with fluorescently-labelled secondary antibodies for 1 h at RT. Membranes were then rinsed three times in 1X PBS supplemented with 0.1% Tween-20 for 5 min and scanned using the Odyssey system (LI-COR). The full list of antibodies used in this study is depicted in **table 2.3**. Quantification of band intensities was performed using Odyssey Imager software. The values obtained were normalised to the loading control (β-actin).

PROTEIN	PROVIDER	PRODUCT CODE	DILUTION
AcH3K9	Cell Signalling	9649	1:2000
Actin	Abcam	ab6276	1:10000
APE1	custom generated to full length protein		1:10000
ARF	Axxora	BET-A300-340A	1:2000
E2F1	Santa Cruz	C-20/sc-193	1:500
H3 TOT	Cell Signalling	9715	1:1000
NAMPT	Bethyl	A300-779A	1:5000
P21	Cell Signalling	12D1/2947	1:2000
p53	Santa Cruz	sc-126	1:500
PAR	Trevigen	4335-AMC-050	1:2000
PARP1	custom generated to full length protein		1:5000
SIRT1	Santa Cruz	sc-15404	1:500
XRCC1	Neomarkers	MS-1393-P0	1:10000
XRCC1	custom generated to full length protein		1:10000
Mouse 680	Alexa Fluor	A21057	1:10000
Mouse 800	LI-COR	926-32210	1:10000
Rabbit 680	Alexa Fluor	A21109	1:10000
Rabbit 800	LI-COR	926-32211	1:10000

Table 2.3: List of antibodies.
Antibodies and working diluitions.

2.5 NAD^+ quantification assay

Cells were seeded and either treated with the inhibitor FK866 or transfected with NAMPT RNAi as described in **sections 2.2.2** and **2.2.3**. Cells for the assay (2 x 10^5 cells) were collected by trypsinization, whereas remaining cells were harvested for western blotting.

Extraction was performed by adding 400 µl of NADH/NAD^+ extraction buffer (Abcam) to each sample followed by two cycles of freezing (20 min on dry-ice) and thawing (10 min at RT) to lyse the cells. The samples were centrifuged at 425 rcf for 5 min at RT and the supernatant was collected into a new tube. To avoid consumption of NADH/NAD^+ by enzymes, the extracts were filtered through a 10 kDa cut off filter. The extracts were recovered after filtration. For quantification, 200 µl of the extracts were incubated at 60°C for 30 min to decompose NAD^+, while the remainder was used to quantify NADt (NAD^+ and NADH).

The assay was performed in a 96-well flat bottom plate. A standard curve was prepared using 0, 20, 40, 60 and 80 pmols of the NADH standard (Abcam). NADH/NAD extraction buffer was used to make the final volume up to 50 µl in each well. For each sample, 50 µl of the NADH and the NADt extracts were analysed in triplicates into the 96-well plate. Samples were analysed in triplicate in a 96-well plate.

A NAD cycling mix containing 100 µl of NAD cycling buffer (Abcam) and 2 µl of NAD cycling enzyme (Abcam) was added to each well. The plate was incubated for 5 min at RT to allow the conversion from NAD^+ to NADH. NADH developer (Abcam) was added to each well and allowed to react for 1 h at RT. Finally, the absorbance at 450 nm was measured using a plate reader (BMG Labtech, polar star omega).

A standard curve equation was used to determine the amount of both NADt and NADH in pmol/10^6cells. NAD^+ final concentration ([NAD^+]) was then calculated as shown in the **equation 2.3**.

2.3 $$[NAD+] = [NADt] - [NADH]$$

It is important to mention the NADH concentration was determined to be negligible, with optical densities determined to be equivalent to that of a ‘0’ pmol amount of NADH according to the obtained standard curve. To accurately determine the amount of NADH present in the samples, the amount of sample loaded for NADH measurement was twice that of NADt. No change was observed in the measured optical densities, leading to the conclusion the NADH levels present in the sample were considered negligible. It was then reasoned the levels of NAD^+ could be considered equal to the levels of NADt. Furthermore, the NAD^+ levels were normalised to the control samples to minimise the variability in terms of measured optical densities from experiment to experiment.

2.6 Comet assay

The comet assay was performed as previously described (Singh et al., 1988). Briefly, cells were trypsinised, treated or mock-treated in suspension with 150 µM H_2O_2 for 15 min or irradiated (10 Gy) on ice. Cells were embedded on a microscope slide in agarose (Bio-Rad, Hemel Hempstead, UK) and the slides were incubated for various times at 37 °C in a humidified chamber to allow for DNA repair. The slides were subsequently placed in lysis buffer containing 2.5 M NaCl, 100 mM EDTA, 10 mM Tris-HCl pH 10.5, 1% (v/v) DMSO and 1% (v/v) Triton X-100 for 1 h at 4°C.

The slides were then incubated in the dark for 30 min in cold electrophoresis buffer (300 mM NaOH, 1 mM EDTA, 1% (v/v) DMSO, pH 13) to allow the DNA to unwind prior to electrophoresis at 25 V for 25 min. After neutralisation with 0.5 M Tris-HCl (pH 8.0), the slides were stained with SYBR Gold (Invitrogen, Paisley, UK) and analysed using the Komet 5.5 image analysis software (Andor Technology, Belfast, Northern Ireland).

2.7 Plasmid manipulation

2.7.1 Bacterial transformation

XL1-blue competent bacterial cells were purchased from Stratagene and transformed as recommended by the manufacturer. Briefly, 50 µl of bacterial cells were used for each transformation and incubated on ice for 10 min with 24 mM β-ME. pCMV XRCC1 plasmid (10 pmol) was then added and incubated on ice for a further 30 min. Tubes were heat-pulsed at 42°C for 45 sec using a heat block (Eppendorf, thermomixer comfort) and placed again on ice for 2 min. Pre-heated LB medium (500 µl) was added and tubes were incubated in a shaking incubator at 250 rpm for 1 h (New Brunswick scientific, Innova 42). To select for transformants, bacterial cells were plated on 30 µg/ml kanamycin positive LB agar plates and allowed to grow overnight at 37°C in a bacterial incubator (Binder). Single clones were then picked and grown overnight at 37°C in 5 ml of LB medium supplemented with 30 µg/ml kanamycin on a shaker at 250 rpm (New Brunswick scientific, Innova 42).

2.7.2 MiniPrep plasmid purification

Overnight cultures were pelleted at 4000 rcf for 10 min at 4°C and re-suspended in 250 µl of buffer P1 (50 mM Tris HCl, pH 8, 10 mM EDTA) supplemented with RNase A (100 µg/ml final concentration). For lysis, 250 µl of buffer P2 (200 mM NaOH, 1% SDS) was added and mixed by inverting the tubes several times. The reaction was stopped by adding 350 µl of high-salt buffer N3 (4.2 M Gu-HCl, 0.9 potassium acetate, pH 4.8). The tubes were then centrifuged for 10 min at 15000 rcf to precipitate the genomic DNA and debris. Supernatants were then transferred to QIAprep spin columns and centrifuged at 15000 rcf for 1 min. The flow-through was discarded and the columns were washed with 750 µl of PE buffer (10 mM Tris HCl, pH 7.5, 80% ethanol) followed by centrifugation to remove any residual PE buffer. To elute DNA, 30-50 µl of buffer EB (10 mM Tris HCl, pH 8.5) was added to the columns, incubated for 1 min followed by centrifugation for 1 min at 15000 rcf. The purified plasmid was then stored at -20°C.

Plasmid concentration was determined using a Nanodrop 1000 (Thermoscientific) and the quality checked on a 1% agarose gel. Sequence analysis was performed to verify that no mutations were inserted into the plasmid during the amplification/replication process.

2.7.3 MaxiPrep plasmid purification

A maxi prep was performed to amplify the amount of plasmid and to improve the quality of the DNA. Bacterial cells were transformed with the previously selected plasmid; colonies were picked and grown in 5 ml of LB selective medium. The bacterial culture was then diluted 1:100 in 100 ml LB selective medium and grown overnight at 37°C at 200-250 rpm on a shaker (New Brunswick scientific, Innova 44).

Bacterial cultures were centrifuged at 4°C for 15 min at 6000 rcf (Beckman Coulter, Avanti J26 XP) and re-suspended in 10 ml buffer P1 (50 mM Tris HCl, pH 8, 10 mM EDTA), supplemented with RNase. For lysis, 10 ml of buffer P2 (200 mM NaOH, 1% SDS) was added and incubated for 5 min at RT. 10 ml of pre-chilled buffer P3 (3 M potassium acetate, pH 5.5) was added; the contents were transferred to a QIAfilter Maxi Cartridge and incubated for 10 min at RT. The lysate was filtered through a QIAGEN-tip 500 pre-equilibrated in 10 ml of buffer QBT (750 mM NaCl, 50 mM MOPS pH 7.0, 15% isopropanol, 0.15% triton X-100), allowed to drain fully, followed by two washes with 30 ml of buffer QC (1 M NaCl, 50 mM MOPS, pH 7.0, 15% isopropanol). Finally, the DNA was eluted in 15 ml of a high-salt buffer QF (1.25 M NaCl, 50 mM Tris HCl, pH 8.5, 15% isopropanol).

DNA was precipitated with 10.5 ml of 100% isopropanol and samples centrifuged at 4000 rcf for 60 min at 4 °C. The supernatant was removed carefully and the DNA pellet washed with 70% ethanol followed by centrifugation at 4000 rcf for 60 min at 4 °C. The ethanol was removed and pellets were left to air dry at RT. The pellets were then dissolved in 200-500 µl TE buffer (10 mM TrisHCl, pH 8, 1 mM EDTA). Plasmid quality and sequence were checked as described in **section 2.7.2**.

2.7.4 Site-directed mutagenesis

Primers, 25-45 bases in length with a melting temperature of (T_m) ≥ 78 °C, were designed for site-directed mutagenesis by using **equation 2.4** as suggested by the manufacturer. *N* corresponds to the primer length in bases, while *% GC* and *% mismatch* respectively correspond to the percentage of GC bases and the percentage of mismatching bases relative to the total number of bases.

2.4 $$Tm = 81.5 + 0.41\ (\%GC) - \ 675/N - \%\ mismatch$$

Primers were designed to generate mutations of two adjacent bases without changing the XRCC1 amino acid sequence in order to obtain an RNAi resistant pCMV XRCC1 plasmid (XRCC1 RNAi-R). The oligonucleotides designed for the mutagenesis site-directed reaction were as follows: forward (5'CTCCCAAAGGGAAGAGGAAACTGGATTTGAACCAAGAAG3'), and reverse (5'CTTCTTGGTTCAAATCCAGTTTCCTCTTCCCTTTGGGAG3').

A PCR reaction was prepared containing 5 ng of DNA template, 1X PfuTurbo buffer (200 mM Tris-HCl pH 8.8, 100 mM $(NH_4)_2SO_4$, 100 mM KCl, 1% (v/v) Triton X-100, 1 mg/mL BSA), 125 ng of both primers, 0.2 mM dNTPs mix, 0.5 U/µl of PfuTurbo DNA polymerase and H_2O to a final volume of 50 µl. The following PCR programme was used: 1 cycle at 95°C for 2 min followed by 25 cycles of 95°C for 30 sec, 50°C for 60 sec, 68°C for 8 min (1min/kb of plasmid length) and a final step at 68°C for 20 min. 0.2 U/ µl of Dpn I restriction enzyme was directly added and incubated at 37°C for 1 h to digest the methylated parental DNA. Finally, PCR products were checked on a 1% agarose gel.

Transformation of XL1 blue competent bacterial cells was performed. Plasmids were purified (MiniPrep) and sequenced (**section 2.7.2**), followed by a MaxiPrep purification step (**section 2.7.3**).

2.8 Cell cycle and apoptosis analysis

2.8.1 Cell cycle assay

Cells were detached using Trypsin-EDTA solution, re-suspended in 5 ml PBS-1%FBS and counted. 5 x 10^5 cells were used for cell cycle analysis, while the remaining cells were used for western blotting.

Cells were centrifuged at 250 rcf for 5 min and the supernatant was then carefully removed. Ice-cold 70% ethanol (1 ml) was added and incubated for 30 min on ice to permeabilise the cells. Ethanol was removed after centrifugation at 250 rcf for 5 min and cells were incubated at 37°C for 30 min in 1 ml PBS supplemented with 100 µg/ml RNase to cleave the RNA. After incubation, the cell suspension was supplemented with 20 µg/ml propidium Iodide (PI) and incubated at RT for 15 min in the dark to stain the DNA. Sample acquisition was then performed using FACSort (BD). Data analysis was performed with ModFit software. An example of the analysis performed using ModFit is shown in **figure 2.1**.

2.8.2 Apoptosis assay

Cells were deatched using Trypsin-EDTA and counted to give 2.5 x 10^5 cells per sample. The remaining cells were used for western blotting analysis. Cells were then centrifuged at 250 rcf for 5 min, re-suspended in 500 µl of 1X AnnexinV binding buffer (Apoptosis kit, Abcam) and incubated for 10 min at RT. For each sample, 5 µl of Annexin V-FITC and 5 µl PI (Apoptosis kit, Abcam) were added to each sample and incubated for 15 min at RT in the dark. Sample acquisition was performed using FACSort (BD). Since FITC and PI emission spectra overlap, compensation techniques were applied to minimise FITC positive cells being considered as PI positive cells, and vice versa. **Figure 2.2** displays a representative acquisition of Annexin V-FITC only and PI only control samples acquired after the compensation was applied. Acquisition of the samples stained with both fluorophores was performed. FlowJo software was used to analyse the acquired data.

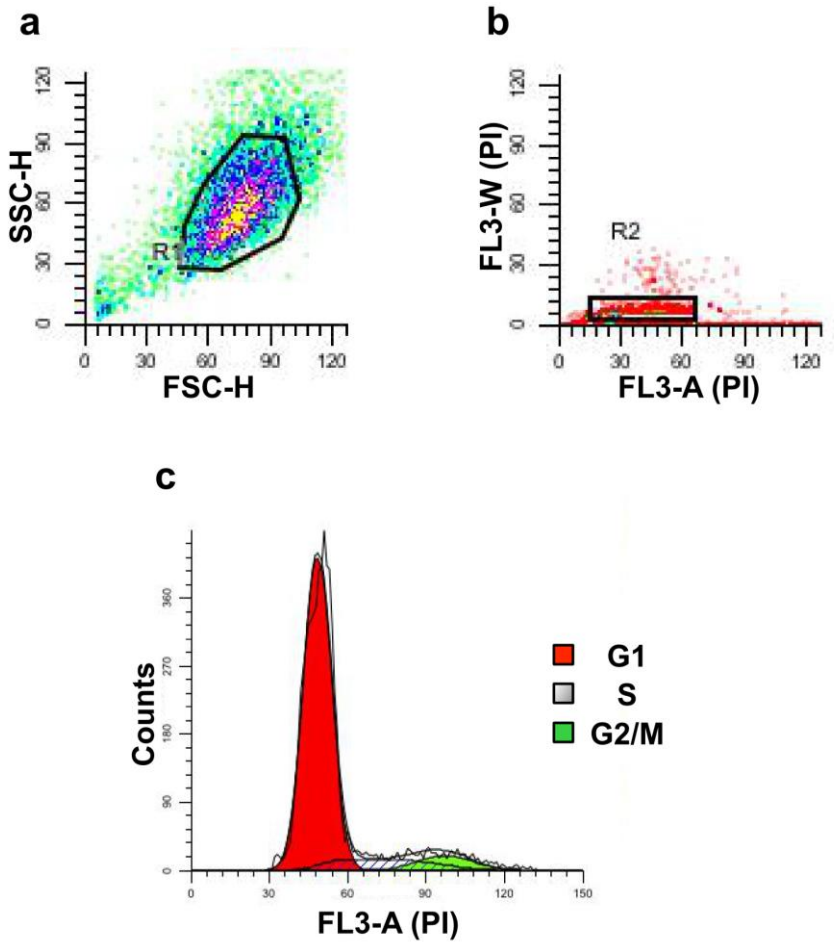

Figure 2.1: Example of the analysis of cell cycle data using ModFit programme.
Gate R1 represents the main cell population (**a**), whereas gate R2 represents the population to be analysed, excluding cell doublets (**b**). The graph represents the distribution of the cells in the cycle phases analysed by ModFit software (**c**).

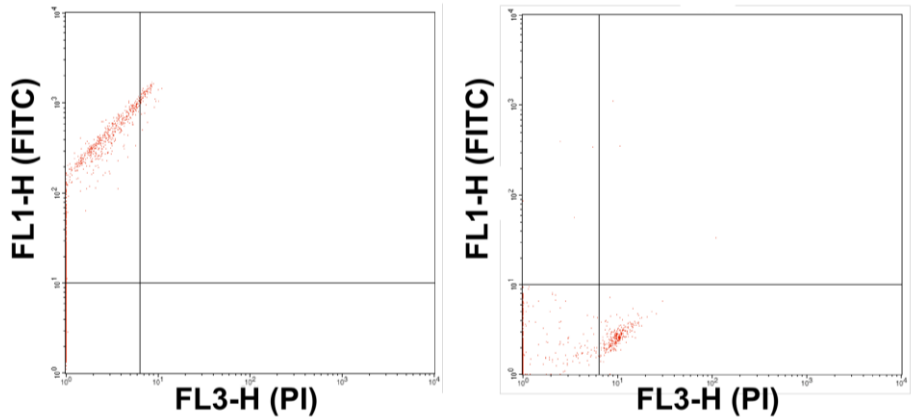

Figure 2.2: Example of the resulting dot plots obtained after compensation was applied.
The left panel displays a dot plot obtained following acquisition of Annexin V-FITC-stained cells. The right panel displays a representative acquisition of PI-stained cells. Cells with Annexin-associated fluorescence only are confined to the upper left quadrant of the dot plot, whereas PI-stained cells are confined to the lower right quadrant. Compensation is then required to facilitate the analysis of cells with both Annexin and PI-associated fluorescence.

2.9 Statistical analysis

When statistical analysis was required, average values and the standard error (S.E.) of three independent experiments were determined. Values were normalised against the control samples and plotted on a histogram graph. The p-values were calculated using a two-tailed Student's t-test. For this study, the following legend was adopted: n.s., non-significant, *p-value < 0.05, **p-value < 0.01, ***p-value < 0.001.

3. Persistent DNA strand breaks lead to induction of *ARF* expression

3.1 ARF induction is triggered by persistent DNA SBs

3.1.1 Moderate induction of ARF protein levels in response to acute DNA damage

To study ARF induction, HeLa cells were chosen as a model since *ARF* expression can be detected and the protein level can be modulated up and down (Zhang et al., 1998). Moreover, ARF induction can be tolerated in these cells without triggering cell cycle arrest or apoptosis, because p53 accumulation is impaired; in fact, p53 degradation is constantly stimulated by the presence of the human papilloma virus E6 protein, which promotes the interaction of p53 with the E3 ubiquitin ligase E6AP (Scheffner et al., 1993).

Firstly, it was assessed if ARF is induced in response to acute DNA damage treatment as has been previously reported (Eymin et al., 2006; Khan et al., 2004). HeLa cells were treated with 150 µm H_2O_2 for 15 min or exposed to 10 Gy IR to generate DNA damage. It is known that PARP1 recognises SBs, binds at the site of the DNA nicks and synthetises PAR polymers due to the activation of its enzymatic activity (Gradwohl et al., 1990; Okano et al., 2003; Singh et al., 1985). Therefore, the synthesis of PAR can be used as a marker for DNA damage formation. Analysis of ARF protein levels detected a 15-20% increase in ARF levels 1-2 h after treatment (**figure 3.1**); however, ARF levels are restored to control levels 4 h post- treatment. This result indicates that ARF is only moderately induced in response to acute DNA damage.

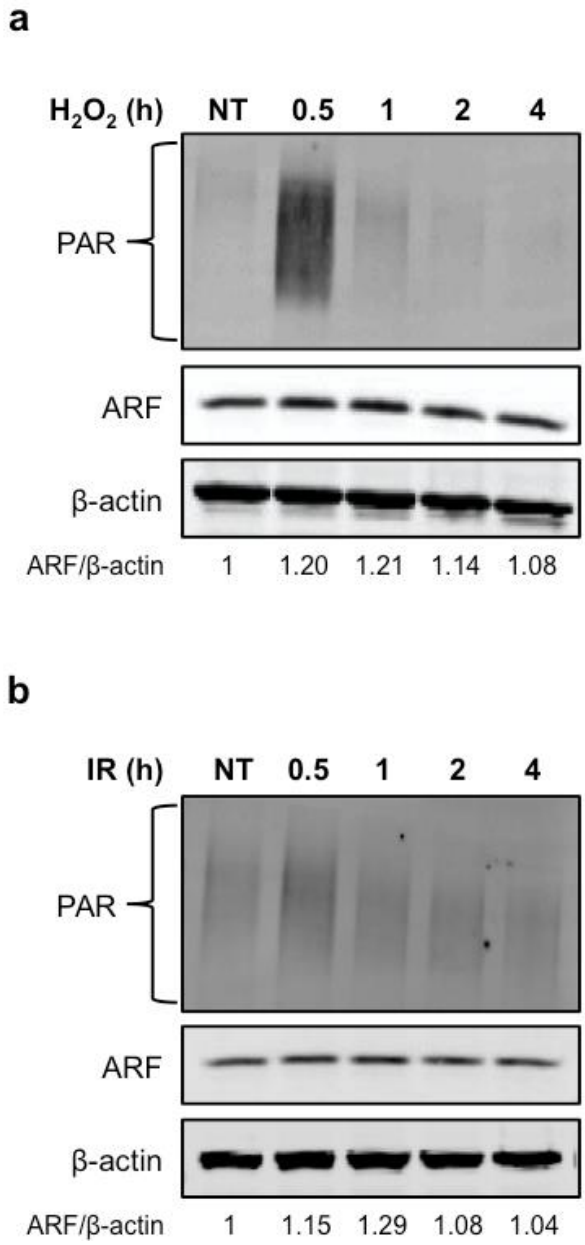

Figure 3.1: Moderate induction of ARF in response to H_2O_2 and IR treatment.
HeLa cells were treated with 150 µm H_2O_2 for 15 min (**a**) or exposed to IR at a dose of 10 Gy (**b**). NT stands for non-treated samples. The cells were harvested at the time points indicated after treatment (h) and WCEs were prepared. The level of ARF was analysed by SDS-PAGE and immunoblotting with ARF, PAR and β-actin (loading control) antibodies. ARF signal was quantified and normalised against β-actin signal. Values were then normalised to the control (NT). The images displayed are representative of three independent experiments.

H_2O_2 and IR treatments generate oxidative and SB lesions. To verify the formation of DNA lesions and to assess the DNA repair kinetics, an alkaline comet assay was performed following treatment with either H_2O_2 or IR. An untreated sample (Cont) was used to check whether the treatment generates DNA SBs (Cont and. 0 h time points). As shown in **figure 3.2**, approximately 80% of the SBs are repaired 30 min after treatment, suggesting that the DNA repair system is capable of promptly repairing the damage generated by these treatments. It was thus concluded that DNA damage itself, if it is promptly repaired, does not lead to the accumulation of ARF.

3.1.2 ARF upregulation occurs in response to unrepaired SBs

ARF accumulates in aging tissue and in senescent cells (Dimri et al., 2000; Krishnamurthy et al., 2004). Senescence can be triggered by the persistence of DNA damage (Rodier et al., 2009). In the previous section, it has been demonstrated that promptly repaired DNA lesions do not lead to ARF accumulation. Thus, it was hypothesised that persistent DNA damage may be the reason for ARF induction. The DNA macromolecule is inherently unstable and the formation of DNA base lesions occurs via the attack of endogenous sources, such as ROS (Lindahl, 1993). The major pathway involved in the repair of base lesions is BER. It has been shown that when XRCC1 is depleted, the ligation step during BER is impaired, leading to the accumulation of DNA SBs (Brem and Hall, 2005). Therefore, the BER pathway was disabled by depleting XRCC1 to test whether persistent DNA damage triggers ARF induction. To do so, HeLa cells were transfected with XRCC1 RNAi for 72 h. **Figure 3.3** shows that XRCC1 is efficiently depleted under the experimental conditions. To assess whether there was an accumulation of unrepaired SB lesions, PAR signal was examined. The PAR signal increases 2-fold when comparing lipofectamine with XRCC1 RNAi samples, thus showing that XRCC1 depletion generates persistent SB lesions (**figure 3.3**). Therefore, the XRCC1-depleted system can be exploited to create persistent DNA lesions and to assess whether ARF is induced in this situation (see **section 7.1**).

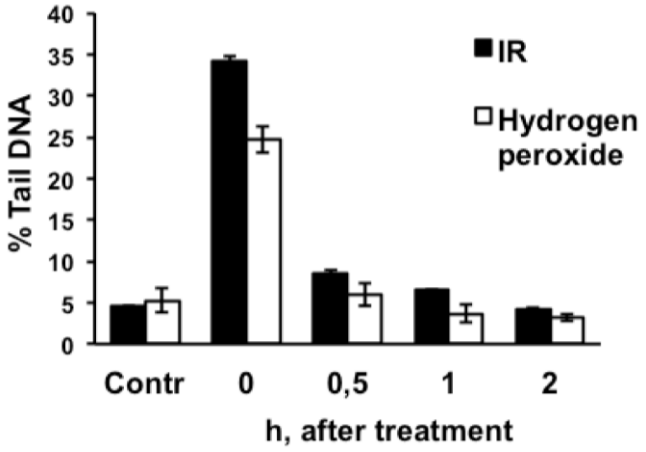

Figure 3.2: SB lesions are efficiently repaired by DNA repair machinery.
HeLa cells were treated for 15 min with 150 µm H_2O_2 (white bars) or exposed to IR at a dose of 10 Gy (black bars). Untreated samples were also prepared (Contr). A comet assay in alkaline conditions was performed at different repair time points. The graph represents the average ± S.E. of three independent experiments.

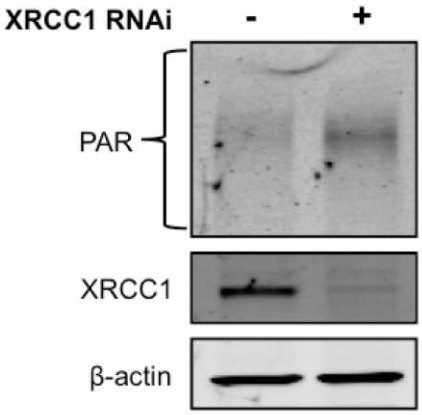

Figure 3.3: XRCC1-depleted cells show an accumulation of unrepaired DNA SBs.
HeLa cells were transfected with either lipofectamine only (-) or in combination with 200 pmol XRCC1 RNAi (+) for 72 h. WCEs were prepared and analysed by SDS-PAGE. XRCC1 and PAR levels were analysed by immunoblotting; β-actin was used as a loading control. The images displayed are representative of three independent experiments.

The level of ARF was assessed 72 h after XRCC1 knockdown. The efficient depletion of XRCC1 and the formation of PAR are confirmed as shown in **figure 3.4.a**. It was then shown that the level of ARF increases 2-fold following the formation of SBs (**Figure 3.4.a**); indeed ARF was upregulated by an average of 3-fold in three independent experiments (**figure 3.4.b**). It was then concluded that ARF is induced in response to the accumulation of unrepaired SB lesions.

To exclude the possibility of RNAi off-target effects, XRCC1 complementation was performed. A pCMV mammalian vector expressing wild type XRCC1 (XRCC1 WT) was used to prepare an RNAi resistant version (XRCC1 RNAi-R). Firstly, to verify that XRCC1 overexpression does not affect ARF protein levels, HeLa cells were transfected with XRCC1 WT and XRCC1 RNAi-R plasmids. It was confirmed that the level of ARF does not change upon XRCC1 overexpression (**figure 3.5.a**).

To perform the rescue of XRCC1, HeLa cells were transfected with either lipofectamine or XRCC1 RNAi followed by transfection with XRCC1 RNAi-R vector. The analysis of ARF levels was carried out by western blotting (**figure 3.5.b**) and the quantification of three independent experiments was performed (**figure 3.5.c**). The increase of ARF levels is reverted following XRCC1 complementation, confirming that the RNAi sequence used has no off-target effects. These data suggest that ARF upregulation is driven by the accumulation of persistent DNA SBs provoked by XRCC1 depletion.

3.1.3 The accumulation of persistent SBs is necessary to trigger the induction of ARF

The majority of endogenous SBs are generated by the endonuclease activity of APE1 during BER. APE1 catalyses the cleavage of the DNA backbone in proximity to AP sites, generated either by DNA glycosylases or by the spontaneous hydrolysis of the nitrogenous bases (Wilson and Barsky, 2001).

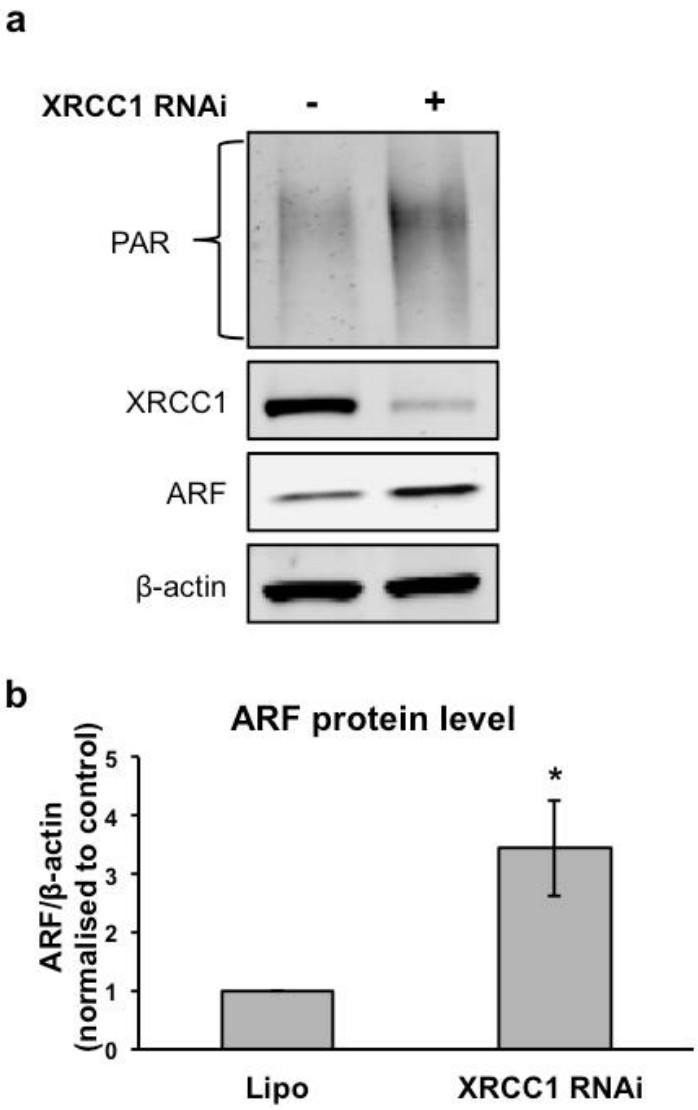

Figure 3.4: ARF levels are upregulated in response to SB accumulation.
a) HeLa cells were transfected with either lipofectamine only (-) or in combination with 200 pmol XRCC1 RNAi (+). PAR, XRCC1 and ARF protein levels were assessed by SDS-PAGE and western blotting; β-actin was used as loading control. The displayed images are representative of three independent experiments.
b) ARF signal for both lanes was quantified and normalised against β-actin signal in lipofectamine only (Lipo) or in XRCC1-depleted (XRCC1 RNAi) samples. Values were then normalised to the control (Lipo). The graph represents the average ± S.E. of three independent experiments. P-value was calculated by the Student's t-test (*p<0.05).

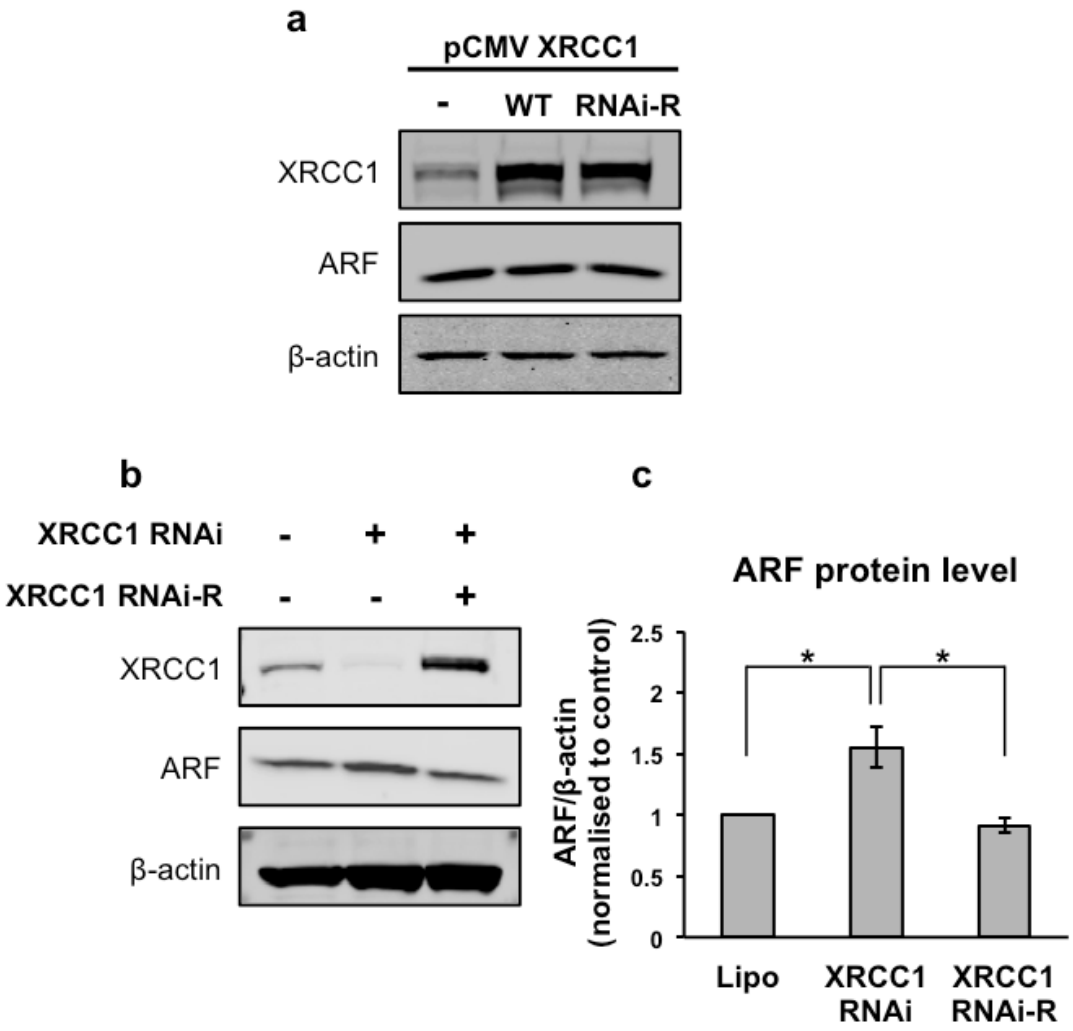

Figure 3.5: Expression of RNAi-resistant XRCC1 plasmid prevents ARF induction generated by XRCC1 knockdown.
a) HeLa cells were transfected with lipofectamine only (-) or in combination with either 250 pmol of XRCC1 WT (WT) or XRCC1 RNAi-R (RNAi-R) plasmids for 18 h. WCEs were prepared and analysed by SDS-PAGE. XRCC1, ARF and β-actin (loading control) protein levels were assessed by immunoblotting. The displayed images are representative of three independent experiments.
b) HeLa cells were transfected with lipofectamine only (-) or in combination with 200 pmol XRCC1 RNAi (+) for 30 h and subsequently transfected with 150 pmol of XRCC1 RNAi-R (RNAi-R) plasmid for an additional 18 h. WCEs were prepared and analysed by SDS-PAGE. XRCC1, ARF and β-actin (loading control) protein levels were assessed by immunoblotting. The displayed images are representative of three independent experiments.
c) Quantification of data shown in (b). ARF signal was normalised against β-actin. Values of each sample were then normalised to the control (Lipo). The graph represents the average ± S.E. of three independent experiments and the p-value was calculated by the Student's t-test (*$p<0.05$).

To assess the possibility that ARF induction was dependent on the persistence of endogenous SBs, APE1 endonuclease was depleted to reduce the amount of SBs generated. HeLa cells were depleted of either XRCC1 or APE1 or both proteins using RNAi for 72 h. **Figure 3.6** shows that ARF levels do not change in APE1-depleted cells (lane 1 and lane 3), suggesting that the accumulation of AP sites does not trigger ARF induction. More importantly, an increase in ARF levels is prevented when cells are depleted of APE1 in a XRCC1 knockdown background (lane 2 and lane 4, **figure 3.6**), showing that ARF is induced when SBs are created (by APE1 endonuclease activity) and when they are persistent (by depleting XRCC1). Hence, the formation and the persistence of SB lesions induce ARF.

To demonstrate that ARF protein levels correlate with the amount of SB lesions produced, a time course experiment following XRCC1 RNAi transfection was performed. HeLa cells were transfected with XRCC1 RNAi and the kinetics of PAR and ARF induction were analysed by western blotting (**figure 3.7**). The figure shows that PAR accumulates in a time-dependent manner, reflecting the accumulation of SBs. As expected, the kinetics of ARF induction follows the same time-dependent pattern of PAR, showing a correlation between the level of PAR and ARF. Thus, an increasing amount of unrepaired SB lesions correlates with increasing amount of ARF levels.

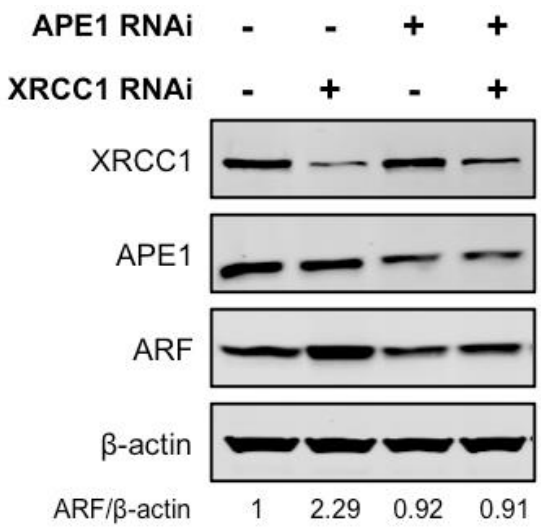

Figure 3.6: APE1 knockdown reduces the induction of ARF by persistent SBs.
HeLa cells were transfected with lipofectamine only (-) or in combination with APE1 RNAi (+) or XRCC1 RNAi (+) or with both the RNAi sequences (200 pmol each). After 72 h cells were harvested and WCEs were prepared. APE1, ARF, XRCC1 and β-actin (loading control) protein levels were assessed by SDS-PAGE and western blotting. ARF signal was quantified and normalised against β-actin signal. Values were then normalised to the control (Lipo). The displayed images are representative of three independent experiments.

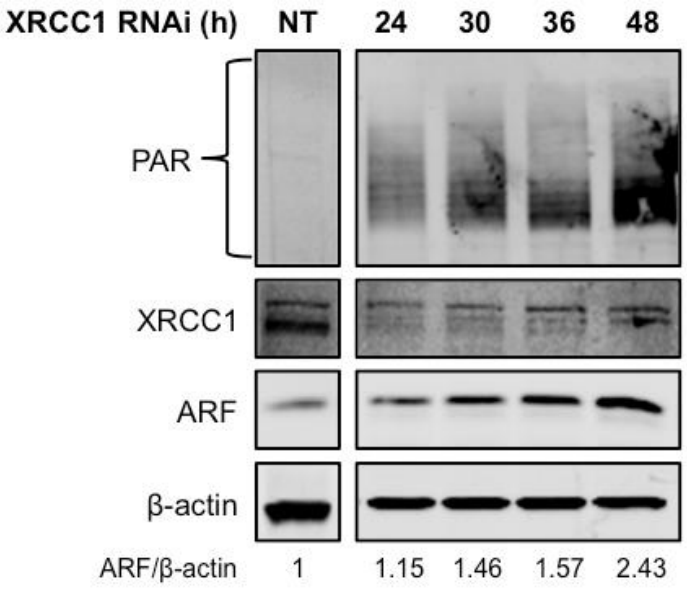

Figure 3.7: Kinetics of PAR and ARF induction following XRCC1 knockdown.
HeLa cells were transfected with 200 pmol XRCC1 RNAi and harvested at the indicated (h) time points after transfection. WCEs were prepared and analysed by SDS-PAGE and western blotting. XRCC1, ARF, PAR and β-actin (loading control) protein levels were assessed. ARF signal was quantified and normalised against β-actin signal. Values were then normalised to the control (NT). The displayed images are representative of three independent experiments. NT stands for non-treated cells.

3.2 Increase in transcription of *ARF* mRNA levels causes ARF accumulationin response to SBs

3.2.1 ARF stability is not affected by persistent SBs

The data presented shows that ARF is induced in response to the accumulation of SB lesions. The level of proteins is regulated through the induction of the mRNA transcription and PTMs, which itself can affect both the stability and the activity. To assess if the molecular mechanism responsible for the increase in ARF levels was affecting ARF stability, CHX treatment following XRCC1 knockdown was performed. CHX inhibits the ribosomal activity by blocking the mRNA translation process (Korner, 1966); therefore, the synthesis of new protein is prevented, allowing the evaluation of the protein lifetime. HeLa cells were transfected with XRCC1 RNAi for 72 h and then treated with 50 µg/ml of CHX. The level of ARF was assessed by western blotting. The resulting images confirm the validity of CHX treatment since ARF protein levels decrease upon treatment (**figure 3.8.a**). The average ARF levels of three independent experiments were plotted as a histogram as displayed in **figure 3.8.b**. By comparing lipofectamine and XRCC1 RNAi samples, it can be observed that ARF kinetics are similar, thus implying SB formation has no impact on ARF stability.

3.2.2 ARF induction is regulated at the transcriptional level

According to the results described in the previous section, it was investigated if ARF induction was regulated at the transcriptional level. To verify this hypothesis *ARF* mRNA levels were assessed after XRCC1 depletion. HeLa cells were seeded and XRCC1 RNAi transfection was performed for 72 h. The RNA quality was checked on an agarose gel to confirm the 2:1 ratio between the 28S and the 18S ribosomal subunits (**figure 3.9.a**). The analysis of *ARF* transcription in three independent experiments indicates that persistent SBs lead to an average 3-fold upregulation of *ARF* mRNA levels (**figure 3.9.b**). It was then concluded that unrepaired SBs increase the transcription of the *ARF* tumour

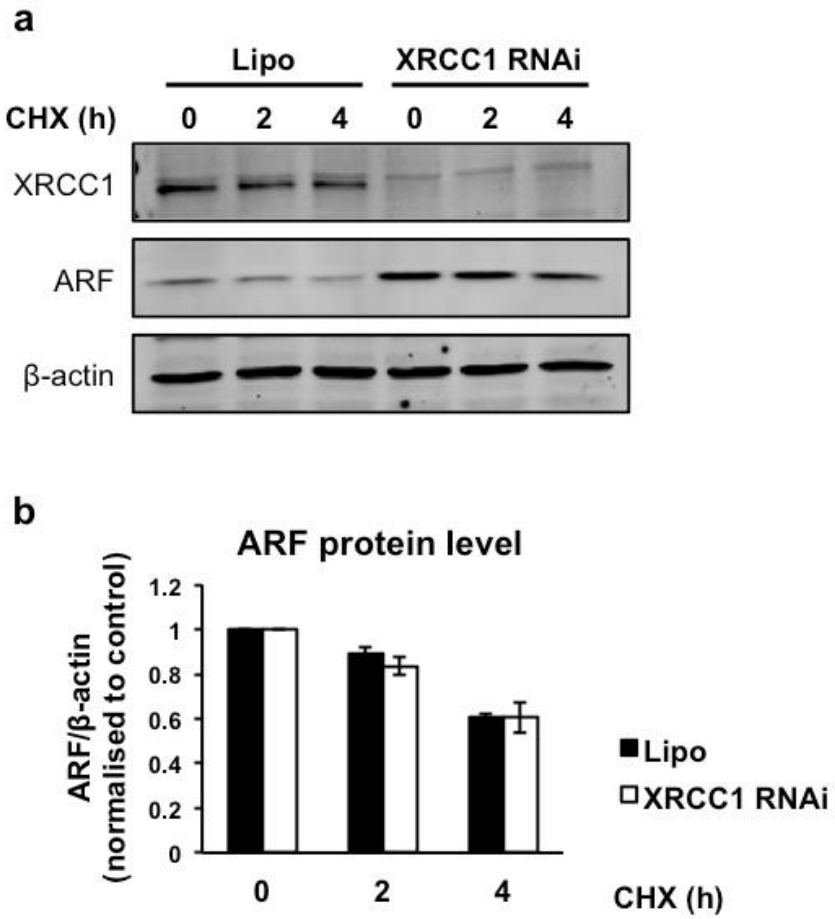

Figure 3.8: ARF stability is not affected by SB formation.
a) HeLa cells were transfected with either lipofectamine only (Lipo) or in combination with 200 pmol XRCC1 RNAi (XRCC1 RNAi). After 72 h cells were treated with 50 µg/ml CHX and harvested at the indicated (h) time points. WCEs were prepared; SDS-PAGE and western blotting assays were carried out. XRCC1, ARF and β-actin (loading control) protein levels were assessed. The displayed images are representative of three independent experiments.
b) Quantification of the data shown in (a). ARF signal was normalised against β-actin. Values of each group of samples were normalised to the respective control (0 h time point). The graph represents the average ± S.E. of three independent experiments.

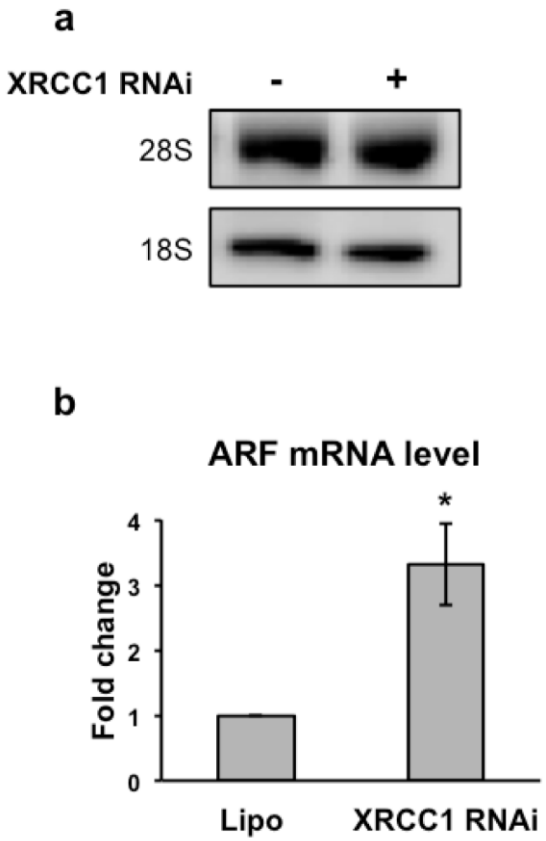

Figure 3.9: Increase of *ARF* transcription in response to unrepaired SBs.
a) HeLa cells were transfected with either lipofectamine only (-) or in combination with 200 pmol XRCC1 RNAi (+). After 72 h, cells were harvested and RNA extraction was performed. 1 µg of total RNA was loaded on a 1% agarose gel. The 2:1 ratio between the amount of the 28S and the 18S rRNA subunits was determined.
b) cDNAs of lipofectamine only (Lipo) and of XRCC1-depleted (XRCC1 RNAi) samples were synthesised and qPCR was performed. *ARF* mRNA levels and *GAPDH* mRNA levels (loading control) were evaluated. Values were normalised to the control (Lipo). The graph represents the average ± S.E. of three independent experiments and the p-value was calculated by the Student's t-test (*$p<0.05$).

suppressor gene, consequently raising ARF protein levels.

The *ARF* gene is known to be part of the *INK4a-ARF* locus (Gazzeri et al., 1998). ARF and p16 (encoded by *INK4a* gene) mRNAs are both transcribed from this locus. The two transcripts shares exon 2 and 3, but they have two distinct exons 1 and two separate promoter regions (Mao et al., 1995; Quelle et al., 1995). To assess whether the entire locus was activated in response to the accumulation of SBs, *p16* mRNA levels were assessed in XRCC1-depleted samples. The graph displayed in **figure 3.10,** representing analysis of three independent experiments, shows that *p16* mRNA levels were not upregulated in response to SBs. This result indicates that the increase in *ARF* mRNA levels is not due to the induction of transcription of the entire locus, but is instead specific for the *ARF* gene.

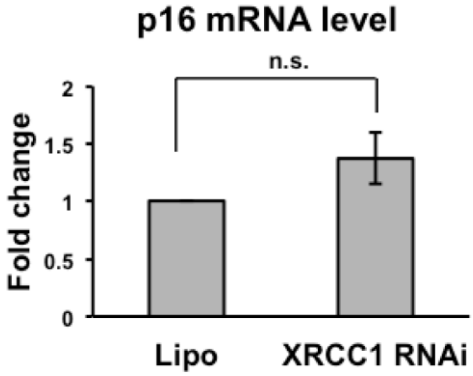

Figure 3.10: SB formation does not lead to the transcriptional activation of the entire INK4-ARF locus.
qPCR was performed using the cDNAs previously synthetised for lipofectamine only (Lipo) and XRCC1-depleted (XRCC1 RNAi) samples. *P16* mRNA levels and *GAPDH* mRNA levels (loading control) were measured. Values were normalised to the control (Lipo). The graph represents the average ± S.E. of three independent experiments and the p-value was calculated by the Student's t-test (p=n.s., non significant).

Altogether, these findings highlight that ARF induction can be driven by unrepaired SBs, thus enforcing the importance of maintaining an intact and functional *ARF* gene. Hence, when DNA repair mechanisms cannot cope with the number of DNA lesions produced, ARF is induced and signals the presence of unrepaired DNA damage that could eventually lead to genomic instability. Moreover, these data support the idea that the *ARF* tumour suppressor gene could be part of the DDR, proposing a novel role for ARF. A work in progress model for the molecular mechanism responsible for ARF induction in response to DNA damage is shown in **figure 3.11**.

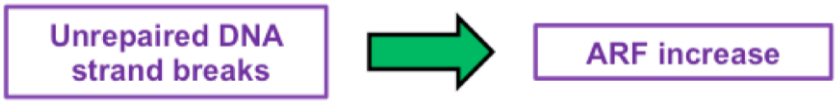

Figure 3.11: Model in progress for ARF induction.
Unrepaired SBs generated upon XRCC1 depletion increase ARF levels through upregulation of *ARF* mRNA levels.

It was then hypothesised that the proteins involved in sensing SBs could be responsible for triggering ARF upregulation. PARP1 is the major sensor of SBs and the synthesis of PAR is stimulated by binding to DNA nicks. In this chapter, a correlation between PARP1 activation and ARF levels has been shown. Therefore, it was then speculated that there is a possible role for PARP1 in inducing the tumour suppressor gene *ARF*. The aim of the following chapter is to address this hypothesis and to better characterise the link between SB formation and the upregulation of ARF levels.

4. PARP1 induces *ARF* transcription by modulating cellular NAD^+ levels

4.1 ARF induction is dependent on PARP1 activation

4.1.1 Induction of ARF by persistent SBs requires PARP1 protein

In accordance with previously published data (Gradwohl et al., 1990; Singh et al., 1985), the formation of SBs can lead to an increase in PAR synthesis following depletion of XRCC1 (**figure 3.3**). Production of PAR is mainly catalysed by PARP1, which is a known sensor of SBs (Ame et al., 1999; Caldecott, 2008). It was then hypothesised that PARP1 could be responsible for the upregulation of *ARF* mRNA levels. To address this possibility, HeLa cells were transfected with XRCC1 and PARP1 RNAi sequences or with a combination of both. The results presented in **figure 4.1** show that PARP1 is knocked down efficiently ~ 80%. ARF is moderately induced upon PARP1 depletion when comparing lane 1 and lane 3, suggesting that PARP1 is not required for maintaining ARF levels in an unperturbed situation. XRCC1-treated cells show both an increase in ARF (3-fold) and PAR formation when comparing lane 1 and lane 2 in **figure 4.1**. However, when PARP1 is depleted in combination with XRCC1 (lane 4, **figure 4.1**), both the synthesis of PAR and the induction of ARF are reduced. Indeed, ARF induction is 1-fold reduced when comparing lane 2 and lane 4. These results show that PARP1 is necessary for an increase in ARF levels in response to unrepaired SBs, suggesting a new role for PARP1 in signalling DNA damage.

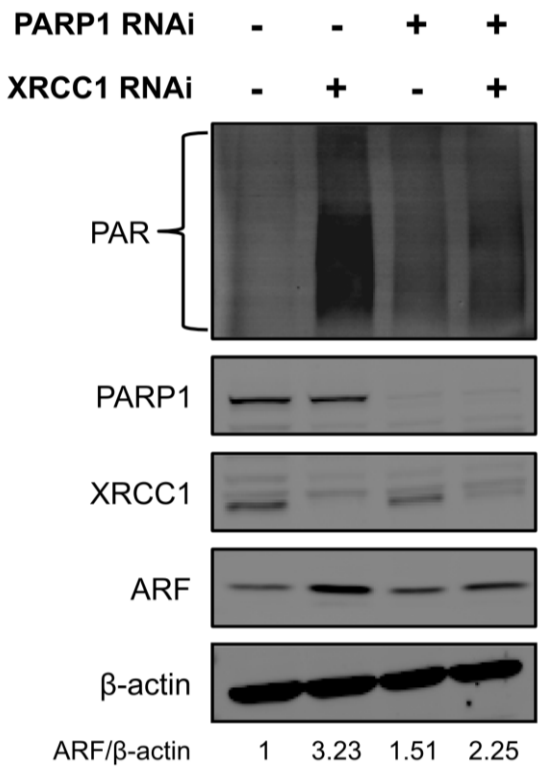

Figure 4.1: ARF induction in response to persistent DNA SBs is reduced in response to PARP1 knockdown.
HeLa cells were transfected with lipofectamine only (-) or in combination with either XRCC1 RNAi (+) or PARP1 RNAi (+) (200 pmol), or a mixture of both for 72 h. WCEs were prepared and analsyed by SDS-PAGE. The level of XRCC1, PAR, PARP1 and ARF were analysed by immunoblotting, probing the membrane with the specific antibodies. β-actin was used as a loading control. ARF signal was quantified and normalised against β-actin signal. Values were then normalised to the control (Lipo). The images displayed are representative of three independent experiments.

However, PAR synthesis and ARF induction are not completely abolished. These results might be a consequence of either an incomplete depletion of PARP1 or it might indicate that other PARP proteins might be involved in the regulation of ARF protein levels in response to SB accumulation.

A second sequence against PARP1 (PARP1_2 RNAi) was employed to rule out the possibility that the effect measured on ARF levels could be caused by an off-target effect produced by the RNAi sequence used. HeLa cells were then transfected with either XRCC1 or PARP1_2 RNAi only or with a combination of both sequences. Similarly, **figure 4.2** shows PARP1 is efficiently knocked down (~ 80%) by PARP1_2 RNAi and that the induction of ARF is prevented by the depletion of PARP1 in XRCC1-depleted cells (lane 2 and lane 4, **figure 4.2**). It is important to note that PARP1_2 RNAi sequence causes a 50% decrease in ARF levels in an unperturbed situation (lane 1 and lane 3, **figure 4.2**); however, the 1.5-fold difference between lane 2 and lane 4 suggests PARP1 requirement for ARF induction in response to SBs despite the use of PARP1_2 RNAi sequence. These data suggest that ARF induction is regulated by PARP1 and not by the off-target effects produced by using the RNAi technology. Altogether, these findings suggest that the increase in ARF levels in response to SB formation requires the presence of PARP1, which is known to be important in the detection and the signalling of SB lesions.

4.1.2 PARP1 activity is necessary to induce *ARF* transcription

To assess if PARP1 activity is required for ARF induction, XRCC1 was depleted in HeLa cells and cells were then treated with 200 μM of the PARP inhibitor, NU1025 (Bowman et al., 1998). XRCC1 depletion was confirmed and accumulation of PAR was used as a marker for PARP1 activation (**figure 4.3**). Analysis of PAR synthesis confirms that treatment with NU1025 leads to PARP1 inhibition; in fact, after 4 h treatment the PAR signal is completely abolished despite the lack of XRCC1 (lane 2 and lane 3, **figure 4.3**).

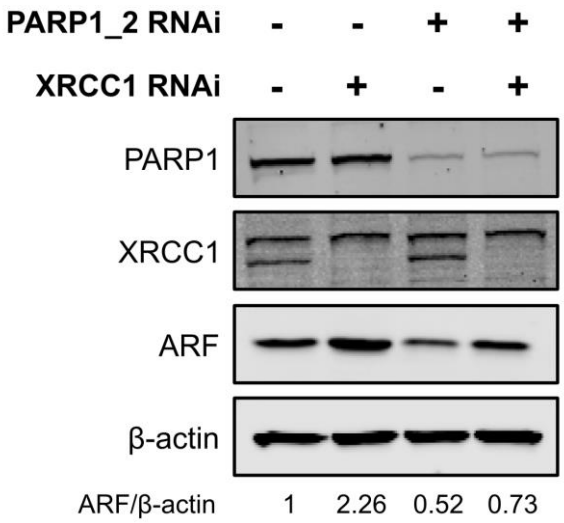

Figure 4.2: The use of a second RNAi sequence against PARP1 suggests that the effect on ARF levels is not caused by any RNAi off-target effects.
HeLa cells were transfected with lipofectamine only (-) or in combination with either XRCC1 RNAi (+) or PARP1_2 RNAi (+) (200 pmol), or a mixture of both for 72 h. WCEs were prepared and assessed by SDS-PAGE. XRCC1, PARP1 and ARF levels were analysed by immunoblotting. β-actin was used as a loading control. ARF signal was quantified and normalised against β-actin signal. Values were then normalised to the control (Lipo). The images displayed are representative of three independent experiments.

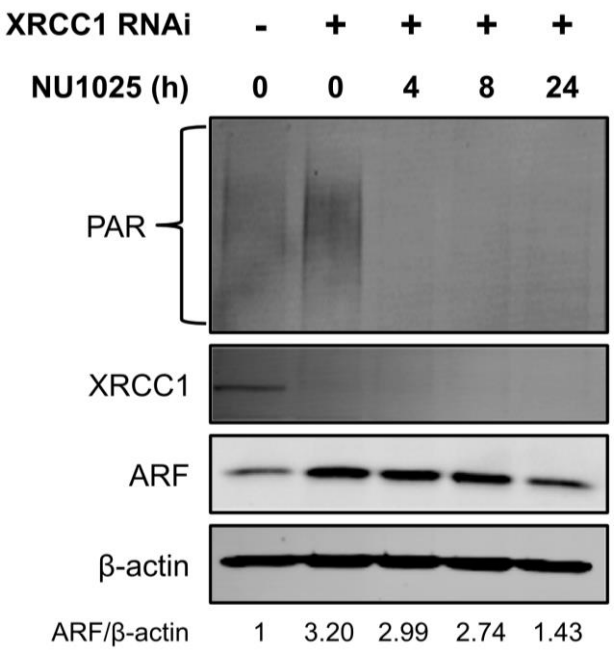

Figure 4.3: Inhibition of PARP1 activity reduces ARF accumulation induced by XRCC1 depletion.
HeLa cells were transfected with lipofectamine only (-) or in combination with XRCC1 RNAi (+) (200 pmol) for 72 h. The cells were then treated with PARP1 inhibitor NU1025 (200 μM) and harvested at the indicated times (h) after treatment. WCEs were prepared and analysed by SDS-PAGE. XRCC1, PAR and ARF levels were analysed by immunoblotting. β-actin was used as a loading control. ARF signal was quantified and normalised against β-actin signal. Values were then normalised to the control (Lipo 0 h). The images displayed are representative of three independent experiments.

ARF is still induced at 4 h and 8 h post-treatment, although ARF levels appear to slightly decrease as shown by the quantification (lane 3 and lane 4 respectively, **figure 4.3**), while a 1.8-fold decrease was identified 24 h after PARP1 inhibition. These results show that an increase in ARF correlates with the sustained PARP1 activity in response to SB formation. Moreover, these data suggest that PAR formation has also got a role in the regulation of proteins which are not part of the DNA repair machinery, such as the ARF tumour suppressor protein.

In chapter 3 it was shown that an increase in ARF correlates with the upregulation of *ARF* mRNA levels; therefore, it was investigated whether PARP1 activation is important for sustaining *ARF* mRNA synthesis in response to SB accumulation. To determine *ARF* mRNA levels, HeLa cells were transfected with XRCC1 RNAi and subsequently treated with 200 μM of the PARP inhibitor NU1025. To check the quality of the RNA isolated, the total RNA was loaded on a 1% agarose gel and the 2:1 ratio between the 28S and the 18S rRNA subunits was determined (**figure 4.4.a**). Analysis of *ARF* mRNA levels confirms an increase in ARF transcription as previously shown in **figure 3.9**, when comparing lipofectamine-treated cells with XRCC1 RNAi-treated cells (**figure 4.4.b**). Interestingly, *ARF* mRNA levels are restored to control levels when PARP1 activity is inhibited (comparing Lipo with NU1025 treated samples, **figure 4.4.b**). It is important to note that a 24 h untreated NU1025 XRCC1-treated control should have been included in the experiment displayed in **figure 4.3** and **figure 4.4** in order to assess whether ARF was remained induced 96 h following XRCC1 knockdown. This additional control would have provided further evidence for a potential correlation between PARP inhibition and a reduction in ARF levels, excluding the possibility of this observation occurring due to a decrease in ARF induction with time. However, *ARF* mRNA levels are 1-fold reduced 4 h and 8 h following NU1025 treatment, suggesting PARP inhibition plays a role in reducing ARF induction in response to persistent SBs.

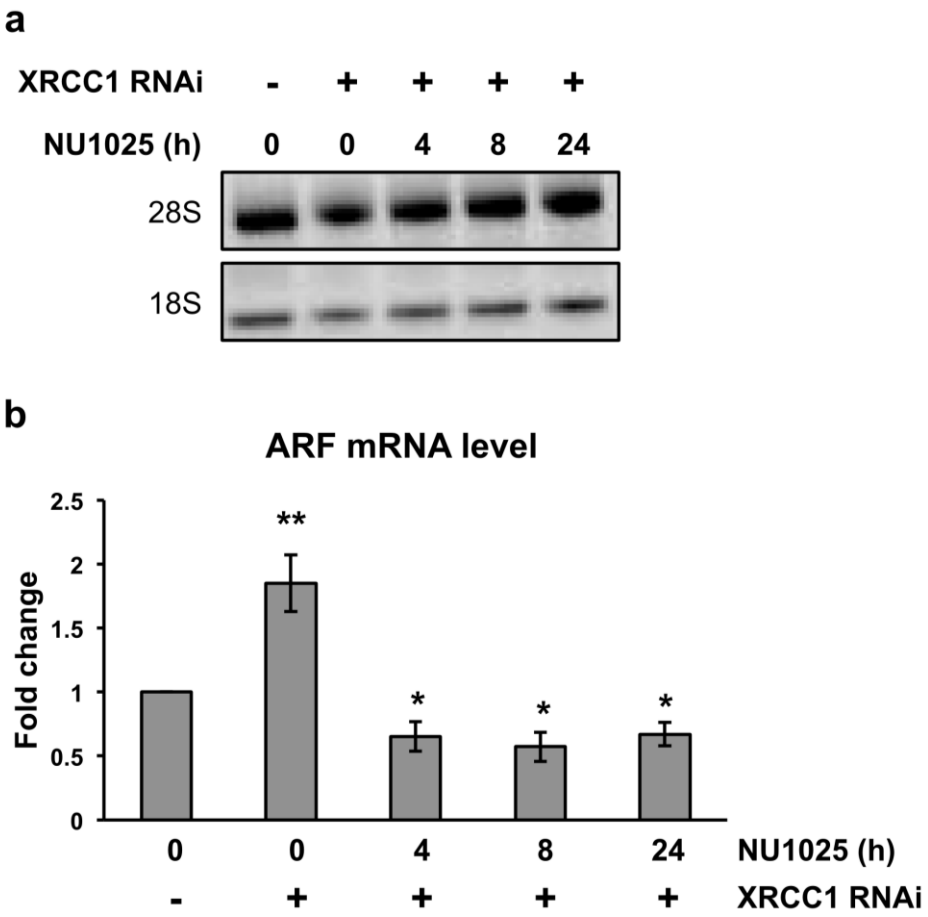

Figure 4.4: Inhibition of PARP1 reduces *ARF* expression.
a) HeLa cells were transfected with lipofectamine only (-) or in combination with XRCC1 RNAi (+) (200 pmol) for 72 h. The cells were then treated with PARP1 inhibitor NU1025 (200 μM) and harvested at the indicated time (h) post treatment. RNA extraction was performed and 1 μg of total RNA was loaded on a 1% agarose gel to assess the RNA quality. The 2:1 ratio between the amount of 28S and 18S rRNA subunits was assessed.
b) cDNA was prepared and qPCR was performed to analyse *ARF* expression. *GAPDH* mRNA was used as a loading control. Values were normalised to the control (Lipo 0 h). The graph represents the average ± S.E. of three independent experiments. The related p-values were calculated using the Student's t-test (*p<0.05; **p<0.01).

These results imply that PARP1 activity is required to stimulate *ARF* mRNA synthesis in response to SB formation. It was then concluded that in response to persistent SBs PARP1 is involved in promoting a signalling transduction cascade which leads to an induction of ARF at the transcriptional level.

4.2 PARP1-dependent NAD^+ consumption triggers ARF upregulation

4.2.1 ARF induction correlates with PARP1-dependent NAD^+ depletion

It is known that the enzymatic reaction catalysed by PARP1 requires NAD^+ as a co-factor, thus allowing the synthesis of the PAR polymer (Singh et al., 1985). It has been reported that the depletion of NAD^+ occurs when PARP1 is activated by genotoxic stress (Nakamura et al., 2003). In previously published work (Brem and Hall, 2005; Nakamura et al., 2003), PARP1 activation has been also evaluated by monitoring the depletion of NAD^+ in XRCC1-depleted cells. It was therefore hypothesised that NAD^+ consumption could be the cellular signal responsible for ARF induction. Therefore, in order to assess whether NAD^+ was consumed by PARP1 in XRCC1-depleted cells, HeLa cells were transfected with XRCC1 RNAi. After 48 h, cells were harvested and half of the pellet was used to quantify the amount of intracellular NAD^+ and the other half was analysed by western blotting. The graph presented in **figure 4.5.a** shows that in XRCC1-depleted cells, the level of NAD^+ was, in fact, significantly reduced compared to the lipofectamine-treated cells in accordance with previously published data (Brem and Hall, 2005; Nakamura et al., 2003). Western blotting confirms that XRCC1 is depleted, PAR is synthesised and ARF is 20% induced (**figure 4.5.b**). The lesser degree of ARF upregulation displayed in **figure 4.5.b** could be explained by the fact that ARF levels were assessed 48 h and not 72 h following XRCC1 knockdown. Such observation is in agreement with the data displayed in **figure 3.5** where ARF protein levels were found to be 50% induced 48 h following XRCC1 knockdown. Taken together, these results suggest that ARF induction might correlate with PARP1-dependent NAD^+ consumption. The following section focuses on proving that ARF upregulation might be triggered by NAD^+ depletion.

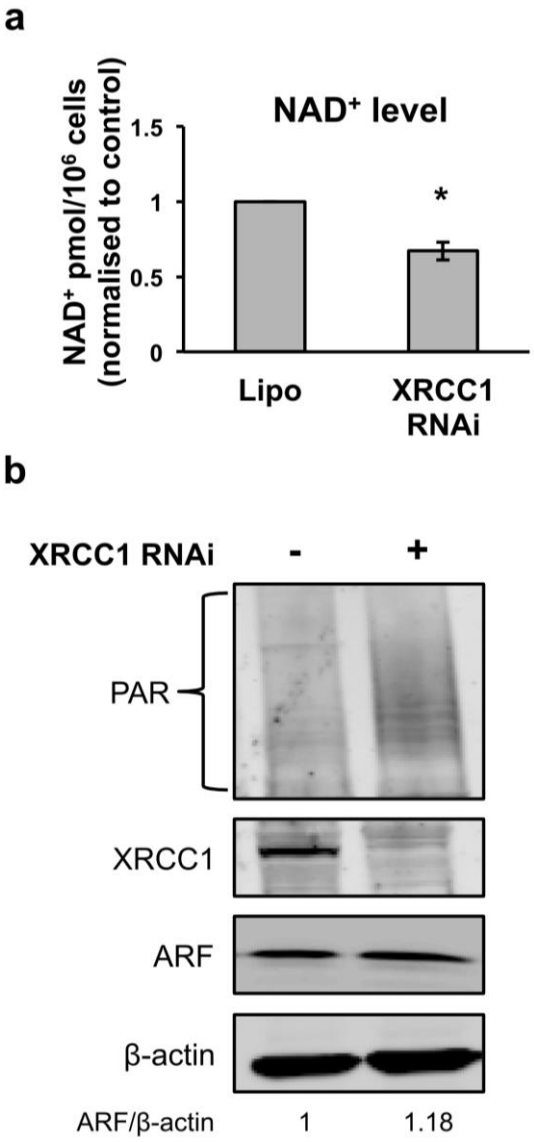

Figure 4.5: ARF induction correlates with PARP1-dependent NAD^+ depletion.
a) HeLa cells were transfected with lipofectamine only (-) or in combination with XRCC1 RNAi (+) (200 pmol) for 48 h. Cells were then harvested and counted. 2 x 10^5 cells were used for measuring the amount of intracellular NAD^+ using a colorimetric assay and the obtained values were normalised to the control (Lipo). The graph represents the average ± S.E. of three independent experiments and the p-value was calculated using the Student's t-test (*$p<0.05$).
b) The remaining treated cells were used to prepare WCEs. The levels of XRCC1, PAR and ARF were analysed by SDS-PAGE and by immunoblotting. β-actin was used as a loading control. ARF signal was quantified and normalised against β-actin signal. Values were then normalised to the control (Lipo). The images displayed are representative of three independent experiments.

4.2.2 Depletion of NAD^+ by NAMPT knockdown triggers ARF induction

According to the above data, it was then suggested that the depletion of NAD^+ could be the “warning signal” for triggering ARF induction. To assess this hypothesis, it was necessary to find a PARP1-independent system to chemically decrease the amount of NAD^+, thus mimicking its consumption. The nicotinamide phosphoribosyltransferase (NAMPT) enzyme has been reported to take part in the NAD^+ salvage pathway, thus contributing to the recovery of the NAD^+ pool (Revollo et al., 2004). Therefore, NAMPT activity was inhibited using the compound FK866 (Thakur et al., 2012). Initially, to confirm that the inhibitor was effectively depleting the intracellular NAD^+ pool, HeLa cells were treated with 30 nM FK866. The chart in **figure 4.6.a** shows that the inhibitor is efficiently depleting NAD^+ from the cells, achieving a 100% decrease in intracellular NAD^+ when comparing treated (TR) to untreated (NT) samples. This result shows that it is, indeed, possible to reduce NAD^+ in a PARP1-independent manner using the inhibitor FK866. It was then assessed whether ARF levels are upregulated by NAD^+ depletion. In order to do this, HeLa cells were treated with 30 nM FK866 and then harvested at different time points after treatment (**figure 4.6.b**). ARF protein levels are incresed in response to NAMPT inhibition, with a 60% increase being observed 24 h following FK866 treatment. These results suggest NAD^+ depletion upon FK866 treatment leads to ARF induction. A 48 h treatment was then performed to assess whether ARF is induced in response to a longer depletion of NAD^+. However, longer treatments with FK866 lead to extensive cell death (data not shown) agreeing with previously published data (Billington et al., 2008; Hasmann and Schemainda, 2003). Therefore there are technical limitations in assessing if long-term depletion of NAD^+ leads to ARF induction using the inhibitor FK866.

However, in multiple myeloma (MM) cancer cells it has been reported that NAMPT depletion effectively decreases the amount of intracellular NAD^+, abolishing the action of the NAD^+ salvage pathway (Cea et al., 2012). It was then possible to test if depletion of NAD^+ for a longer period increases ARF levels.

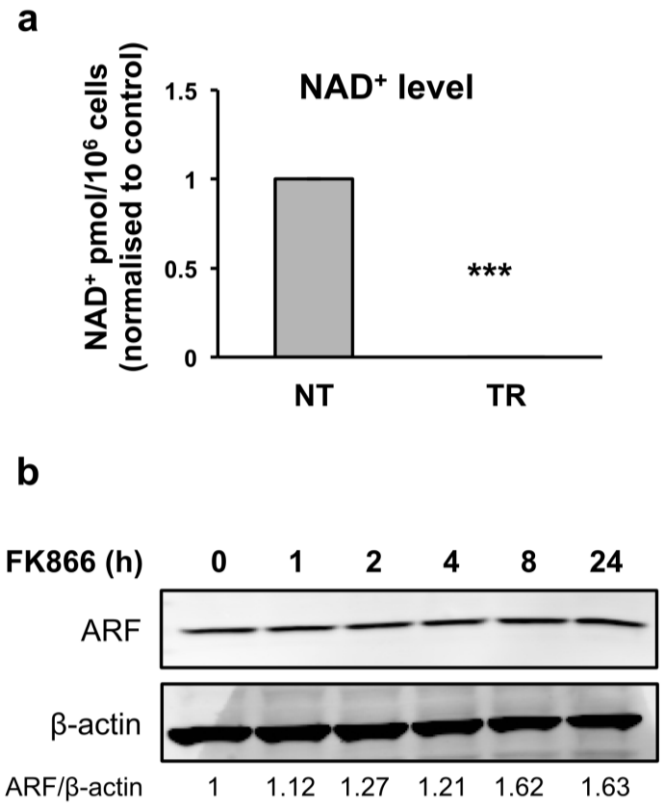

Figure 4.6: ARF levels increase in response to FK866 treatment.
a) HeLa cells were treated with 30 nM FK866. After 24 h, untreated (NT) and treated (TR) cells were harvested and counted. 2 X 10^5 cells were used for measuring the intracellular NAD^+ concentration and the obtained values were normalised to the control (NT). The graph represents the average ± S.E. of three independent experiments and the p-value was calculated using the Student's t-test (***p<0.001).
b) HeLa cells were treated with 30 nM FK866 and harvested at the indicated time points (h). WCEs were prepared and analysed by SDS-PAGE. The level of ARF was analysed by immunoblotting; β-actin was used as a loading control. ARF signal was quantified and normalised against β-actin signal. Values were then normalised to the control (FK866 0h). The images displayed are representative of three independent experiments.

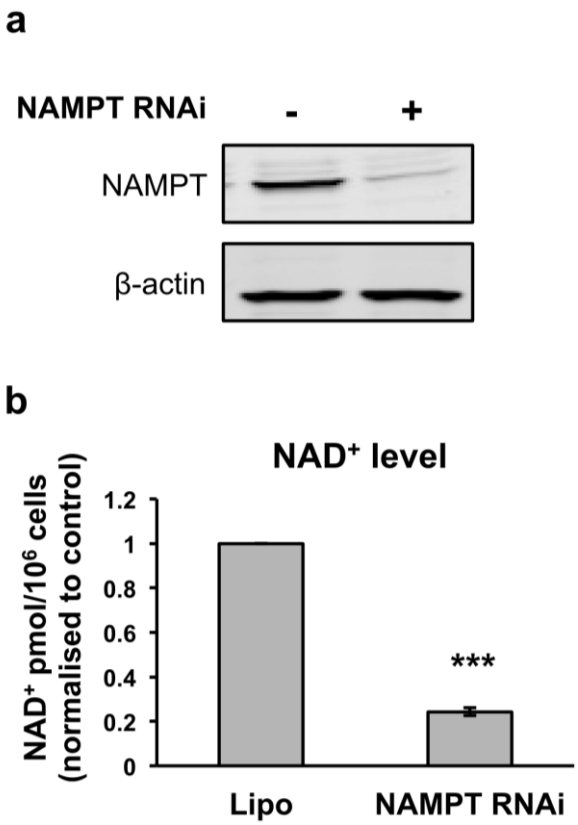

Figure 4.7: NAMPT knockdown leads to NAD^+ depletion.
a) HeLa cells were transfected with lipofectamine only (-) or in combination with NAMPT RNAi (+) (200 pmol) for 72 h. WCEs were prepared and analysed by SDS-PAGE. The level of NAMPT was assessed by immunoblotting; β-actin was used as a loading control. The images displayed are representative of three independent experiments.
b) Following RNAi trasfection, 2 X 10^5 cells were used to measure the intracellular NAD^+ concentration and the obtained values were normalised to the control (Lipo). The graph represents the average ± S.E. of three independent experiments and the p-value was calculated using the Student's t-test (***$p<0.001$).

To do so, HeLa cells were transfected with NAMPT RNAi for 72 h. **Figure 4.7.a** shows efficient depletion of NAMPT (80-90%) using RNAi. To measure the amount of NAD^+ in NAMPT-depleted cells, HeLa cells were transfected with NAMPT RNAi and a NAD^+/NADH colorimetric assay was carried out. The graph in **figure 4.7.b** represents the average amount of NAD^+ in three independent experiments following NAMPT depletion. The intracellular NAD^+ level decreases by 80% after 72 h compared to lipofectamine only treated cells (Lipo) with NAMPT knockdown cells (NAMPT RNAi). Therefore, NAMPT depletion can be used as a tool to study the effect of prolonged NAD^+ depletion on the *ARF* tumour suppressor gene.

To analyse the effect on ARF levels following NAMPT depletion, HeLa cells were transfected for 72 h. NAMPT protein is efficiently depleted as shown in **figure 4.8** and NAMPT depletion leads to a 1.7-fold increase in ARF levels. To exclude the possibility that this increase is caused by changes in the level of both XRCC1 and PARP1 in NAMPT-depleted cells, XRCC1 and PARP1 levels were also determined. Since neither XRCC1 nor PARP1 are affected by the reduction of NAMPT as shown in **figure 4.8**, it was concluded that an increase in ARF is caused by a decrease in the intracellular level of NAD^+. These data suggest that the concentration of NAD^+ is the intracellular messenger reporting an accumulation of SBs, thus triggering ARF upregulation.

Since ARF induction was previously shown to occur via upregulation of its mRNA levels, it was speculated that NAD^+ depletion could trigger the increase in ARF levels by activating a transcriptional mechanism. To evaluate the level of the *ARF* mRNA in NAD^+ depleted conditions, HeLa cells were transfected with NAMPT RNAi for 72 h. To assess the quality of the mRNA, the total mRNA was loaded on 1% agarose gel and the 2:1 ratio between the 28S and the 18S rRNA subunits was determined (**figure 4.9.a**). *ARF* mRNA levels were measured and *GAPDH* mRNA levels were used as loading control.

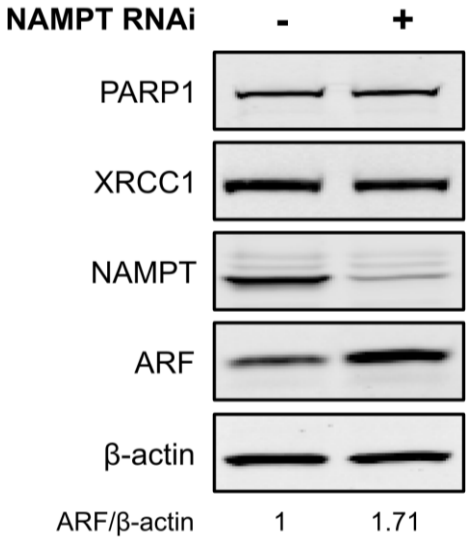

Figure 4.8: NAMPT knockdown promotes ARF increase by depleting NAD$^+$.
HeLa cells were transfected with lipofectamine only (-) or in combination with NAMPT RNAi (+) (200 pmol) for 72 h. WCEs were prepared and analysed by SDS-PAGE. The levels of PARP1, XRCC1, NAMPT and ARF were assessed by immunoblotting; β-actin was used as a loading control. ARF signal was quantified and normalised against β-actin signal. Values were then normalised to the control (Lipo). The images displayed are representative of three independent experiments.

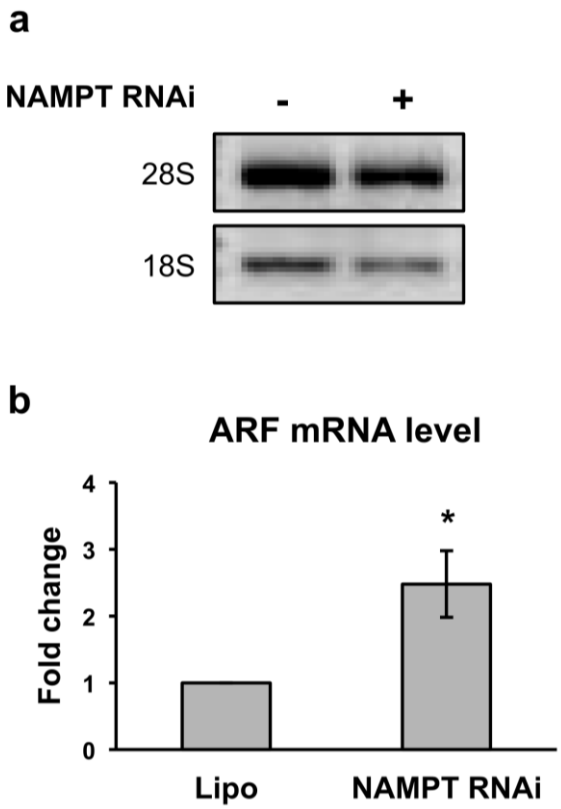

Figure 4.9: NAMPT knockdown promotes *ARF* transcription.
a) HeLa cells were transfected with lipofectamine only (-) or in combination with NAMPT RNAi (+) (200 pmol) for 72 h. RNA extraction was performed and 1 µg of total RNA was loaded on a 1% agarose gel to assess the RNA quality. The 2:1 ratio between the 28S and the 18S rRNA subunits was then determined.
b) cDNA was prepared and qPCR was performed to analyse *ARF* expression. *GAPDH* mRNA levels were used as a loading control. Values were normalised to the Lipo-treated control. The graph represents the average ± S.E. of three independent experiments. The p-value was calculated using the Student's t-test (*$p<0.05$).

Figure 4.9.b shows that in NAMPT-depleted samples (NAMPT RNAi), *ARF* mRNA levels are increased by 2-fold compared to the control samples (Lipo). These results provide the link between SB formation, PARP1 activation and *ARF* mRNA upregulation.

These findings suggest that in response to persistent SBs *ARF* mRNA levels are upregulated, through the activation of DNA damage signalling via PARP1, by modulating the NAD^+ pool. A work in progress model for ARF regulation in response to persistent SBs is represented in **figure 4.10**.

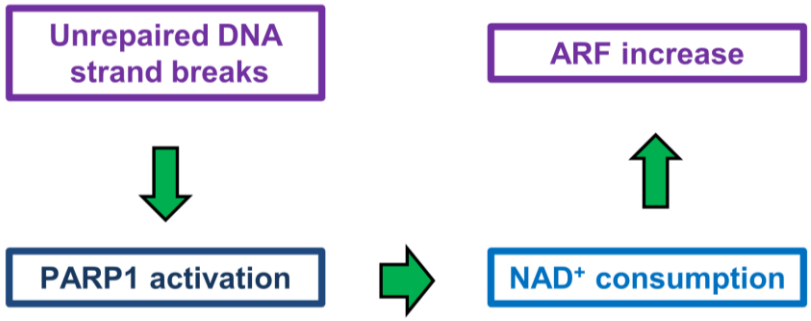

Figure 4.10: Model in progress for ARF induction.
Persistent SBs lead to PARP1 activation followed by NAD^+ depletion and consequently ARF upregulation.

In this chapter, PARP1 activity was linked to an increase in the *ARF* tumour suppressor gene for the first time, strengthening the function of this enzyme in response to unrepaired SBs. Hence, unrepaired SBs are detected by PARP1 and signalled via NAD^+ consumption. This process can be considered as a mechanism to assess the amount of DNA damage; in fact, the more SBs, the more PARP1 units are activated, the more NAD^+ is consumed and the more *ARF* mRNA synthesis (and possibly other components) is induced. It can be speculated that once the minimal threshold of intracellular NAD^+ is reached, ARF levels are upregulated to convey the message that the DNA damage accumulated cannot be resolved and perhaps to activate other types of cellular responses, such as cell cycle arrest.

Finally, it was demonstrated that ARF is induced by persistent SBs at the transcriptional level and that PARP1 activation and consumption of NAD^+ are required. Since it was

previously shown that the ARF promoter is regulated by the transcription factor E2F1 (Komori et al., 2005) which is in turn regulated by the NAD^+-dependent deacetylase SIRT1 (Wang et al., 2006), it was next tested whether induction of ARF by SBs is SIRT1 and E2F1-dependent.

5. SIRT1 and E2F1 regulate *ARF* transcription in response to unrepaired SBs

5.1 SIRT1 inhibition leads to ARF induction

5.1.1 SIRT1 activity is inhibited through PARP1-dependent depletion of NAD^+

As discussed in the previous chapter, PARP1-dependent regulation of ARF requires the reduction of the intracellular level of NAD^+. However, the PARP protein family is not the only class of enzymes that use NAD^+ as a co-factor. The class III histone deacetylase proteins, called sirtuins, are the major consumers of NAD^+ in a cell together with PARP1 (Frye, 1999; Langley et al., 2002). Indeed, SIRT1 and PARP1 have been reported to regulate each other's activity throughout the consumption of the available NAD^+ (Bai et al., 2011; Caito et al., 2010; Kolthur-seetharam et al., 2006), suggesting that SIRT1 was the possible candidate to be potentially involved in the regulation of ARF levels.

To test this hypothesis, it was first assessed whether SIRT1 activity is inhibited in XRCC1-depleted cells by checking the acetylation status of known-targets of SIRT1. Deacetylation of histone 3 on lysine 9 (H3K9) has been reported to increase in SIRT1-depleted cells (Vaquero et al., 2004). Therefore, HeLa cells were transfected with a SIRT1 specific RNAi sequence to confirm that SIRT1 depletion affects the acetylation status of H3K9 in this cellular system. **Figure 5.1**. shows that SIRT1 knockdown was efficiently achieved with a ~ 80% decrease of SIRT1 levels. Moreover, SIRT1 depletion mildly increases total H3 (H3 TOT) levels (10%), whereas a 1.9-fold increase is observed in acetylation of H3K9

(H3AcK9). Therefore acetylated H3K9 can be used to indirectly monitor SIRT1 activity in HeLa cells and if SIRT1 inhibition were to occur, the upregulation of the H3AcK9 would be detected. To confirm if SIRT1 activity was inhibited in response to unrepaired SBs, HeLa cells were transfected with XRCC1 RNAi for 72 h. **Figure 5.2.a** shows that XRCC1 knockdown is efficiently achieved and the SIRT1 protein level is not affected by XRCC1 depletion, thus proving that any effects on SIRT1 targets are not caused by changes in the protein level. Analysis of the acetylation status of H3K9 reveals that the XRCC1-depleted samples show an increase in the H3AcK9 form compared to the lipofectamine treated samples. The ratio between the acetylated form and total H3 was calculated and the average of three independent experiments is displayed in **figure 5.2.b**. The chart shows that a consistent 50% increase in the acetylated H3K9 form was obtained in XRCC1 knockdown cells. These results suggest that SIRT1 activity is inhibited in response to the formation of persistent SBs. Together, these data indicate that SB formation leads to inhibition of SIRT1 deacetylase activity as a consequence of PARP1-dependent NAD^+ consumption. In accordance with previously published data (Bai et al., 2011; Liu et al., 2009; Pang et al., 2011), these results suggest that the interplay between PARP1 activation and SIRT1 inhibition might be important for the regulation of their downstream targets, such as the newly identified target ARF.

5.1.2 SIRT1 depletion leads to ARF upregulation

To test whether SIRT1 inhibition is necessary for triggering an increase in ARF, HeLa cells were treated with SIRT1 RNAi, thus mimicking the inhibition of the protein itself. **Figure 5.3** shows that there is indeed a 3.3-fold upregulation in the ARF protein level in SIRT1-depleted cells suggesting that SIRT1 activity antagonises an increase in ARF. XRCC1 was assessed to rule out that its protein level was not affected by SIRT1 knockdown. As shown in **figure 5.3**, XRCC1 protein levels show only a slight decrease (~15%) in SIRT1-depleted cells.

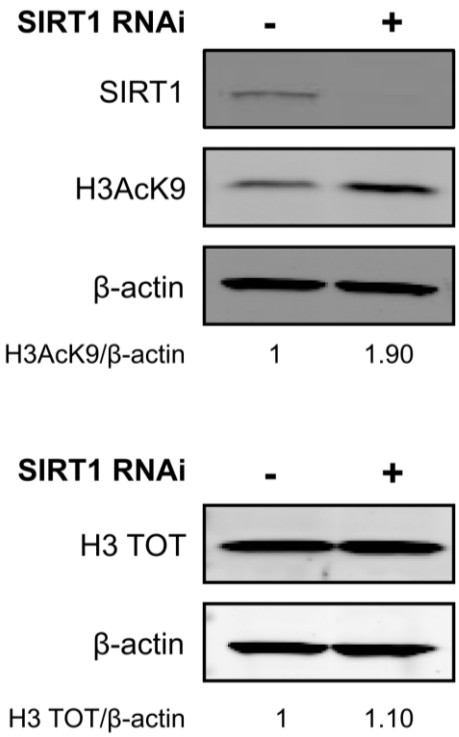

Figure 5.1: SIRT1 depletion increases the acetylation status of H3K9.
HeLa cells were transfected with lipofectamine only (-) or in combination with SIRT1 RNAi (+) (200 pmol) for 72 h. WCEs were prepared and analsyed by SDS-PAGE. The level of SIRT1, H3 TOT and H3AcK9 were analysed by immunoblotting. β-actin was used as a loading control. H3AcK9 and H3 TOT signals were quantified and normalised against β-actin signal. Values were then normalised to the control (Lipo). The displayed images are representative of three independent experiments.

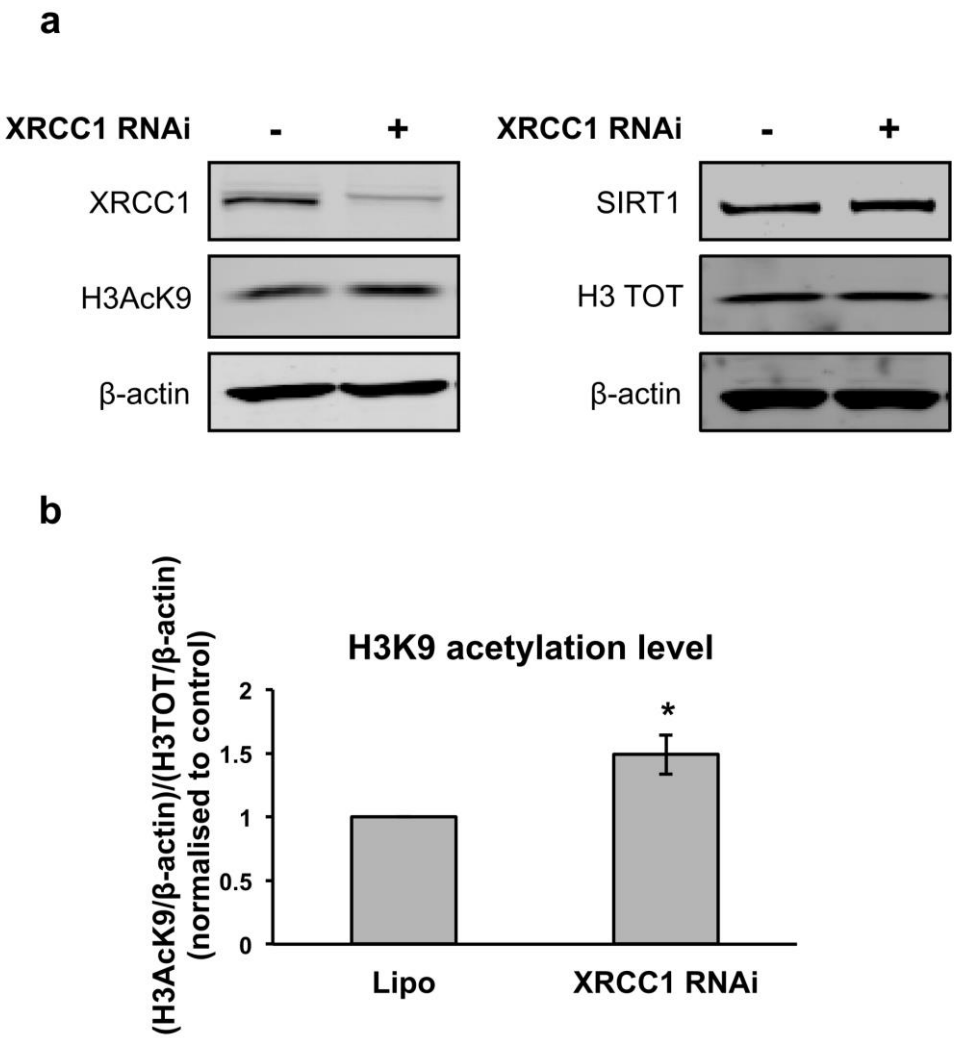

Figure 5.2: XRCC1 depletion reduces SIRT1 activity.
a) HeLa cells were transfected with lipofectamine only (-) or in combination with XRCC1 RNAi (+) (200 pmol) for 72 h. WCEs were prepared and analsyed by SDS-PAGE. The level of SIRT1, XRCC1, H3 TOT and H3AcK9 were analysed by immunoblotting. β-actin was used as a loading control. The displayed images are representative of three independent experiments.
b) H3TOT and H3AcK9 signals were quantified and normalised against the β-actin signal. The H3AcK9/H3 TOT ratio was calculated and the average values were plotted on an histogram graph. Values were normalised to the control (Lipo). The graph represents the average ± S.E. of three independent experiments and the p-value was calculated by the Student's t-test (*$p<0.05$).

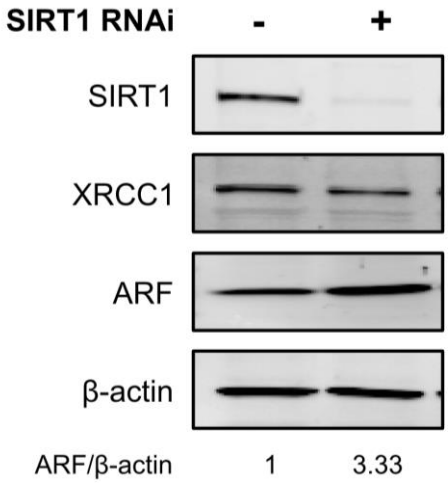

Figure 5.3: SIRT1 depletion triggers ARF induction.
HeLa cells were transfected with lipofectamine only (-) or in combination with SIRT1 RNAi (+) (200 pmol) for 72 h. WCEs were prepared and analsyed by SDS-PAGE. The level of SIRT1, XRCC1 and ARF were analysed by immunoblotting. β-actin level was used as a loading control. ARF signal was quantified and normalised against β-actin signal. Values were then normalised to the control (Lipo). The displayed images are representative of three independent experiments.

Therefore, these results indicate that SIRT1 inhibition is necessary to increase ARF levels, suggesting that SIRT1 deacetylase activity might prevent the upregulation of expression of the *ARF* tumour suppressor gene.

5.1.3 *ARF* transcription is induced in SIRT1-depleted cells

In **chapters 3** and **4**, it has been shown that ARF regulation occurs at transcriptional level by increasing the synthesis of *ARF* mRNA levels. Therefore, to further study the molecular mechanism leading to ARF upregulation in SIRT1 knockdown cells, it was firstly examined whether ARF stability is affected by SIRT1 depletion. To assess this hypothesis, HeLa cells were transfected with SIRT1 RNAi for 72 h and then treated with 50 µg/ml of CHX. **Figure 5.4.a** shows that an efficient SIRT1 knockdown is achieved and that ARF levels decrease in response to treatment, thus confirming the validity of CHX treatment. However, ARF stability does not change when comparing lipofectamine-treated (Lipo) and SIRT1-depleted (SIRT1 RNAi) sample kinetics following treatment (**figure 5.4.a**). Finally, the average of the obtained values from three independent experiments was then plotted on a bar chart as shown in **figure 5.4.b**.

The analysis of *ARF* mRNA levels was carried out after SIRT1 depletion. HeLa cells were treated with SIRT1 RNAi for 72 h. To verify the quality of the RNA obtained, the total RNA was loaded on agarose gel and the 2:1 ratio between the 28S and the 18S rRNA subunits was determined (**figure 5.5.a**). Once the quality of the total RNA was verified, *ARF* mRNA levels were assessed and then normalised against *GAPDH* mRNA levels. The graph displayed in **figure 5.5.b** shows that there is a 2-fold increase in *ARF* mRNA levels in SIRT1 RNAi samples compared to lipofectamine-treated (Lipo) samples.

These findings indicate that inhibition, mimicked by downregulating SIRT1 by RNAi, triggers the upregulation of *ARF* mRNA levels. Together, these data suggest that persistent SBs lead to PARP1-dependent NAD^+ depletion, thus inhibiting SIRT1 deacetylase activity and enabling the induction of *ARF* expression.

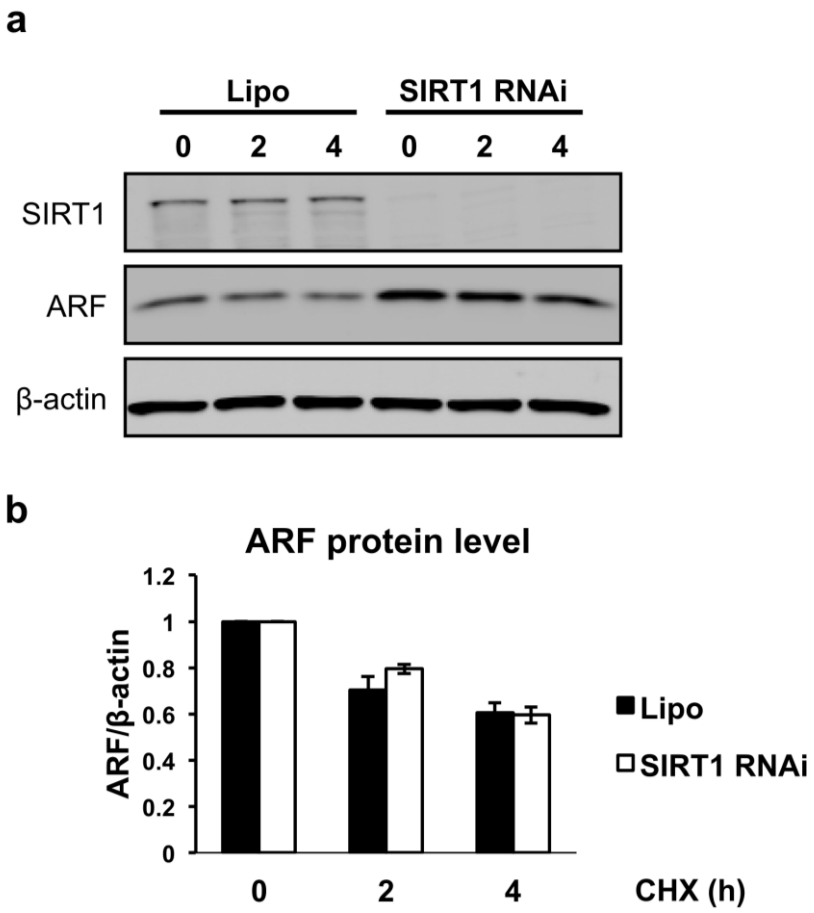

Figure 5.4: ARF stability is not affected by SIRT1 depletion.
a) HeLa cells were transfected with either lipofectamine only (Lipo) or in combination with 200 pmol SIRT1 RNAi. After 72 h cells were treated with 50 µg/ml CHX and harvested at the indicated (h) time points. WCEs were prepared; SDS-PAGE and western blotting assays were carried out. SIRT1, ARF and β-actin (loading control) protein levels were assessed. The displayed images are representative of three independent experiments.
b) ARF signals (a) were quantified and normalised against β-actin signals. Values of each group of samples were normalised to the respective control (0 h time point). The graph represents the average ± S.E. of three independent experiments.

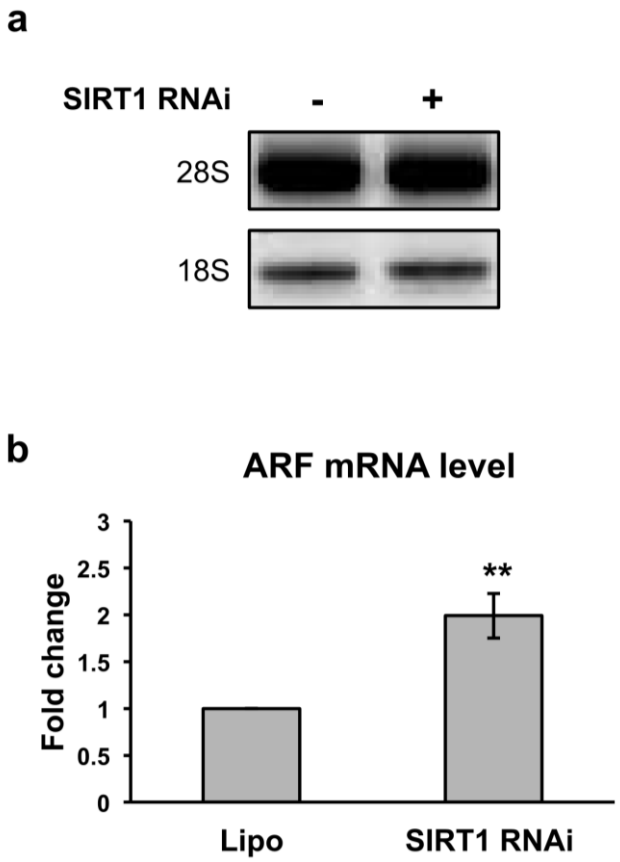

Figure 5.5: SIRT1 depletion triggers an increase of *ARF* transcription.
a) HeLa cells were transfected with either lipofectamine only (-) or in combination with 200 pmol SIRT1 RNAi (+). After 72 h, cells were harvested and RNA extraction was performed. 1 µg of total RNA was loaded on a 1% agarose gel .The 2:1 ratio between the amount of the 28S and the 18S rRNA subunits was determined.
b) cDNAs of lipofectamine only (Lipo) and of SIRT1-depleted (SIRT1 RNAi) samples were synthesised and qPCR was performed. *ARF* mRNA levels and *GAPDH* mRNA levels (loading control) were evaluated. Values were normalised to the control (Lipo). The graph represents the average ± S.E. of three independent experiments and the p-value was calculated by the Student's t-test (**p<0.01).

5.2 E2F1 transcription factor is required for ARF induction in response to unrepaired SBs

SIRT1 deacetylase activity has been reported to have a role in directly regulating gene expression by targeting histone tails, thus promoting chromatin condensation and suppression of gene transcription (Fatoba and Okorokov, 2011; He et al., 2011; Vaquero et al., 2004). Even though SIRT1 has a role in regulating the status of histone proteins, SIRT1 has also been shown to target non-histone proteins, such as the E2F1 transcription factor (Wang et al., 2006). Moreover, it has been shown that E2F1 overexpression leads to ARF upregulation by binding the *ARF* gene promoter, thus stimulating *ARF* mRNA transcription (Komori et al., 2005). Therefore, it was hypothesised that an *ARF* mRNA increase requires SIRT1 inhibition to enhance E2F1 activity, thus promoting *ARF* transcription.

To test this hypothesis, E2F1 acetylation was assessed in response to SIRT1 and XRCC1 knockdown. Since antibodies which recognise acetylated E2F1 were not commercially available, immunoprecipitation (IP) of endogenous E2F1 was performed by using two different antibodies (data not shown). The IP samples were analysed by SDS-PAGE and the membrane probed with two different pan-acetylated antibodies. However, it was not possible to assess the E2F1 acetylated status since no band of with the correct molecular weight was observed (data not shown). Despite the fact it was not feasible to assess whether E2F1 acetylation increases in response to unrepaired SBs, it was investigated whether ARF upregulation requires the presence of E2F1. In fact, if E2F1 is indispensable for ARF increase, then the depletion of the transcription factor should abolish ARF induction.

Firstly, it was evaluated if E2F1 was required for ARF upregulation in SIRT1-depleted cells. To test this hypothesis, HeLa cells were treated with SIRT1 RNAi or E2F1 RNAi or with a combination of both for 72 h. The efficiency of E2F1 and SIRT1 knockdowns was

checked (**figure 5.6**). E2F1 depletion leads to a 40% decrease in ARF levels (lane 1 and lane 2, **figure 5.6**), thus suggesting that in this cellular system *ARF* expression requires the presence of the E2F1 transcription factor. The simultaneous depletion of both E2F1 and SIRT1 abolishes the 3-fold upregulation of ARF following SIRT1 knockdown (lane 3 and lane 4, **figure 5.6**). These results show that the E2F1 protein is important for ARF induction in response to SIRT1 depletion. To assess whether E2F1 is required for ARF regulation as described in the previous model, it was necessary to verify that the E2F1 protein is essential for ARF induction in response to NAD^+ depletion (discussed in **chapter 4**) and to persistent SBs formation (discussed in **chapter 3**). HeLa cells were transfected with E2F1 RNAi sequence only or in combination with either NAMPT or XRCC1 RNAi sequences for 72 h. **Figures 5.7.a** and **5.7.b** show that E2F1, NAMPT and XRCC1 proteins are efficiently depleted. NAMPT depletion leads to a 2.2-fold increase in ARF (lane 3, **figure 5.7.a**) and this effect is reverted when E2F1 is simultaneously depleted (lane 4, **figure 5.7.a**), thus indicating that E2F1 is required for ARF upregulation in response to NAD^+ depletion. **Figure 5.7.b** further confirms that ARF induction depends on the presence of E2F1 in response to SB formation following XRCC1 knockdown (lane 3 and lane 4, **figure 5.7.b**).

It is important to note that ARF levels are 40-50% decreased in E2F1-depleted cells (lane 1 and lane 3, **figure 5.6** and **figure 5.7**), suggesting a role for E2F1 in maintaining ARF basal levels. However, the reduction in ARF protein levels when cells are simultaneously depleted of E2F1 and either SIRT1, NAMPT or XRCC1, is 1-2-fold (lane 2 and lane 4, **figure 5.6** and **figure 5.7**), suggesting that E2F1 may also be required for the induction of ARF in the assessed conditions.

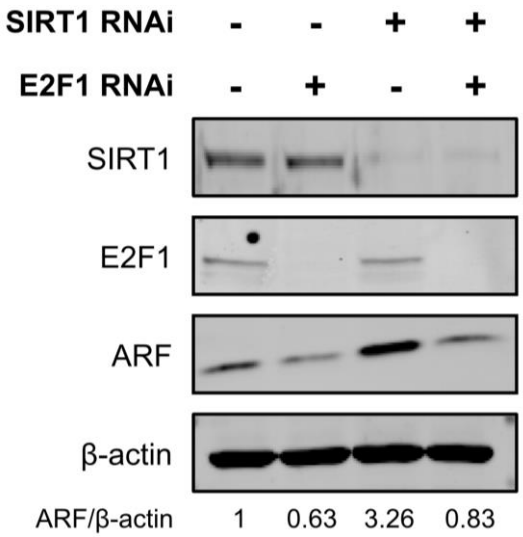

Figure 5.6: E2F1 is required for ARF induction in SIRT1-depleted cells.
HeLa cells were transfected with lipofectamine only (-) or in combination with either SIRT1 RNAi (+) or E2F1 RNAi (+) (200 pmol), or a mixture of both for 72 h. WCEs were prepared and analsyed by SDS-PAGE. The level of SIRT1, E2F1 and ARF were analysed by immunoblotting. β-actin level was used as a loading control. ARF signal was quantified and normalised against β-actin signal. Values were then normalised to the control (Lipo). The images displayed are representative of three independent experiments.

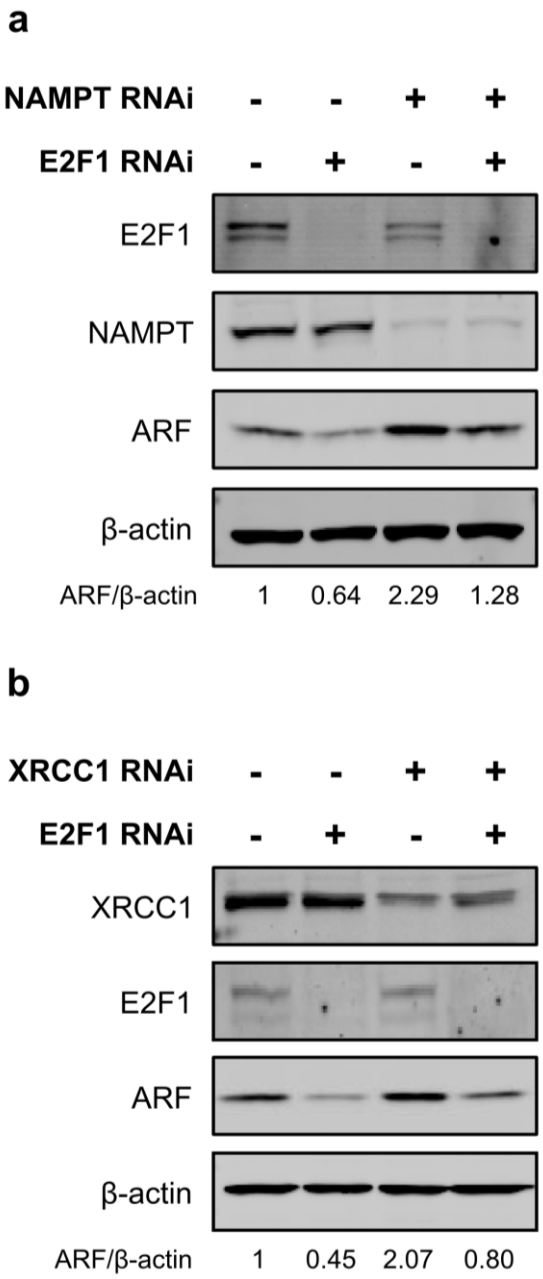

Figure 5.7: E2F1 is required for ARF induction in response to NAD^+ depletion and, ultimately, to persistent SBs.
a) HeLa cells were transfected with lipofectamine only (-) or in combination with either NAMPT RNAi (+) or E2F1 RNAi (+) (200 pmol), or a mixture of both for 72 h. WCEs were prepared and analsyed by SDS-PAGE. The level of NAMPT, E2F1 and ARF were analysed by immunoblotting. β-actin level was used as a loading control. ARF signal was quantified and normalised against β-actin signal. Values were then normalised to the control (Lipo). The images displayed are representative of three independent experiments.
b) HeLa cells were transfected with lipofectamine only (-) or in combination with either XRCC1 RNAi (+) or E2F1 RNAi (+) (200 pmol), or a mixture of both for 72 h. WCEs were prepared and analsyed by SDS-PAGE. The level of XRCC1, E2F1 and ARF were analysed by immunoblotting. β-actin level was used as a loading control. ARF signal was quantified and normalised against β-actin signal. Values were then normalised to the control (Lipo). The images displayed are representative of three independent experiments.

Altogether these novel findings uncover a new molecular mechanism of regulation of *ARF* gene expression that involves PARP1-dependent NAD^+ depletion, SIRT1 inhibition and E2F1 activation as shown in **figure 5.8**.

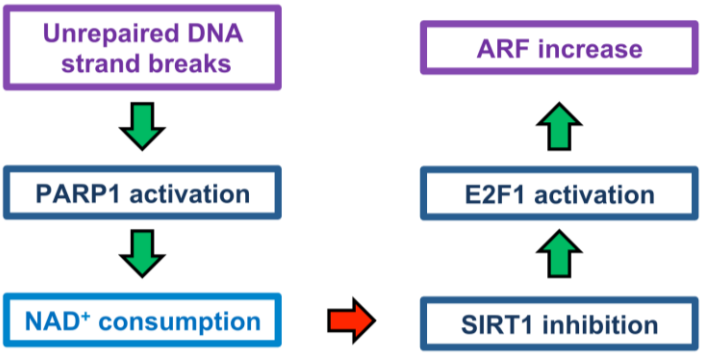

Figure 5.8: Proposed model for *ARF* gene induction in response to unrepaired SBs. Activation of PARP1 following the detection of SBs leads to the depletion of NAD^+ and consequently to the inhbition of the NAD-dependent SIRT1 enzyme, activation of E2F1 and induction of *ARF* gene transcription, eventually resulting in an increase in ARF protein levels.

It was then decided to address what are the physiological consequences of ARF induction in HeLa cells. The following chapter focuses on getting a better understanding on whether ARF upregulation plays a role in triggering cell cycle arrest or apoptosis.

6. ARF induction delays cell cycle progression in normal human fibroblasts

6.1 ARF accumulation does not affect cell cycle and cell viability following SB formation in p53-deficient cells

It was decided to assess whether an increase in ARF perturbs cell cycle progression in a p53-independent way in response to the accumulation of unrepaired SBs. To do so, HeLa cells were used since p53 accumulation is prevented by the E6 protein (Scheffner et al., 1993). Cells were depleted of XRCC1 using RNAi for 72 h and $5x10^5$ cells were subsequently prepared for the cell cycle assay, whereas the remaining cells were used for western blotting. Analysis of XRCC1 and ARF levels confirms XRCC1 depletion and ARF induction as shown in **figure 6.1.a**. Analysis of three independent experiments shows that cell cycle progression is not affected by the accumulation of persistent SBs (**figure 6.1.b**) (cell cycle profiles displayed in **Appendix II**). It was then concluded that ARF induction does not trigger the activation of checkpoint in a p53-independent in response to persistent SBs in HeLa cells. These data are in accordance with previously published results (Hemmati et al., 2005; Weber et al., 2002) which show ARF-dependence on p53 for modulating the cell cycle following cellular stress. It was then evaluated whether ARF induction affects cell viability by measuring cell death. To do so, HeLa cells were transfected with XRCC1 RNAi for 72 h and apoptosis assay was carried out. XRCC1 depletion and ARF induction was confirmed by western blotting (**figure 6.2.a**). ARF

induction does not trigger cell-death in HeLa cells as seen in **figure 6.2.b** which represents data from three independent experiments (FlowJo dot plots displayed in **Appendix III**). It was then concluded that ARF accumulation in response to persistent SBs might require p53 for eliciting both cell cycle arrest and apoptosis in HeLa cells.

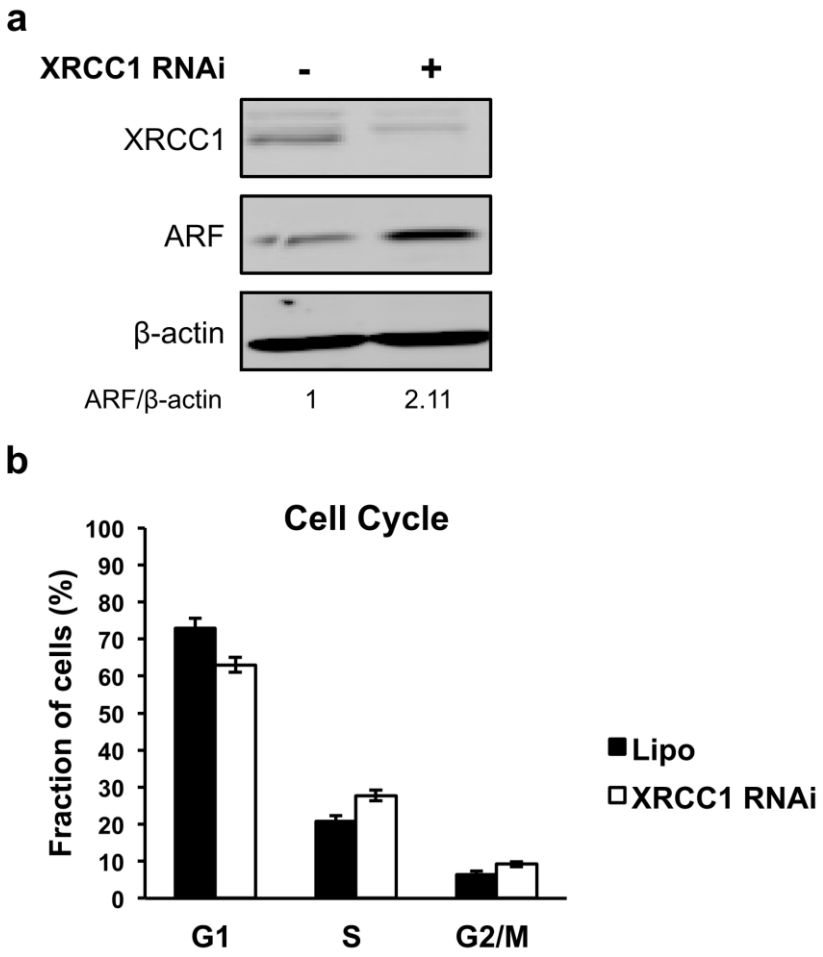

Figure 6.1: ARF induction does not affect cell cycle progression in p53-deficient HeLa cells.

a) HeLa cells were transfected with lipofectamine only (Lipo) or in combination with XRCC1 RNAi (200 pmol) for 72 h. Cells were collected, counted and $5x10^5$ cells were used for cell cycle analysis, whereas the remaining cells were used for western blotting. WCEs were prepared and analsyed by SDS-PAGE. The level of ARF and XRCC1 were analysed by immunoblotting. β-actin was used as a loading control. ARF signal was quantified and normalised against β-actin signal. Values were then normalised to the control (Lipo). Images are representative of three independent experiments.

b) Cells were fixed in ethanol and subsequently stained with PI. Sample acquisition was performed by using a FACSort machine and the cell cycle profile was analysed by Mod-Fit software. The graph shows the distribuition of the percentage of cells in the different cell cycle phases of lipofectamine-treated (black bars) and XRCC1-depleted (white bars) samples. Data represents the average ± S.E. of three independent experiments.

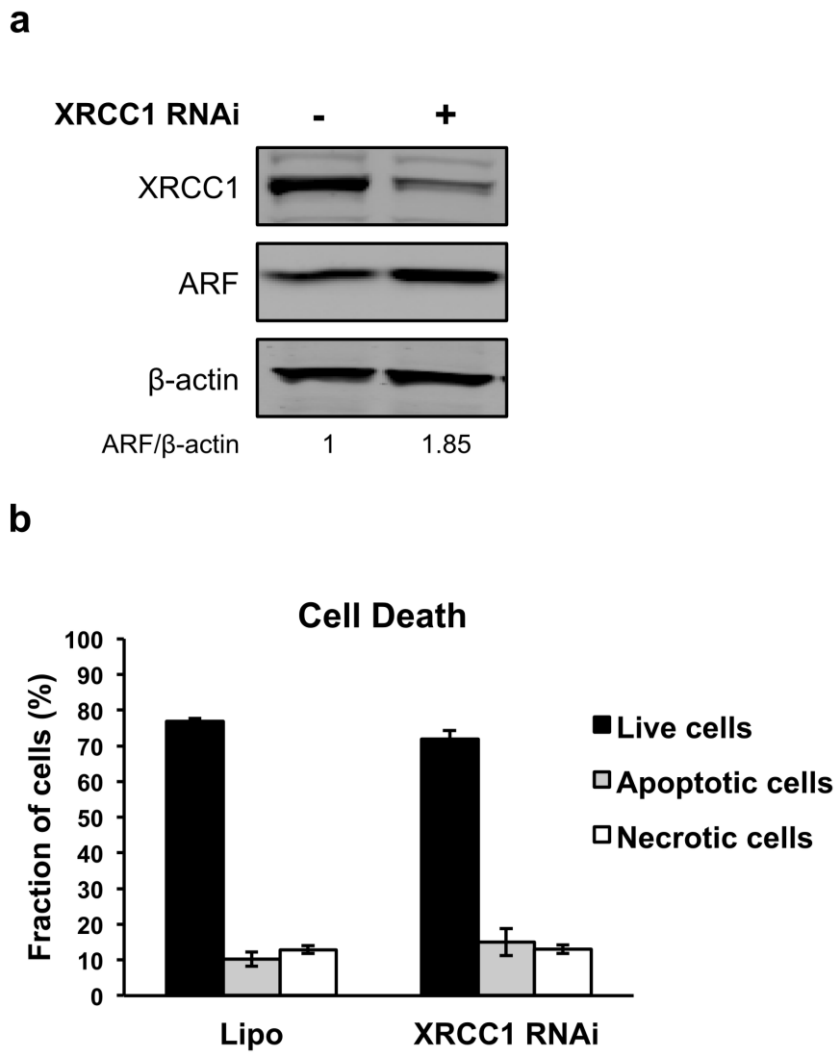

Figure 6.2: ARF increase does not trigger cell death in p53-deficient HeLa cells.
a) HeLa cells were transfected with lipofectamine only (Lipo) or in combination with XRCC1 RNAi (200 pmol) for 72 h. Cells were collected, counted and $2.5x10^5$ cells were used for the apoptosis assay, whereas the remaining cells were used for western blotting. WCEs were prepared and analsyed by SDS-PAGE. The level of ARF and XRCC1 were analysed by immunoblotting. β-actin was used as a loading control. ARF signal was quantified and normalised against β-actin signal. Values were then normalised to the control (Lipo). Images are representative of three independent experiments.
b) Cells were stained with PI and Annexin V for the apoptosis assay. Sample acquisition was performed using a FACSort machine and analysed by FlowJo software. The graph shows the percentage of live cells (black bars), apoptotic cells (grey bars) and necrotic cells (white bars) in either lipofectamine-treated (Lipo) or XRCC1-treated (XRCC1 RNAi) samples. Data represents the average of ± S.E. of three independent experiments.

6.2 ARF induction is required for G1 arrest in response to SB formation in normal human fibroblasts

6.2.1 SB formation triggers an ARF increase in human primary fibroblasts

It was then decided to characterise the downstream effects of an increase in ARF using p53-proficient human primary TIG-1 fibroblasts. Firstly, it was investigated whether ARF could be induced in response to SB accumulation. To do so, TIG-1 cells were transfected with XRCC1 RNAi for 72 h. **Figure 6.3** shows that XRCC1 is efficiently depleted and the synthesis of PAR occurs, suggesting that formation of persistent SBs also occurs in normal cells when BER is disabled. Once it was demonstrated that the same conditions obtained in HeLa cells could be reproduced in TIG-1 cells, ARF protein levels were assessed. Upon XRCC1 depletion, ARF levels display a 30% increase in TIG-1 cells (lane 1 and lane 3, **figure 6.4**). Furthermore, p53 levels are slightly increased in response to SB formation. It was then hypothesised that ARF accumulation may be limited due to the presence of functional p53. In fact, ARF expression has been reported to be regulated by a p53 negative feedback loop (Robertson and Jones, 1998; Zeng et al., 2011); therefore when ARF is upregulated, p53 increases and restores ARF basal levels. It was then speculated that p53 depletion would indeed allow a greater detection of ARF accumulation by SB formation. To verify this hypothesis, TIG-1 cells were transfected with a combination of XRCC1 or p53 RNAi sequences. **Figure 6.4** shows that p53-depletion does not affect ARF levels when compared to lipofectamine-treated samples (lane 1 and lanes 2); however, when XRCC1 and p53 are simultaneously depleted, a 50% increase in ARF protein levels is observed, suggesting ARF levels are maintained low by the action of the p53 negative feedback loop (lane 1 and lane 4).

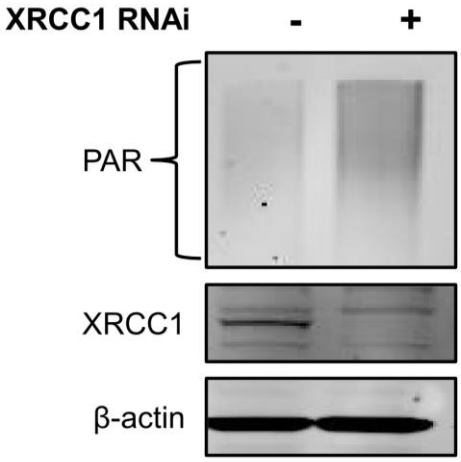

Figure 6.3: XRCC1-depletion leads to SB formation in TIG-1 cells.
TIG-1 cells were transfected with lipofectamine only (-) or in combination with XRCC1 RNAi (+) (200 pmol) for 72 h. WCEs were prepared and analsyed by SDS-PAGE. The level of PAR and XRCC1 were analysed by immunoblotting. β-actin was used as a loading control. Images are representative of three independent experiments.

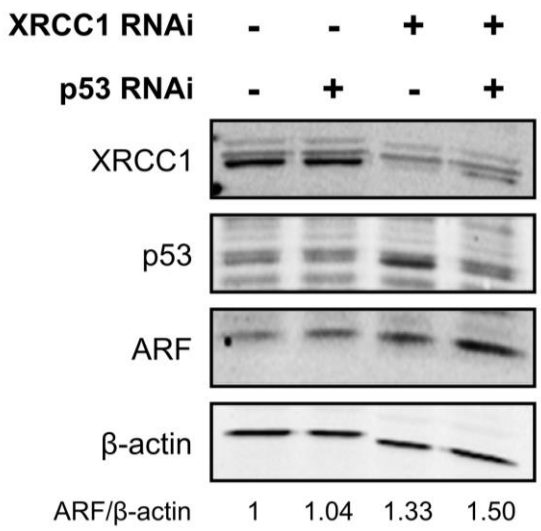

Figure 6.4: ARF induction in response to unrepaired SBs is controlled by the p53 negative feedback loop in TIG-1 cells.
TIG-1 cells were transfected with lipofectamine only (-) or in combination with either XRCC1 RNAi (+) or p53 RNAi (+) (200 pmol), or a mixture of both for 48 h. WCEs were prepared and analsyed by SDS-PAGE. The level of XRCC1, p53 and ARF were analysed by immunoblotting. β-actin level was used as a loading control. ARF signal was quantified and normalised against β-actin signal. Values were then normalised to the control (Lipo). Images displayed are representative of three independent experiments.

In order to also assess whether ARF upregulation is triggered by NAD^+ depletion and SIRT1 inhibition in normal cells, TIG-1 cells were seeded and transfected using NAMPT, SIRT1 and p53 RNAi sequences or a combination of those ones as indicated in **figure 6.5.a** and **figure 6.5.b**. NAMPT and SIRT1 silencing leads to an increase in ARF protein levels as displayed in **figure 6.5.a** and **figure 6.5.b** respectively. However, when p53 is depleted in combination with either NAMPT or SIRT1 proteins, ARF accumulation is substantially increased, further suggesting that the p53 feedback loop limits an ARF increase.

Together these data indicate that ARF is induced in response to persistent SBs in normal TIG-1 fibroblasts and that p53 keeps the accumulation of ARF under control in this pathway.

6.2.2 DNA SB signalling leads to ARF-dependent G1 arrest in human primary fibroblasts

It has been previously shown that ARF accumulation does not influence cell cycle progression and does not trigger apoptosis in HeLa cells (**figure 6.1** and **figure 6.2**). To assess whether the formation of SBs would lead to cell cycle arrest, TIG-1 cells were transfected with XRCC1. Furthermore, to assess whether ARF is required for coordinating cell cycle progression in response to persistent SBs, ARF was depleted using RNAi. **Figure 6.6** represents the average amount of cells distributed between the cell cycle phases in three independent experiments (cell cycle profiles displayed in **Appendix IV**). XRCC1-depleted samples show a statistically significant increase in the amount of cells in G1-phase when compared to lipofectamine-treated samples, suggesting that the accumulation of SBs leads to G1 arrest. Moreover, the amount of cells entering S-phase is reproducibly reduced (lipo and XRCC1 RNAi samples), confirming the arrest in G1. The cells lacking ARF show a similar cell cycle profile compared to the lipofectamine ones, thus indicating that ARF is not required in unperturbed situation and does not affect the cell cycle progression.

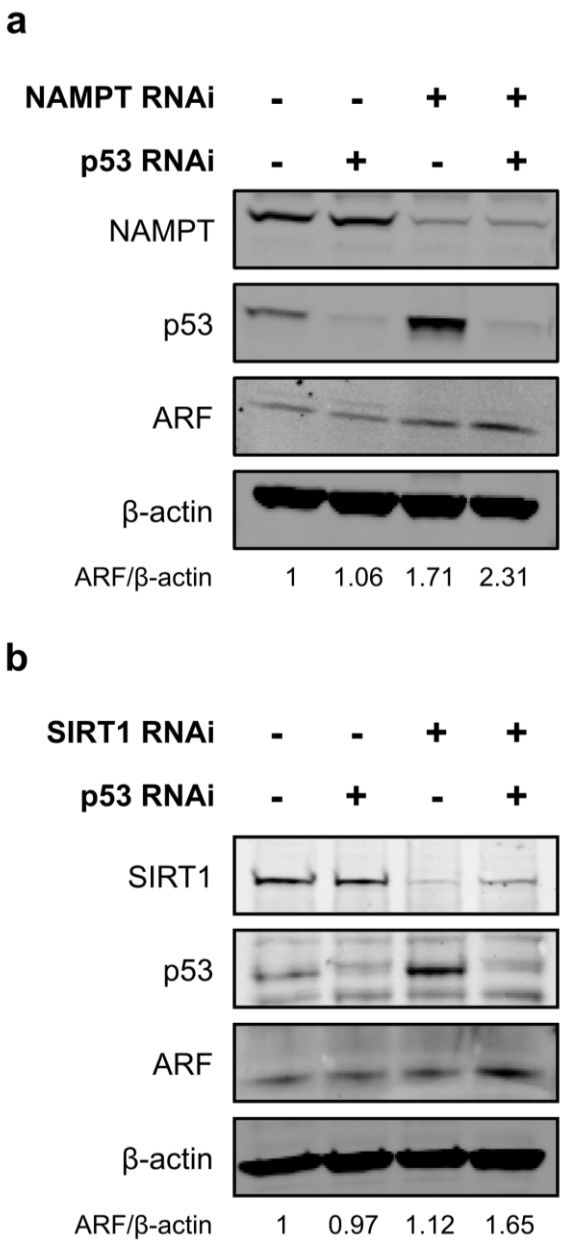

Figure 6.5: ARF is induced in response to NAMPT and SIRT1 depletion in TIG-1 cells when p53 is knocked down.
a) TIG-1 cells were transfected with lipofectamine only (-) or in combination with either NAMPT RNAi (+) or p53 RNAi (+) (200 pmol), or a mixture of both for 48 h. WCEs were prepared and analsyed by SDS-PAGE. The level of NAMPT, p53 and ARF were analysed by immunoblotting. β-actin level was used as a loading control. ARF signal was quantified and normalised against β-actin signal. Values were then normalised to the control (Lipo). Images displayed are representative of three independent experiments.
b) TIG-1 cells were transfected with lipofectamine only (-) or in combination with either SIRT1 RNAi (+) or p53 RNAi (+) (200 pmol), or a mixture of both for 48 h. WCEs were prepared and analsyed by SDS-PAGE. The level of SIRT1, p53 and ARF was analysed by immunoblotting. β-actin was used as a loading control. ARF signal was quantified and normalised against β-actin signal. Values were then normalised to the control (Lipo). Images are representative of three independent experiments.

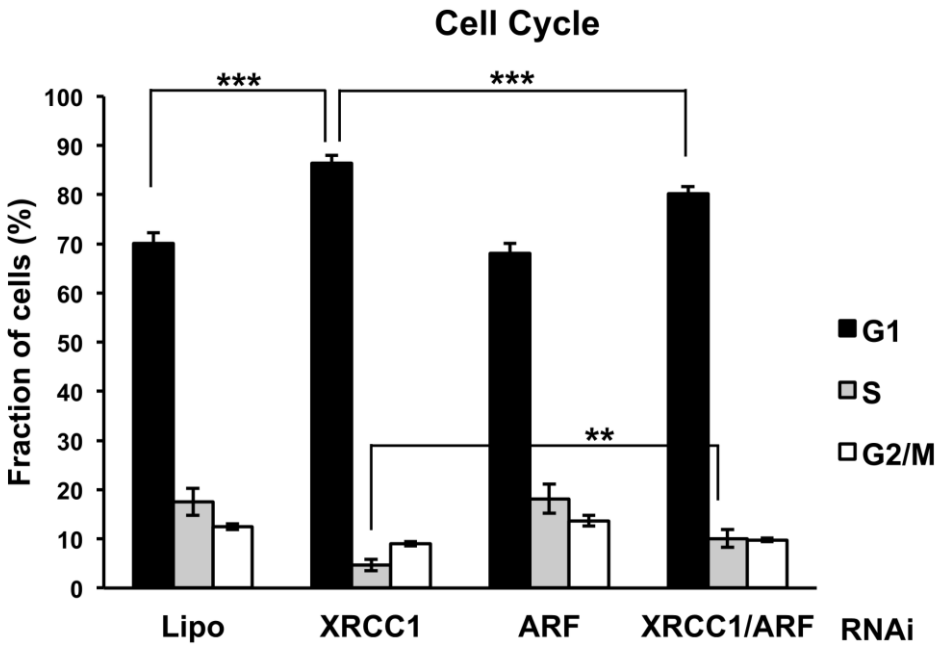

Figure 6.6: ARF is required for G1 arrest in response to persistent SBs in TIG-1 cells. TIG-1 cells were transfected with lipofectamine only (Lipo) or in combination with either XRCC1 RNAi or ARF RNAi (200 pmol), or a mixture of both for 48 h. Cells were harvested, counted, fixed in ethanol and subsequently stained with PI. Sample acquisition was performed using a FACSort machine and the cell cycle profile was analysed by Mod-Fit software. The graph shows the distribuition of the percentage of cells in the different cell cycle phases (black bars for the G1 phase, grey bars for the S-phase and white bars for the G2/M phase). Data represents the average ± S.E. of three independent experiments. The p-values were calculated by the Student's t-test (**p<0.01; ***<0.001).

However, in response to the formation of SBs, the cells depleted of ARF show a defective G1 arrest along with a partially restored S-phase population compared to the cells lacking XRCC1 only. These data indicate that ARF is required for G1 cell cycle arrest in response to persistent SBs in p53-proficient TIG-1 cells.

To complete the above data, it was investigated whether ARF-dependent regulation of the cell cycle is p53-mediated by checking the level of p21, the main p53 target responsible for cell cycle arrest. TIG-1 cells were transfected using either XRCC1 or ARF RNAi sequences or with a combination of both. In response to the formation of SBs upon XRCC1 depletion, p53 increases is ~ 10%; however, p21 level is 60% increased as shown in **figure 6.7**. When ARF is downregulated in a XRCC1 background, the p21 level is reduced (30%) suggesting that ARF may have a role in triggering G1 arrest by sustaining p21 induction. However, it is important to note that ARF depletion leads to a decrease in p21 basal levels (lane 1 and lane 3, **figure 6.7**), suggesting that ARF may also have a role in maintaining p21 levels in unperturbated conditions. Altogether these data indicate that an increase in ARF is important in reporting DNA damage, thus regulating cell-cycle progression and avoiding the accumulation of DNA mutations which could lead to genomic instability.

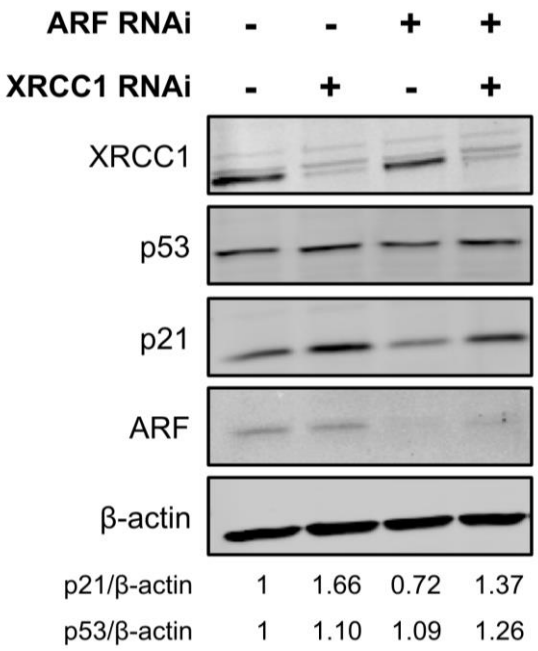

Figure 6.7: ARF downregulation reduces p21 induction in response to SBs in TIG-1 cells. TIG-1 cells were transfected with lipofectamine only (Lipo) or in combination with either XRCC1 RNAi or ARF RNAi (200 pmol), or a mixture of both for 48 h. WCEs were prepared and analsyed by SDS-PAGE. The level of XRCC1, p53, p21 and ARF were analysed by immunoblotting. β-actin level was used as a loading control. p21 and p53 signals were quantified and normalised against β-actin signal. Values were then normalised to the control (Lipo). Images are representative of three independent experiments.

7. Discussion

7.1 Overview

The data presented in this thesis provide a novel mechanism of induction for the tumour suppressor gene *ARF* in response to persistent DNA damage **(Figure 7.1)**. As shown in **chapter 3**, XRCC1 depletion has been used as a tool to create persistent DNA damage. PAR accumulation was used to monitor the incurrence of persistent DNA damage. Moreover, XRCC1-depleted cells have been shown to accumulate DNA damage as assessed by alkaline comet assay (data not shown). These data are in agreement with other previously published data suggesting accumulation of DNA damage upon XRCC1 depletion, eventually leading to the induction of SCEs (Brem and Hall, 2005; Fan et al., 2007). Moreover, deficiency in the repair of SBs has been also investigated in *XRCC1* -/- CHO E9 cells, suggesting that the lack of XRCC1 leads to unrepaired SBs (Caldecott, 2003b). Indeed, XRCC1 depletion disables the ligation step of the BER pathway, thus creating a situation in which the repair of endogenous lesions cannot be completed (Brem and Hall, 2005; Fan et al., 2007; Shen et al., 1998). In this study, it has been shown that XRCC1 depletion correlates with an increase in the ARF protein levels as a consequence of induction of *ARF* transcription. Moreover, a correlation between PARP1 activation and ARF upregulation has been described. Indeed, as shown in **chapter 4**, PARP1 activity is required for the upregulation of ARF at both protein and mRNA levels. Since, PARP1 uses NAD^+ for its catalytic activity (Singh et al., 1985), it has been shown that NAD^+ depletion correlates with the induction of ARF, possibly through the consumption of the metabolite by PARP1. To mimic the depletion of NAD^+ in a PARP1-independent manner, the NAD^+

salvage pathway has been disabled by knocking down NAMPT, one of the enzymes responsible for the reconstitution of the NAD^+ pool (Cea et al., 2012; Revollo et al., 2004). Indeed, ARF induction is directly triggered by a decrease in NAD^+, thus suggesting that PARP1-dependent depletion of NAD^+ is the stimulus necessary for upregulating ARF. NAD^+ is used as a co-factor by other proteins such as the SIRT1 deacetylase protein (Frye, 1999; Langley et al., 2002). As detailed in **chapter 5**, SIRT1 inhibition is necessary to increase ARF levels and to stimulate *ARF* transcription, linking PARP1-dependent NAD^+ depletion and ARF upregulation. Finally in this chapter, the E2F1 transcription factor, which is negatively regulated by SIRT1 deacetylase activity (Wang et al., 2006), has been shown to be required for an increase in ARF levels in response to SB formation. It is important to note that the amplitude of ARF upregulation was found to be variable between experiments from 0.5 to 3-fold induction. It was observed that early passage cells display a greater ARF induction compared to late passage cells, suggesting that upregulation of ARF might be affected by the prolonged maintenance of cells in culture. Since cells accumulate DNA damage overtime, it can be speculated that ARF might be gradually induced until a plateau is reached. Thus, when XRCC1 is depleted the amplitude of the induction would be smaller if ARF levels are already high. However, further investigation is required to assess such hypothesis.

Finally, the biological relevance of ARF upregulation has been investigated in **chapter 6**. Since ARF function is linked to p53 function (Sherr, 2006), it is necessary to study the downstream effects of ARF upregulation in a p53-proficient cell line. HeLa cells were used since in these cells ARF induction can be tolerated because p53 accumulation is impaired in the presence of the E6 protein (Scheffner et al., 1993). However, to assess the consequences of ARF induction in response to SB accumulation in a p53-profiencent cellular system TIG-1 cells were used. Firstly, in response to persistent SBs ARF induction is limited by the negative p53 feedback loop which maintains low levels of ARF. More importantly, it has been shown that ARF is required for G1 arrest in response to SB

formation, thus suggesting an important role for ARF in reporting DNA damage and avoiding genomic instability.

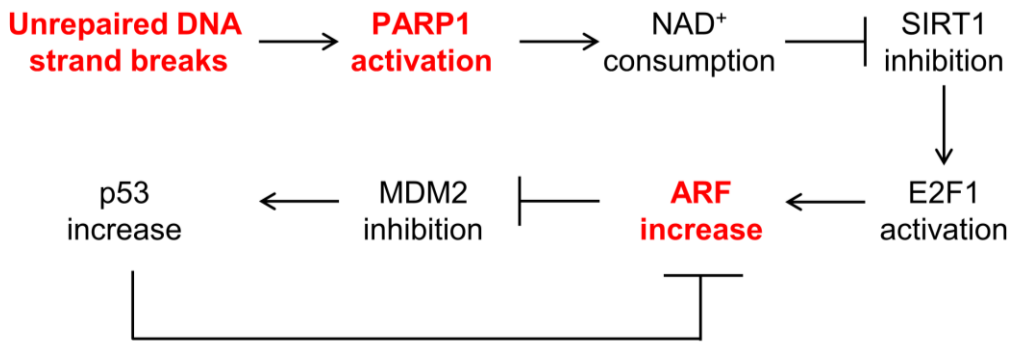

Figure 7.1: Proposed model for ARF upregulation in response to persistent DNA SBs. Unrepaired SBs lead to *arf* upregulation via PARP1-dependent NAD^+ consumption which leads to SIRT1 inhibition and E2F1 activation. In normal human fibroblasts the amplitude of ARF upregulation in response to persistent SBs is kept under control by the p53 negative feedback loop.

7.2 ARF is induced in response to persistent DNA damage

The *ARF* tumour suppressor gene has been found to be deleted, mutated or the promoter hypermethylated in several cancers (Ozenne et al., 2010), such as breast cancer (Silva et al., 2001) and colorectal carcinoma (Esteller et al., 2000; Zheng et al., 2000). Thus, the loss of *ARF* expression correlates with tumour development, indicating that the correct regulation of ARF levels is important to avoid the onset of cancer.

At the molecular level, ARF function is regulated by modulating the expression of the *ARF* gene and by protein levels. The E3 ubiquitin ligase ULF and SIVA1 have been found to promote ARF degradation through the ubiquitination of the N-terminus (Chen et al., 2010; Wang et al., 2013). At the transcriptional level, E2F1 has been found to bind to the ARF promoter stimulating its transcription (Komori et al., 2005), whereas overexpression of c-MYC has been found to upregulate *ARF* mRNA (Zindy et al., 1998). Additionally, c-MYC has been reported to stabilise ARF levels by limiting the ARF-ULF interaction (Chen et al., 2010). In mouse cells, Arf induction has been shown to be triggered by hyperproliferative stimuli. For instance, abnormal oncogene activation, such as Ras hyperactivation, leads to Arf upregulation (Barradas et al., 2009; Lin and Lowe, 2001).

Regarding the regulation of ARF in response to DNA damage, results in the current literature are still contradictory. For example, the upregulation of ARF in response to genotoxic treatment has been reported in several studies (Eymin et al., 2006; Khan et al., 2004; Li et al., 2012), whereas other studies suggest that DNA damage does not trigger ARF upregulation (Chen et al., 2013; Velimezi et al., 2013). Moreover, the molecular mechanism that leads to ARF induction in response to DNA damage has not been investigated. In this study, a novel model for ARF upregulation has been described. The creation of endogenous lesions and the persistency of SBs have been shown to stimulate the transcription of the *ARF* gene and, as a consequence, protein accumulation. Interestingly, a recent publication reports that ARF levels are induced in response to ATM depletion (Velimezi et al., 2013). The authors describe a mechanism which regulates ARF

protein levels in response to the loss of ATM, excluding the possibility of transcriptionally inducing *ARF* gene. However, they do not exclude the possibility that ATM depletion could induce an accumulation of endogenous DNA damage. Indeed, ATM regulates the activity of several proteins involved in DNA repair and is responsible for correct checkpoint activation to avoid genomic instability (Shiloh and Ziv, 2013). Therefore, it is reasonable to speculate that the induction of ARF could still be a consequence of persistent DNA damage which accumulates as a result of the loss of ATM. Indeed, results presented in this work correlate with the findings that ARF is upregulated in response to BRCA2 deletion, confirming that the accumulation of DNA damage is responsible for ARF induction (Carlos et al., 2013). However, the molecular mechanism of ARF induction has not been addressed in this paper, although ATM and ATR have been found to be necessary for triggering ARF upregulation.

An important role for E2F1 in controlling *ARF* mRNA levels has been described. Indeed, E2F1 has been reported to be important for the transcription of G1/S transition genes (Gregori et al., 1995); however, in response to DNA damage treatments with etoposide and doxocycline, it has been shown that E2F1 activates the transcription of pro-apoptotic genes, such as *TP73* (which encodes for p73), by directly binding to the promoter of the gene (Pediconi et al., 2009; Stanelle et al., 2002; Wang et al., 2006). These results confirm that the specificity of E2F1 binding to promoters might change according to the cellular conditions. Under normal conditions, E2F1 could sustain cell cycle progression, whereas in a stress-induced situation, other genes such as *ARF*, might be preferentially activated to help make the decision between cell cycle progression and cell death.

The major role for ARF is to regulate the amount of p53 by inhibiting the E3 ubiquitin ligase MDM2, thus allowing p53 accumulation (Zhang et al., 1998). p53 has been reported to bind to the *ARF* gene promoter and to repress *ARF* expression; in this way, the upregulation of p53 by ARF leads eventually to ARF downregulation via a negative feedback loop (Stott et al., 1998). This study has shown that ARF upregulation is indeed

kept under control by the presence of p53. In response to an accumulation of DNA damage, ARF levels are detectable only when the p53 negative feedback loop is abrogated, by depleting p53 itself. Therefore, in p53-proficient cells, ARF levels are tightly controlled in the presence of p53, thus making it difficult to study ARF induction under these conditions. However, these results confirm that ARF induction indeed occurs in normal cells in response to unrepaired SBs, indicating the importance of maintaining the *ARF* gene intact, in order to avoid genomic instability. Indeed, analysis of the cell cycle profiles of normal cells suggests that ARF is required for blocking the cell cycle in G1 in response to unrepaired SBs in a p53-p21-dependent way, indicating a fundamental role for ARF in triggering the p53 response. These data are in agreement with previously published results that show that ARF overexpression leads to cell cycle arrest in p53-proficient cells (Weber et al., 2002).

Finally, in this study ARF induction in response to persistent SBs has been unveiled, suggesting a role for ARF in reporting DNA damage accumulation, thus avoiding genome instability. It can be then speculated that the loss of *ARF* expression could contribute to create the conditions necessary for genome instability to occur, eventually leading to cancer development.

7.3 A novel role for PARP1 in the DDR

DNA base lesions and SBs are mainly repaired by the BER pathway. SBs have been shown to dramatically induce the activation of PARP1, enabling recruitment of the BER proteins and to protect the DNA nicks until repair occurs (Caldecott et al., 1996; El-Khamisy et al., 2003; Woodhouse et al., 2008). The binding of PARP1 to the DNA nicks stimulates its activation, thus leading to the synthesis of PAR polymers using NAD^+ as a co-factor (Okano et al., 2003). Despite PARP1 having been reported to be important for the recruitment of BER enzymes, it does not have a direct role during the repair itself.

In the last ten years, several studies have investigated the possibility of other roles for PARP1 as a regulator in cell biology (Gibson and Kraus, 2012; Luo and Kraus, 2012). Generally speaking, PARP1 has been identified to be a stress response protein. Indeed, it has been found to be part of different signalling networks, such as the NF-κB inflammatory pathway and the heat shock protein response (Luo and Kraus, 2012). A role for PARP1 in DNA damage signalling has been hypothesised. For instance, PARP1-dependent p53 parylation has been found to positively regulate the binding of the transcription factor in response to 5-FU treatment, suggesting a possible role for PARP1 in sensing and signalling the presence of DNA damage to p53 (Lee et al., 2012). However, little is known about other possible tumour suppressor proteins activated by PARP1. The findings described in this work are in agreement with a putative role for PARP1 in the induction of tumour suppressor proteins. The novel discovery that PARP1 activation is indeed required for *ARF* upregulation through a complex cascade of signal transduction highlights the broad spectrum of functions of this enzyme in avoiding tumour development. Indeed, *Parp1* KO mice are known to be more sensitive to DNA damage, eventually developing tumours (Masutani et al., 2000; de Murcia et al., 1997). Therefore, the loss of PARP1 could be responsible not only for the accumulation of DNA lesions, but also for the lack of induction of tumour suppressor mechanisms governed by ARF and p53.

More interestingly, this work shows that the depletion of NAD^+ by PARP1 triggers *ARF* upregulation. NAD^+ depletion by PARP1 has been described to be able to trigger cell death in neuronal cells, but also in cancer cells and MEFs (Alano et al., 2004, 2010; Andrabi et al., 2006; Wang et al., 2011). This type of cell death, called parthanatos, is activated by hyperactivation of PARP1 in response to DNA damage and is characterised by NAD^+ depletion, ATP depletion and AIF release from mitochondria through a caspase-independent mechanism (Luo and Kraus, 2012). It can be speculated that the level of damage correlates with a certain level of PARP1 activation; once the minimum threshold of the intracellular concentration of NAD^+ is reached, cell death is triggered to avoid the accumulation of unrepaired DNA lesions and genome instability. In this way, PARP1 detection of SBs can be seen as a way of measuring the amount of DNA damage to be repaired. If the cells can cope with the amount of lesions generated, DNA repair will occur; otherwise hyperactivation of PARP1 will lead to cell death as a mechanism to avoid genomic instability. The upregulation of ARF in response to PARP1 hyperactivation (obtained in this study following XRCC1 depletion) is probably a mechanism that works in parallel and with a final aim to accumulate p53 in order to trigger cell cycle arrest (or even senescence) and eventually cell death. It can be speculated that ARF is not the only targets activated by PARP1-dependent NAD^+ depletion, but possibly other proteins could be regulated by this mechanism.

The intracellular depletion of NAD^+ by PARP1 inhibits the activity of proteins which exercise their catalytic activity using NAD^+ as a cofactor. For instance, sirtuin proteins use NAD^+ to deacetylase and/or monoribosylate their substrates (Frye, 1999; Langley et al., 2002). Among the seven sirtuins family members, SIRT6 and SIRT1 localise both in the nucleus and are therefore likely to share the nuclear NAD^+ pool with PARP1. Indeed, SIRT1 deacetylase and PARP1 have been reported to regulate each other's activity through the consumption of the available NAD^+ (Bai et al., 2011; Caito et al., 2010; Kolthur-seetharam et al., 2006; El Ramy et al., 2009). For instance, *SIRT1* KO cells show

an increase in the activity of PARP1 in response to DNA damage, indicating the presence of an interplay between PARP1 and SIRT1 in the regulation of each other's activity (El Ramy et al., 2009). In this work, an additional outcome of this interplay has been described. Indeed, it has been shown that in response to unrepaired SBs SIRT1 activity is inhibited possibly as a consequence of PARP1-dependent depletion of NAD^+, thus leading to ARF upregulation. These data are in accordance with previous published data in which it has been shown that the amount of DNA damage increases with age and this correlates with PARP1 activation and NAD^+ depletion (Braidy et al., 2011). In this work, although ARF levels have not been assessed, an increase in the acetylation of p53, a known target of SIRT1, has been found, confirming that PARP1-SIRT1 interplay regulates the cellular response to DNA damage (Braidy et al., 2011).

It is important to consider that PARP1 activation has been targeted for the treatment of cancer (Rouleau et al., 2010). The use of PARP inhibitors in cancer treatment has been debated by the scientific community over the last ten years. PARP inhibition leads to the accumulation of unrepaired SB lesions which are converted to replicative DSBs, which are repaired by HR. Nonsense and frameshift mutations or deletions at either the *BRCA1* or *BRCA2* genes, combined with LOH, results in HR-deficiency. Thus, the combination of PARP inhibitory treatment with the genetic background of these cancers leads to a synthetic lethality phenomena, which affects the tumour, but not the normal tissue (Bryant et al., 2005; Helleday, 2011). However, PARP1 has been shown to have multiple functions in cellular biology beyond its role in DNA repair. Indeed, the protein might also act as a tumour suppressor in different genetic backgrounds by stimulating cellular death in response to an excessive accumulation of DNA damage. Moreover, the recent finding that PARP1 activation is important for p53 activity and for ARF upregulation, as described in this thesis, confirms the importance of this protein for the activation of a tumour suppressive response. Therefore the use of PARP inhibitors might actually be deleterious for normal cells, because of the reduction of a potential tumour suppressive ability. Hence,

the evaluation of the use of these drugs for cancer treatment needs to be carefully assessed because of the possibility of creating tumour prone conditions for normal tissues.

Finally, a new tumour suppressive role for PARP1 during the DDR has been described by linking PARP1 activation to ARF upregulation, via NAD^+ depletion and SIRT1 inhibition. A better understanding of the multiple function of this enzyme is fundamental to developing new personalised strategies for cancer treatment based on the genetic background of the tumour.

7.4 Genome instability, cellular metabolism and cancer

Genomic instability has recently been classified as one of the characteristics which promotes tumour formation, enabling accumulation of mutations (Hanahan and Weinberg, 2011). Cancer metabolism has been also inserted amongst the emerging hallmarks which characterise tumour biology (Hanahan and Weinberg, 2011). It is then reasonable to hypothesise that an increase in DNA damage might promote a metabolic shift which might contribute to sustaining tumour development. However, very little is known about the link between genomic instability and cellular metabolism.

A connection between nucleotide metabolism and genomic instability has been shown. Indeed, the production of nucleotides has been found to decrease in cancer, leading to genomic instability (Bester et al., 2011; Hu et al., 2012). The fragile histidine triad (*FHIT*) gene, which encodes for a protein involved in purine metabolism, has been found deleted in several cancers, such as colon and lung (Ohta et al., 1996; Sozzi et al., 1996). Studies in mice have shown that the loss of this gene promotes genome instability and eventually tumour formation (Saldivar et al., 2012). The ribonucleotide reductase enzyme (RNR), which catalyses the conversion of ribonucleotides to deoxyribonucleotides, is another possible candidate (Xu et al., 2008). The expression of a stable mutant of the small subunit of RNR, the RRM2 subunit, leads to genome instability due to an imbalance in the nucleotide pool. More interestingly, RRM2 ubiquitination is abrogated in response to DNA damage to allow stabilisation of the protein and the production of nucleotides for DNA repair (D'Angiolella et al., 2012).

It is important to consider an alternative scenario- that genome instability might contribute to the reprogramming of cellular metabolism. Reprogramming of metabolism during neoplastic transformation has been the focus of several studies which underline the difference between normal proliferating cells and cancer cells (Cantor and Sabatini, 2012; Locasale, 2013; Schulze and Harris, 2012). Cancer metabolism has been found to rely on the uptake of glutamine and glucose for sustaining a high rate of cell proliferation and an

increase in both protein and lipid biosynthesis (DeBerardinis et al., 2007; Vander Heiden et al., 2009). Moreover, cancer cells do not rely on the tricarboxylic acid (TCA) cycle for energy, because of the hypoxic growth conditions within the tumour microenvironment. However, mitochondrial function is still important for lipid biosynthesis and for restoring the NAD^+ pool, necessary for glycolysis (Schulze and Harris, 2012). The NAD^+ molecule and its derivate NADH are fundamental for production of the energy necessary to achieve cellular function. In particular, the intracellular levels of NAD^+ are also involved in the regulation of the activity of several enzymes, such as sirtuins, which coordinate chromatin status, DNA repair, stress responses and cellular fate (Michan and Sinclair, 2007). Also, PARP1 consumes NAD^+ for the synthesis of PAR in response to SB formation (Okano et al., 2003). Therefore, the NAD^+ metabolite seems to work as a bridge between DNA damage and cellular metabolism (Luna et al., 2013). It can be hypothesised that PARP1 chronic activation stimulates the depletion of NAD^+ and this might contribute to a reprogramming of the metabolism towards a cancer-like metabolism. For instance, it can be speculated that a decrease in the amount of NAD^+ would impair the TCA cycle; indeed, each cycle of TCA uses 6 NAD^+ molecule, reducing NAD^+ to NADH.

More interestingly, NAD^+ depletion is the trigger for the activation of the p53 tumour suppressor protein, through the abrogation of the activity of SIRT1 (Braidy et al., 2011). The change in the intracellular levels of NAD^+ activates a p53 response, indicating that the homeostasis of the cellular metabolism might represent another important sensor to check tissue health and potentially an activator of a stress response mechanism. Indeed, PARP1-dependent depletion of NAD^+ leads to ARF upregulation. Moreover, prolonged NAD^+ depletion triggers both p53 and ARF upregulation in normal cells, indicating that NAD^+ levels might tightly control the cellular response, suggesting the activation of tumour suppressive barrier. Although these are preliminary findings, they suggest a connection between DNA damage and cellular metabolism, in particular with NAD^+ metabolism, showing that the two entities are interlinked and they contribute to the activation of a

tumour suppressive response. Investigating whether and how the activity of the proteins involved in these biological processes are interlinked would be important in gaining a better understanding on the concomitant role of these proteins in tumour development.

7.5 Future work

7.5.1 Investigating whether PARP1-ARF axis in response to persistent SBs triggers cellular senescence

In **chapter 6** it has been shown that ARF is important for the activation of G1 arrest in response to SBs (**figure 6.6**), suggesting that cell cycle progression is blocked until the DNA damage is repaired. Persistent DDR is known to trigger senescence. Thus, it would be interesting to investigate if a prolonged XRCC1 depletion could eventually lead to senescence. In order to do that, it would be necessary to establish an inducible XRCC1 shRNA system using human primary fibroblasts, such as the TIG-1 cell line as a cellular model. The induction of senescence-markers, such as β-galactosidase and p21, could be assessed along with the accumulation of ARF. Moreover, the link between PARP1 chronic activation and senescence has not been characterised. Therefore, it would be interesting to assess the role of PARP1 in this process. To do so, it would be necessary to create a *PARP1* KO cell line and subsequently establish the same inducible XRCC1 shRNA system using TIG-1 cells. In this way, it would be possible to investigate whether PARP1 is involved in triggering senescence in response to persistent DNA damage.

7.5.2 Investigating the role of PARP1 in triggering changes in gene expression in response to SB accumulation

Results presented in this thesis show a link between DNA damage accumulation, PARP1 activation and the induction of the tumour suppressor gene *ARF*. However, other genes might be regulated by PARP1 activation. It would be interesting to find other potential targets of this network by doing a microarray analysis of the gene expression levels between non-treated and XRCC1-treated cells. To ensure that the change in the mRNA levels of the target gene is dependent on PARP1, XRCC1 and PARP1-cotreated RNAi samples would be included in the microarray analysis as a control. The validation of the targets would be assessed by qPCR and priority would be given to the targets that are

known to be involved in cancer development. The further steps of this work will be to elucidate the molecular mechanisms of activation of the candidates and to investigate the biological relevance in terms of DDR and cell fate.

References

Abbas, T., and Dutta, A. (2009). P21 in Cancer: Intricate Networks and Multiple Activities. Nat. Rev. Cancer *9*, 400–414.

Agarwal, M.L., Agarwal, A., Taylor, W.R., and Stark, G.R. (1995). p53 controls both the G2/M and the G1 cell cycle checkpoints and mediates reversible growth arrest in human fibroblasts. Proc. Natl. Acad. Sci. U. S. A. *92*, 8493–8497.

Ahel, I., Rass, U., El-Khamisy, S.F., Katyal, S., Clements, P.M., McKinnon, P.J., Caldecott, K.W., and West, S.C. (2006). The neurodegenerative disease protein aprataxin resolves abortive DNA ligation intermediates. Nature *443*, 713–716.

Alano, C.C., Ying, W., and Swanson, R. a (2004). Poly(ADP-ribose) polymerase-1-mediated cell death in astrocytes requires NAD+ depletion and mitochondrial permeability transition. J. Biol. Chem. *279*, 18895–18902.

Alano, C.C., Garnier, P., Ying, W., Higashi, Y., Kauppinen, T.M., and Swanson, R. a (2010). NAD+ depletion is necessary and sufficient for poly(ADP-ribose) polymerase-1-mediated neuronal death. J. Neurosci. *30*, 2967–2978.

Almeida, K.H., and Sobol, R.W. (2007). A unified view of base excision repair: lesion-dependent protein complexes regulated by post-translational modification. DNA Repair (Amst). *6*, 695–711.

Ame, J.-C., Rolli, V., Schreiber, V., Niedergang, C., Apiou, F., Decker, P., Muller, S., Hoger, T., Murcia, J.M. -d., and de Murcia, G. (1999). PARP-2, A Novel Mammalian DNA Damage-dependent Poly(ADP-ribose) Polymerase. J. Biol. Chem. *274*, 17860–17868.

Andrabi, S. a, Kim, N.S., Yu, S.-W., Wang, H., Koh, D.W., Sasaki, M., Klaus, J. a, Otsuka, T., Zhang, Z., Koehler, R.C., et al. (2006). Poly(ADP-ribose) (PAR) polymer is a death signal. Proc. Natl. Acad. Sci. U. S. A. *103*, 18308–18313.

Bai, P., Cantó, C., Oudart, H., Brunyánszki, A., Cen, Y., Thomas, C., Yamamoto, H., Huber, A., Kiss, B., Houtkooper, R.H., et al. (2011). PARP-1 inhibition increases mitochondrial metabolism through SIRT1 activation. Cell Metab. *13*, 461–468.

Bailey, S.L., Gurley, K.E., Hoon-Kim, K., Kelly-Spratt, K.S., and Kemp, C.J. (2008). Tumor suppression by p53 in the absence of Atm. Mol. Cancer Res. *6*, 1185–1192.

Bakkenist, C.J., and Kastan, M.B. (2003). DNA damage activates ATM through intermolecular autophosphorylation and dimer dissociation. Nature *421*, 499–506.

Banerjee, A., Yang, W., Karplus, M., and Verdine, G.L. (2005). Structure of a repair enzyme interrogating undamaged DNA elucidates recognition of damaged DNA. Nature *434*, 612–618.

Barradas, M., Anderton, E., Acosta, J.C., Li, S., Banito, A., Rodriguez-Niedenführ, M., Maertens, G., Banck, M., Zhou, M.-M., Walsh, M.J., et al. (2009). Histone demethylase

JMJD3 contributes to epigenetic control of INK4a/ARF by oncogenic RAS. Genes Dev. *23*, 1177–1182.

Bartek, J., and Lukas, J. (2003). Chk1 and Chk2 kinases in checkpoint control and cancer. Cancer Cell *3*, 421–429.

Bartkova, J., Rezaei, N., Liontos, M., Karakaidos, P., Kletsas, D., Issaeva, N., Vassiliou, L.-V.F., Kolettas, E., Niforou, K., Zoumpourlis, V.C., et al. (2006). Oncogene-induced senescence is part of the tumorigenesis barrier imposed by DNA damage checkpoints. Nature *444*, 633–637.

Barzilay, G., Walker, L.J., Robson, C.N., and Hickson, I.D. (1995). Site-directed mutagenesis of the human DNA repair enzyme HAPi : identification of residues important for AP endonuclease and RNase H activity. Nucleic Acids Res. *23*, 1544–1550.

Beard, W. a, and Wilson, S.H. (2006). Structure and mechanism of DNA polymerase Beta. Chem. Rev. *106*, 361–382.

Bennett, R. a, Wilson, D.M., Wong, D., and Demple, B. (1997). Interaction of human apurinic endonuclease and DNA polymerase beta in the base excision repair pathway. Proc. Natl. Acad. Sci. U. S. A. *94*, 7166–7169.

Bergoglio, V., Pillaire, M., Lacroix-triki, M., Raynaud-messina, B., Canitrot, Y., Bieth, A., Wright, M., Delsol, G., Loeb, L.A., and Cazaux, C. (2002). Deregulated DNA Polymerase β Induces Chromosome Instability and Tumorigenesis. Cancer Res. *62*, 3511–3514.

Berkovich, E., Lamed, Y., and Ginsberg, D. (2003). E2F and Ras Synergize in Transcriptionally Activating p14 ARF Expression. Cell Cycle *2:2*, 127–133.

Bester, A.C., Roniger, M., Oren, Y.S., Im, M.M., Sarni, D., Chaoat, M., Bensimon, A., Zamir, G., Shewach, D.S., and Kerem, B. (2011). Nucleotide deficiency promotes genomic instability in early stages of cancer development. Cell *145*, 435–446.

Billington, R.A., Genazzani, A.A., Travelli, C., and Condorelli, F. (2008). NAD depletion by FK866 induces autophagy nd es io s en ce . D o no t st r ib u te La nd es io s ci en ce o r u. Autophagy 385–387.

Bokobza, S.M., Jiang, Y., Weber, A.M., Devery, A.M., and Ryan, A.J. (2014). Short-course treatment with gefitinib enhances curative potential of radiation therapy in a mouse model of human non-small cell lung cancer. Int. J. Radiat. Oncol. Biol. Phys. *88*, 947–954.

Bowman, K.J., White, a, Golding, B.T., Griffin, R.J., and Curtin, N.J. (1998). Potentiation of anti-cancer agent cytotoxicity by the potent poly(ADP-ribose) polymerase inhibitors NU1025 and NU1064. Br. J. Cancer *78*, 1269–1277.

Bradford, M.M. (1976). A rapid and sensitive method for the quantitation of microgram quantities of protein utilizing the principle of protein-dye binding. Anal. Biochem. *72*, 248–254.

Braidy, N., Guillemin, G.J., Mansour, H., Chan-Ling, T., Poljak, A., and Grant, R. (2011). Age related changes in NAD+ metabolism oxidative stress and Sirt1 activity in wistar rats. PLoS One *6*, e19194.

Brem, R., and Hall, J. (2005). XRCC1 is required for DNA single-strand break repair in human cells. Nucleic Acids Res. *33*, 2512–2520.

Brown, J.P., Wei, W., and Sedivy, J.M. (1997). Bypass of Senescence After Disruption of p21CIP1/WAF1 Gene in Normal Diploid Human Fibroblasts. Science (80-.). *277*, 831–834.

Brunet, A., Sweeney, L.B., Sturgill, J.F., Chua, K.F., Greer, P.L., Lin, Y., Tran, H., Ross, S.E., Mostoslavsky, R., Cohen, H.Y., et al. (2004). Stress-dependent regulation of FOXO transcription factors by the SIRT1 deacetylase. Science *303*, 2011–2015.

Bryant, H.E., Schultz, N., Thomas, H.D., Parker, K.M., Flower, D., Lopez, E., Kyle, S., Meuth, M., Curtin, N.J., and Helleday, T. (2005). Specific killing of BRCA2-deficient tumours with inhibitors of poly(ADP-ribose) polymerase. Nature *434*, 913–917.

Bulavin, D. V, Saito, S., Hollander, M.C., Sakaguchi, K., Anderson, C.W., Appella, E., and Fornace, a J. (1999). Phosphorylation of human p53 by p38 kinase coordinates N-terminal phosphorylation and apoptosis in response to UV radiation. EMBO J. *18*, 6845–6854.

Bunz, F., Dutriaux, A., Lengauer, T., Waldmann, T., Zhou, S., Brown, J.P., Sedivy, J.M., Kinzler, K.W., and Vogelstein, B. (1998). Requirement for p53 and p21 to Sustain G2 Arrest After DNA Damage. Science (80-.). *282*, 1497–1501.

Burma, S., Chen, B., Murphy, M., Kurimasa, A., and Chen, D.J. (2001). ATM phosphorylates histone H2AX in response to DNA double-strand breaks. J. Biol. Chem. *276*, 42462–42467.

Busino, L., Donzelli, M., Chiesa, M., Guardavaccaro, D., Ganoth, D., and Dorrello, N.V. (2003). Degradation of Cdc25A by b -TrCP during S phase and in response to DNA damage. Nature *426*, 87–91.

Busso, C.S., Iwakuma, T., and Izumi, T. (2009). Ubiquitination of mammalian AP endonuclease (APE1) regulated by the p53-MDM2 signaling pathway. Oncogene *28*, 1616–1625.

Busso, C.S., Wedgeworth, C.M., and Izumi, T. (2011). Ubiquitination of human AP-endonuclease 1 (APE1) enhanced by T233E substitution and by CDK5. Nucleic Acids Res. *39*, 8017–8028.

Cabelof, D.C., Guo, Z., Raffoul, J.J., Sobol, R.W., Wilson, S.H., Richardson, A., and Heydari, A.R. (2003). Base Excision Repair Deficiency Caused by Polymerase β Haploinsufficiency : Accelerated DNA Damage and Increased Mutational Response to Carcinogens. Cancer Res. *65*, 5799–5807.

Caito, S., Hwang, J.-W., Chung, S., Yao, H., Sundar, I.K., and Rahman, I. (2010). PARP-1 inhibition does not restore oxidant-mediated reduction in SIRT1 activity. Biochem. Biophys. Res. Commun. *392*, 264–270.

Caldecott, K.W. (2003a). Protein-protein interactions during mammalian DNA single-strand break repair. Biochem. Soc. Trans. *31*, 247–251.

Caldecott, K.W. (2003b). XRCC1 and DNA strand break repair. DNA Repair (Amst). *2*, 955–969.

Caldecott, K.W. (2008). Single-strand break repair and genetic disease. Nat. Rev. Genet. *9*, 619–631.

Caldecott, K.W., Tucker, J.D., Stanker, L.H., and Thompson, L.H. (1995). Characterization of the XRCC1-DNA ligase III complex in vitro and its absence from mutant hamster cells. Nucleic Acids Res. *23*, 4836–4843.

Caldecott, K.W., Aoufouchi, S., Johnson, P., and Shall, S. (1996). XRCC1 polypeptide interacts with DNA polymerase beta and possibly poly (ADP-ribose) polymerase, and DNA ligase III is a novel molecular “nick-sensor” in vitro. Nucleic Acids Res. *24*, 4387–4394.

Campalans, A., Kortulewski, T., Amouroux, R., Menoni, H., Vermeulen, W., and Radicella, J.P. (2013). Distinct spatiotemporal patterns and PARP dependence of XRCC1 recruitment to single-strand break and base excision repair. Nucleic Acids Res. *41*, 3115–3129.

Campisi, J. (2013). Aging, cellular senescence, and cancer. Annu. Rev. Physiol. *75*, 685–705.

Campisi, J., and d’Adda di Fagagna, F. (2007). Cellular senescence: when bad things happen to good cells. Nat. Rev. Mol. Cell Biol. *8*, 729–740.

Canitrot, Y., Cazaux, C., Fréchet, M., Bouayadi, K., Lesca, C., Salles, B., and Hoffmann, J.S. (1998). Overexpression of DNA polymerase beta in cell results in a mutator phenotype and a decreased sensitivity to anticancer drugs. Proc. Natl. Acad. Sci. U. S. A. *95*, 12586–12590.

Cantó, C., Gerhart-Hines, Z., Feige, J.N., Lagouge, M., Noriega, L., Milne, J.C., Elliott, P.J., Puigserver, P., and Auwerx, J. (2009). AMPK regulates energy expenditure by modulating NAD+ metabolism and SIRT1 activity. Nature *458*, 1056–1060.

Cantor, J.R., and Sabatini, D.M. (2012). Cancer cell metabolism: one hallmark, many faces. Cancer Discov. *2*, 881–898.

Carlos, A.R., Escandell, J.M., Kotsantis, P., Suwaki, N., Bouwman, P., Badie, S., Folio, C., Benitez, J., Gomez-Lopez, G., Pisano, D.G., et al. (2013). ARF triggers senescence in Brca2-deficient cells by altering the spectrum of p53 transcriptional targets. Nat. Commun. *4*, 2697.

Carvajal, L. a, and Manfredi, J.J. (2013). Another fork in the road--life or death decisions by the tumour suppressor p53. EMBO Rep. *14*, 414–421.

Cea, M., Cagnetta, A., Fulciniti, M., Tai, Y., Hideshima, T., Roccaro, A., Sacco, A., Calimeri, T., Cottini, F., Jakubikova, J., et al. (2012). Targeting NAD+ salvage pathway induces autophagy in multiple myeloma cells via mTORC1 and extracellular signal-regulated kinase (ERK1 / 2) inhibition. Blood 3519–3529.

Chagovetz, A.M., Sweasy, J.B., and Preston, B.D. (1997). Increased activity and fidelity of DNA polymerase beta on single-nucleotide gapped DNA. J. Biol. Chem. *272*, 27501–27504.

Chan, K.K.L., Zhang, Q.-M., and Dianov, G.L. (2006). Base excision repair fidelity in normal and cancer cells. Mutagenesis *21*, 173–178.

Chen, D., Kon, N., Li, M., Zhang, W., Qin, J., and Gu, W. (2005). ARF-BP1/Mule is a critical mediator of the ARF tumor suppressor. Cell *121*, 1071–1083.

Chen, D., Shan, J., Zhu, W.-G., Qin, J., and Gu, W. (2010). Transcription-independent ARF regulation in oncogenic stress-mediated p53 responses. Nature *464*, 624–627.

Chen, D., Kon, N., Zhong, J., Zhang, P., Yu, L., and Gu, W. (2013). Differential effects on ARF stability by normal versus oncogenic levels of c-Myc expression. Mol. Cell *51*, 46–56.

Chen, D.S., Herman, T., and Demple, B. (1991). Two distinct human DNA diesterases that hydrolyze 3'-blocking deoxyribose fragments from oxidized DNA. Nucleic Acids Res. *19*, 5907–5914.

Chevillard, S., Radicella, J.P., Levalois, C., Lebeau, J., Poupon, M.F., Oudard, S., Dutrillaux, B., and Boiteux, S. (1998). Mutations in OGG1, a gene involved in the repair of oxidative DNA damage, are found in human lung and kidney tumours. Oncogene *16*, 3083–3086.

Chio, I.I.C., Sasaki, M., Ghazarian, D., Moreno, J., Done, S., Ueda, T., Inoue, S., Chang, Y.-L., Chen, N.J., and Mak, T.W. (2012). TRADD contributes to tumour suppression by regulating ULF-dependent p19Arf ubiquitylation. Nat. Cell Biol. *14*, 625–633.

Clair, S.S., and Manfredi, J.J. (2006). The Dual Specificity Phosphatase Cdc25C is a Direct Target for transcriptional repression by the tumor suppressor p53. Cell Cycle *5*, 709–713.

Clements, P.M., Breslin, C., Deeks, E.D., Byrd, P.J., Ju, L., Bieganowski, P., Brenner, C., Moreira, M.-C., Taylor, a M.R., and Caldecott, K.W. (2004). The ataxia-oculomotor apraxia 1 gene product has a role distinct from ATM and interacts with the DNA strand break repair proteins XRCC1 and XRCC4. DNA Repair (Amst). *3*, 1493–1502.

Collado, M., Blasco, M. a, and Serrano, M. (2007). Cellular senescence in cancer and aging. Cell *130*, 223–233.

CONSURTIUM (2005). [Finishing the euchromatic sequence of the human genome]. Tanpakushitsu Kakusan Koso. *50*, 162–168.

Copani, A., Hoozemans, J.J.M., Caraci, F., Calafiore, M., Van Haastert, E.S., Veerhuis, R., Rozemuller, A.J.M., Aronica, E., Sortino, M.A., and Nicoletti, F. (2006). DNA polymerase-beta is expressed early in neurons of Alzheimer's disease brain and is loaded into DNA replication forks in neurons challenged with beta-amyloid. J. Neurosci. *26*, 10949–10957.

d'Adda di Fagagna, F., Reaper, P.M., Clay-Farrace, L., Fiegler, H., Carr, P., Von Zglinicki, T., Saretzki, G., Carter, N.P., and Jackson, S.P. (2003). A DNA damage checkpoint response in telomere-initiated senescence. Nature *426*, 194–198.

D'Angiolella, V., Donato, V., Forrester, F.M., Jeong, Y.-T., Pellacani, C., Kudo, Y., Saraf, A., Florens, L., Washburn, M.P., and Pagano, M. (2012). Cyclin F-mediated degradation of ribonucleotide reductase M2 controls genome integrity and DNA repair. Cell *149*, 1023–1034.

Dantzer, F., de La Rubia, G., Ménissier-De Murcia, J., Hostomsky, Z., de Murcia, G., and Schreiber, V. (2000). Base excision repair is impaired in mammalian cells lacking Poly(ADP-ribose) polymerase-1. Biochemistry *39*, 7559–7569.

Davidovic, L., Vodenicharov, M., Affar, E.B., and Poirier, G.G. (2001). Importance of poly(ADP-ribose) glycohydrolase in the control of poly(ADP-ribose) metabolism. Exp. Cell Res. *268*, 7–13.

DeBerardinis, R.J., Mancuso, A., Daikhin, E., Nissim, I., Yudkoff, M., Wehrli, S., and Thompson, C.B. (2007). Beyond aerobic glycolysis: transformed cells can engage in glutamine metabolism that exceeds the requirement for protein and nucleotide synthesis. Proc. Natl. Acad. Sci. U. S. A. *104*, 19345–19350.

Demple, B., Herman, T., and Chen, D.S. (1991). Cloning and expression of APE, the cDNA encoding the major human apurinic endonuclease: definition of a family of DNA repair enzymes. Proc. Natl. Acad. Sci. U. S. A. *88*, 11450–11454.

Dianov, G.L., and Parsons, J.L. (2007). Co-ordination of DNA single strand break repair. DNA Repair (Amst). *6*, 454–460.

Dianov, G.L., Prasad, R., Wilson, H., and Bohr, V.A. (1999). Role of DNA Polymerase β in the Excision Step of Long Patch Mammalian Base Excision Repair. J. Biol. Chem. *274*, 13741–13743.

Dianov, G.L., Sleeth, K.M., Dianova, I.I., and Allinson, S.L. (2003). Repair of abasic sites in DNA. Mutat. Res. Mol. Mech. Mutagen. *531*, 157–163.

Dimri, G.P., Lee, X., Basile, G., Acosta, M., Scott, G., Roskelley, C., Medrano, E.E., Linskens, M., Rubelj, I., and Pereira-Smith, O. (1995). A biomarker that identifies senescent human cells in culture and in aging skin in vivo. Proc. Natl. Acad. Sci. U. S. A. *92*, 9363–9367.

Dimri, G.P., Itahana, K., Acosta, M., and Campisi, J. (2000). Regulation of a Senescence Checkpoint Response by the E2F1 Transcription Factor and p14 ARF Tumor Suppressor. Mol. Cell. Biol. *20*, 273–285.

El-Andaloussi, N., Valovka, T., Toueille, M., Steinacher, R., Focke, F., Gehrig, P., Covic, M., Hassa, P.O., Schär, P., Hübscher, U., et al. (2006). Arginine methylation regulates DNA polymerase beta. Mol. Cell *22*, 51–62.

El-Khamisy, S.F., Masutani, M., Suzuki, H., and Caldecott, K.W. (2003). A requirement for PARP-1 for the assembly or stability of XRCC1 nuclear foci at sites of oxidative DNA damage. Nucleic Acids Res. *31*, 5526–5533.

El-khamisy, S.F., Saifi, G.M., Weinfeld, M., and Caldecott, K.W. (2005). Defective DNA single-strand break repair in spinocerebellar ataxia with axonal neuropathy-1. Nature *434*, 108–113.

Esteller, M., Tortola, S., Toyota, M., Capella, G., Peinado, M. a, Baylin, S.B., and Herman, J.G. (2000). Hypermethylation-associated inactivation of p14(ARF) is independent of p16(INK4a) methylation and p53 mutational status. Cancer Res. *60*, 129–133.

Evan, G.I., and d'Adda di Fagagna, F. (2009). Cellular senescence: hot or what? Curr. Opin. Genet. Dev. *19*, 25–31.

Eymin, B., Leduc, C., Coll, J.-L., Brambilla, E., and Gazzeri, S. (2003). p14ARF induces G2 arrest and apoptosis independently of p53 leading to regression of tumours established in nude mice. Oncogene *22*, 1822–1835.

Eymin, B., Claverie, P., Salon, C., Leduc, C., Col, E., Brambilla, E., Khochbin, S., and Gazzeri, S. (2006). p14ARF activates a Tip60-dependent and p53-independent ATM/ATR/CHK pathway in response to genotoxic stress. Mol. Cell. Biol. *26*, 4339–4350.

Falck, J., Mailand, N., Syljuåsen, R.G., Bartek, J., and Lukas, J. (2001). The ATM-Chk2-Cdc25A checkpoint pathway guards against radioresistant DNA synthesis. Nature *410*, 842–847.

Fan, J., Wilson, P.F., Wong, H., Urbin, S.S., Thompson, L.H., and Iii, D.M.W. (2007). XRCC1Down-Regulation in Human Cells Leads to DNA-Damaging Agent Hypersensitivity , Elevated Sister Chromatid Exchange , and Reduced Survival of BRCA2 Mutant Cells. Envionmental Mol. Mutagen. *500*, 491–500.

Fatoba, S.T., and Okorokov, A.L. (2011). Human SIRT1 associates with mitotic chromatin and contributes to chromosomal condensation. Cell Cycle *10*, 2317–2322.

Ferbeyre, G., Stanchina, E. De, Lin, A.W., Querido, E., Mccurrach, M.E., Hannon, G.J., and Lowe, S. (2002). Oncogenic ras and p53 Cooperate To Induce Cellular Senescence. Mol. Cell. Biol. *22*, 3497–3508.

Ferro AM, and Olivera, B. (1982). Poly(ADP-ribosylation) in vitro. Reaction parameters and enzyme mechanism. J. Biol. Chem. *257*, 7808–7813.

Fisher, A.E.O., Hochegger, H., Takeda, S., and Caldecott, K.W. (2007). Poly(ADP-ribose) polymerase 1 accelerates single-strand break repair in concert with poly(ADP-ribose) glycohydrolase. Mol. Cell. Biol. *27*, 5597–5605.

Flynn, R.L., and Zou, L. (2011). ATR: a master conductor of cellular responses to DNA replication stress. Trends Biochem. Sci. *36*, 133–140.

Fortini, P., Pascucci, B., Parlanti, E., Sobol, R.W., Wilson, S.H., Dogliotti, E., and Elena, V.R. (1998). Different DNA Polymerases Are Involved in the Short- and Long-Patch Base Excision Repair in Mammalian Cells. Biochemistry *37*, 3575–3580.

Fortini, P., Parlanti, E., Olga, M., Chem, J.B., Sidorkina, O.M., Laval, J., and Dogliotti, E. (1999). The Type of DNA Glycosylase Determines the Base Excision Repair Pathway in Mammalian Cells. J. Biol. Chem. *274*, 15230–15236.

Fortini, P., Pascucci, B., Parlanti, E., D'Errico, M., Simonelli, V., and Dogliotti, E. (2003). The base excision repair: mechanisms and its relevance for cancer susceptibility. Biochimie *85*, 1053–1071.

Friedman, J.I., Majumdar, A., and Stivers, J.T. (2009). Nontarget DNA binding shapes the dynamic landscape for enzymatic recognition of DNA damage. Nucleic Acids Res. *37*, 3493–3500.

Frye, R.A. (1999). Characterization of five human cDNAs with homology to the yeast SIR2 gene: Sir2-like proteins (sirtuins) metabolize NAD and may have protein ADP-ribosyltransferase activity. Biochem. Biophys. Res. Commun. *260*, 273–279.

Fu, D., Calvo, J. a, and Samson, L.D. (2012). Balancing repair and tolerance of DNA damage caused by alkylating agents. Nat. Rev. Cancer *12*, 104–120.

Fung, H., and Demple, B. (2005). A vital role for Ape1/Ref1 protein in repairing spontaneous DNA damage in human cells. Mol. Cell *17*, 463–470.

García-Díaz, M., Bebenek, K., Kunkel, T. a, and Blanco, L. (2001). Identification of an intrinsic 5'-deoxyribose-5-phosphate lyase activity in human DNA polymerase lambda: a possible role in base excision repair. J. Biol. Chem. *276*, 34659–34663.

Gary, R., Kim, K., Cornelius, H.L., Park, M.S., and Matsumoto, Y. (1999). Proliferating Cell Nuclear Antigen Facilitates Excision in Long-patch Base Excision Repair. J. Biol. Chem. *274*, 4354–4363.

Gazzeri, S., Valle, V. Della, Chaussade, L., Valle, V.Ã., and Brambilla, C. (1998). The Human p19 ARF Protein Encoded by the β Transcript of the p16 INK4a Gene Is Frequently Lost in Small Cell Lung Cancer. Cancer Res. *58*, 3926–3931.

Gibson, B. a, and Kraus, W.L. (2012). New insights into the molecular and cellular functions of poly(ADP-ribose) and PARPs. Nat. Rev. Mol. Cell Biol. *13*, 411–424.

Gil, J., and Peters, G. (2006). Regulation of the INK4b-ARF-INK4a tumour suppressor locus: all for one or one for all. Nat. Rev. Mol. Cell Biol. *7*, 667–677.

Godon, C., Cordelières, F.P., Biard, D., Giocanti, N., Mégnin-Chanet, F., Hall, J., and Favaudon, V. (2008). PARP inhibition versus PARP-1 silencing: different outcomes in terms of single-strand break repair and radiation susceptibility. Nucleic Acids Res. *36*, 4454–4464.

Goto, Y., Hayashi, R., Kang, D., and Yoshida, K. (2006). Acute Loss of Transcription Factor E2F1 Induces Mitochondrial Biogenesis in HeLa Cells. *934*, 923–934.

Gradwohl, G., Menissier de Murcia, J., Molinete, M., Simonin, F., Koken, M., Hoeijmakers, J.H.J., and Murcia, G.D.E. (1990). The second zinc-finger domain of poly(ADP-ribose) polymerase determines specificity for single-stranded breaks in DNA. Proc. Natl. Acad. Sci. U. S. A. *87*, 2990–2994.

Gregori, J.D.E., Kowalik, T., and Nevins, J.R. (1995). Cellular targets for activation by the E2F1 transcription factor include DNA synthesis- and G1 / S-regulatory genes. Mol. Cell. Biol. *15*, 4215–4224.

Grønbaek, K., Worm, J., Ralfkiaer, E., Ahrenkiel, V., Hokland, P., and Guldberg, P. (2002). ATM mutations are associated with inactivation of the ARF-TP53 tumor suppressor pathway in diffuse large B-cell lymphoma. Blood *100*, 1430–1437.

Ha, L., Ichikawa, T., Anver, M., Dickins, R., Lowe, S., Sharpless, N.E., Krimpenfort, P., Depinho, R. a, Bennett, D.C., Sviderskaya, E. V, et al. (2007). ARF functions as a melanoma tumor suppressor by inducing p53-independent senescence. Proc. Natl. Acad. Sci. U. S. A. *104*, 10968–10973.

Haince, J.-F., Kozlov, S., Dawson, V.L., Dawson, T.M., Hendzel, M.J., Lavin, M.F., and Poirier, G.G. (2007). Ataxia telangiectasia mutated (ATM) signaling network is modulated by a novel poly(ADP-ribose)-dependent pathway in the early response to DNA-damaging agents. J. Biol. Chem. *282*, 16441–16453.

Hampel, B., Malisan, F., Niederegger, H., Testi, R., and Jansen-Dürr, P. (2004). Differential regulation of apoptotic cell death in senescent human cells. Exp. Gerontol. *39*, 1713–1721.

Hanahan, D., and Weinberg, R. a (2011). Hallmarks of cancer: the next generation. Cell *144*, 646–674.

Hanahan, D., Weinberg, R.A., and Francisco, S. (2000). The Hallmarks of Cancer. Cell *100*, 57–70.

Harland, M., Taylor, C.F., Chambers, P. a, Kukalizch, K., Randerson-Moor, J. a, Gruis, N. a, de Snoo, F. a, ter Huurne, J. a C., Goldstein, A.M., Tucker, M. a, et al. (2005). A mutation hotspot at the p14ARF splice site. Oncogene *24*, 4604–4608.

Hasan, S., El-Andaloussi, N., Hardeland, U., Hassa, P.O., Bürki, C., Imhof, R., Schär, P., and Hottiger, M.O. (2002). Acetylation regulates the DNA end-trimming activity of DNA polymerase beta. Mol. Cell *10*, 1213–1222.

Hasmann, M., and Schemainda, I. (2003). FK866 , a Highly Specific Noncompetitive Inhibitor of Nicotinamide Phosphoribosyltransferase , Represents a Novel Mechanism for Induction of Tumor Cell Apoptosis FK866 , a Highly Specific Noncompetitive Inhibitor of Nicotinamide Phosphoribosyltransferase. Cancer Res. 7436–7442.

Hayflick, L. (1965). The limited in vitro lifetime of human diploid cell strains. Exp. Cell Res. *37*, 614–636.

He, H., Yu, F.-X., Sun, C., and Luo, Y. (2011). CBP/p300 and SIRT1 are involved in transcriptional regulation of S-phase specific histone genes. PLoS One *6*, e22088.

Vander Heiden, M.G., Cantley, L.C., and Thompson, C.B. (2009). Understanding the Warburg effect: the metabolic requirements of cell proliferation. Science *324*, 1029–1033.

Helleday, T. (2011). The underlying mechanism for the PARP and BRCA synthetic lethality: clearing up the misunderstandings. Mol. Oncol. *5*, 387–393.

Helleday, T., Petermann, E., Lundin, C., Hodgson, B., and Sharma, R. a (2008). DNA repair pathways as targets for cancer therapy. Nat. Rev. Cancer *8*, 193–204.

Hemmati, P.G., Gillissen, B., Haefen, C. Von, Wendt, J., Sta, L., Daniel, P.T., and Do, B. (2002). Adenovirus-mediated overexpression of p14 ARF induces p53 and Bax-independent apoptosis. Oncogene *21*, 3149–3161.

Hemmati, P.G., Normand, G., Verdoodt, B., von Haefen, C., Hasenjäger, A., Güner, D., Wendt, J., Dörken, B., and Daniel, P.T. (2005). Loss of p21 disrupts p14 ARF-induced G1 cell cycle arrest but augments p14 ARF-induced apoptosis in human carcinoma cells. Oncogene *24*, 4114–4128.

Hemmati, P.G., Normand, G., Gillissen, B., Wendt, J., Dörken, B., and Daniel, P.T. (2008). Cooperative effect of p21Cip1/WAF-1 and 14-3-3sigma on cell cycle arrest and apoptosis induction by p14ARF. Oncogene *27*, 6707–6719.

Hermeking, H., Lengauer, C., Polyak, K., He, T.C., Zhang, L., Thiagalingam, S., Kinzler, K.W., and Vogelstein, B. (1997). 14-3-3 sigma is a p53-regulated inhibitor of G2/M progression. Mol. Cell *1*, 3–11.

Hill, J.W., Hazra, T.K., Izumi, T., and Mitra, S. (2001). Stimulation of human 8-oxoguanine-DNA glycosylase by AP-endonuclease: potential coordination of the initial steps in base excision repair. Nucleic Acids Res. *29*, 430–438.

Hirano, M., Asai, H., Kiriyama, T., Furiya, Y., Iwamoto, T., Nishiwaki, T., Yamamoto, A., Mori, T., and Ueno, S. (2007). Short half-lives of ataxia-associated aprataxin proteins in neuronal cells. Neurosci. Lett. *419*, 184–187.

Hoeijmakers, J.H.J. (2009). DNA damage, aging, and cancer. N. Engl. J. Med. *361*, 1475–1485.

Hofmann, T.G., Möller, A., Sirma, H., Zentgraf, H., Taya, Y., Dröge, W., Will, H., and Schmitz, M.L. (2002). Regulation of p53 activity by its interaction with homeodomain-interacting protein kinase-2. Nat. Cell Biol. *4*, 1–10.

Hollstein, M., Sidransky, D., Vogelstein, B., and Harris, C. (1991). P53 Mutations in Human Cancers. Science (80-.). *253*, 49–53.

Honda, R., and Yasuda, H. (1999). Association of p19(ARF) with Mdm2 inhibits ubiquitin ligase activity of Mdm2 for tumor suppressor p53. EMBO J. *18*, 22–27.

Horton, J.K., Watson, M., Stefanick, D.F., Shaughnessy, D.T., Taylor, J. a, and Wilson, S.H. (2008). XRCC1 and DNA polymerase beta in cellular protection against cytotoxic DNA single-strand breaks. Cell Res. *18*, 48–63.

Hu, C.-M., Yeh, M.-T., Tsao, N., Chen, C.-W., Gao, Q.-Z., Chang, C.-Y., Lee, M.-H., Fang, J.-M., Sheu, S.-Y., Lin, C.-J., et al. (2012). Tumor cells require thymidylate kinase to prevent dUTP incorporation during DNA repair. Cancer Cell *22*, 36–50.

Huang, E., Qu, D., Zhang, Y., Venderova, K., Haque, M.E., Rousseaux, M.W.C., Slack, R.S., Woulfe, J.M., and Park, D.S. (2010). The role of Cdk5-mediated apurinic/apyrimidinic endonuclease 1 phosphorylation in neuronal death. Nat. Cell Biol. *12*, 563–571.

Izumi, T., Hazra, T.K., Boldogh, I., Tomkinson, a E., Park, M.S., Ikeda, S., and Mitra, S. (2000). Requirement for human AP endonuclease 1 for repair of 3'-blocking damage at DNA single-strand breaks induced by reactive oxygen species. Carcinogenesis *21*, 1329–1334.

Izumi, T., Brown, D.B., Naidu, C. V, Bhakat, K.K., Macinnes, M. a, Saito, H., Chen, D.J., and Mitra, S. (2005). Two essential but distinct functions of the mammalian abasic endonuclease. Proc. Natl. Acad. Sci. U. S. A. *102*, 5739–5743.

Jackson, J.G., and Pereira-Smith, O.M. (2006). p53 is preferentially recruited to the promoters of growth arrest genes p21 and GADD45 during replicative senescence of normal human fibroblasts. Cancer Res. *66*, 8356–8360.

Jackson, S.P., and Bartek, J. (2009). The DNA-damage response in human biology and disease. Nature *461*, 1071–1078.

Jacobs, A.L., and Schär, P. (2012). DNA glycosylases: in DNA repair and beyond. Chromosoma *121*, 1–20.

Jilani, A., Ramotar, D., Ong, C., Yang, X.M., Scherer, W., Lasko, D.D., Slack, C., and Scherer, S.W. (1999). Molecular Cloning of the Human Gene, PNKP, Encoding a Polynucleotide Kinase 3′ -Phosphatase and Evidence for Its Role in Repair of DNA Strand Breaks Caused by Oxidative Damage. J. Biol. Chem. *274*, 24176–24186.

Jones, S., Emmerson, P., Maynard, J., Best, J.M., Jordan, S., Williams, G.T., Sampson, J.R., and Cheadle, J.P. (2002). Biallelic germline mutations in MYH predispose to multiple colorectal adenoma and somatic G:C-->T:A mutations. Hum. Mol. Genet. *11*, 2961–2967.

Kameoka, M., Nukuzuma, S., Itaya, A., Tanaka, Y., Ota, K., Ikuta, K., and Yoshihara, K. (2004). RNA Interference Directed against Poly (ADP-Ribose) Polymerase 1 Efficiently Suppresses Human Immunodeficiency Virus Type 1 Replication in Human Cells RNA Interference Directed against Poly (ADP-Ribose) Polymerase 1 Efficiently Suppresses Human Immuno. J. Virol. *78*, 8931–8934.

Kamijo, T., Zindy, F., Roussel, M.F., Quelle, D.E., Downing, J.R., Ashmun, R. a, Grosveld, G., and Sherr, C.J. (1997). Tumor suppression at the mouse INK4a locus mediated by the alternative reading frame product p19ARF. Cell *91*, 649–659.

Kamijo, T., Weber, J.D., Zambetti, G., Zindy, F., Roussel, M.F., and Sherr, C.J. (1998). Functional and physical interactions of the ARF tumor suppressor with p53 and Mdm2. Proc. Natl. Acad. Sci. U. S. A. *95*, 8292–8297.

Kamijo, T., Kamp, E. Van De, Chong, M.J., Zindy, F., Diehl, J.A., Sherr, C.J., and Mckinnon, P.J. (1999a). Loss of the ARF Tumor Suppressor Reverses Premature Replicative Arrest but not Radiation Hypersensitivity Arising from Disabled Atm Function. Cancer Res. *59*, 2464–2469.

Kamijo, T., Bodner, S., Kamp, E. Van De, Randle, D.H., and Sherr, C.J. (1999b). Tumor Spectrum in ARF -deficient Mice. Cancer Res. *59*, 2217–2222.

Kang, H.C., Lee, Y.-I., Shin, J.-H., Andrabi, S. a, Chi, Z., Gagné, J.-P., Lee, Y., Ko, H.S., Lee, B.D., Poirier, G.G., et al. (2011). Iduna is a poly(ADP-ribose) (PAR)-dependent E3

ubiquitin ligase that regulates DNA damage. Proc. Natl. Acad. Sci. U. S. A. *108*, 14103–14108.

Katyal, S., el-Khamisy, S.F., Russell, H.R., Li, Y., Ju, L., Caldecott, K.W., and McKinnon, P.J. (2007). TDP1 facilitates chromosomal single-strand break repair in neurons and is neuroprotective in vivo. EMBO J. *26*, 4720–4731.

Kavli, B., Slupphaug, G., Mol, C.D., Arvai, a S., Peterson, S.B., Tainer, J. a, and Krokan, H.E. (1996). Excision of cytosine and thymine from DNA by mutants of human uracil-DNA glycosylase. EMBO J. *15*, 3442–3447.

Khan, S., Guevara, C., Fujii, G., and Parry, D. (2004). p14ARF is a component of the p53 response following ionizing irradiation of normal human fibroblasts. Oncogene *23*, 6040–6046.

Kim, E.-J., Kho, J.-H., Kang, M.-R., and Um, S.-J. (2007). Active regulator of SIRT1 cooperates with SIRT1 and facilitates suppression of p53 activity. Mol. Cell *28*, 277–290.

Kirkwood, T.B.L., and Austad, S.N. (2000). Why do we age? Nature *408*, 233–238.

Kolthur-seetharam, U., Dantzer, F., Mcburney, M.W., Murcia, G. De, and Sassone-corsi, P. (2006). Control of AIF-mediated Cell Death by the Functional Interplay of SIRT1 and PARP-1 in Response to DNA Damage. Cell Cycle *5:8*, 873–877.

Komori, H., Enomoto, M., Nakamura, M., Iwanaga, R., and Ohtani, K. (2005). Distinct E2F-mediated transcriptional program regulates p14ARF gene expression. EMBO J. *24*, 3724–3736.

Korner, A. (1966). Effect of cycloheximide on protein biosynthesis in rat liver. Biochem. J. *101*, 627–631.

Koutsodontis, G., Vasilaki, E., Chou, W.-C., Papakosta, P., and Kardassis, D. (2005). Physical and functional interactions between members of the tumour suppressor p53 and the Sp families of transcription factors: importance for the regulation of genes involved in cell-cycle arrest and apoptosis. Biochem. J. *389*, 443–455.

Krishnamurthy, J., Torrice, C., Ramsey, M.R., Kovalev, G.I., Al-regaiey, K., Su, L., and Sharpless, N.E. (2004). Ink4a / Arf expression is a biomarker of aging. J. Clin. Invest. *114*, 1299–1307.

Kubota, Y., Nash, R.A., Klungland, A., Schar, P., Barnes, D.E., and Lindahl, T. (1996). Reconstitution excision-repair purified proteins: polymerase protein. *15*, 6662–6670.

Kuo, M.-L., den Besten, W., Bertwistle, D., Roussel, M.F., and Sherr, C.J. (2004). N-terminal polyubiquitination and degradation of the Arf tumor suppressor. Genes Dev. *18*, 1862–1874.

Kuzminov, A. (2001). Single-strand interruptions in replicating chromosomes cause double-strand breaks. Proc. Natl. Acad. Sci. U. S. A. *98*, 8241–8246.

Ladiges, W., Wiley, J., and MacAuley, A. (2003). Polymorphisms in the DNA repair gene XRCC1 and age-related disease. Mech. Ageing Dev. *124*, 27–32.

Lane, D.P. (1992). p53 the guardian of the genome.pdf. Nature *358*, 15–16.

Langley, E., Pearson, M., Faretta, M., Bauer, U.-M., Frye, R. a, Minucci, S., Pelicci, P.G., and Kouzarides, T. (2002). Human SIR2 deacetylates p53 and antagonizes PML/p53-induced cellular senescence. EMBO J. *21*, 2383–2396.

Lee, J.-H., and Paull, T.T. (2005). ATM activation by DNA double-strand breaks through the Mre11-Rad50-Nbs1 complex. Science *308*, 551–554.

Lee, C., Smith, B. a, Bandyopadhyay, K., and Gjerset, R. a (2005). DNA damage disrupts the p14ARF-B23(nucleophosmin) interaction and triggers a transient subnuclear redistribution of p14ARF. Cancer Res. *65*, 9834–9842.

Lee, M.H., Na, H., Kim, E.-J., Lee, H.-W., and Lee, M.-O. (2012). Poly(ADP-ribosyl)ation of p53 induces gene-specific transcriptional repression of MTA1. Oncogene *31*, 5099–5107.

Lee, Y.-M., Shin, S.-I., Shin, K.-S., Lee, Y.-R., Park, B.-H., and Kim, E.-C. (2011). The role of sirtuin 1 in osteoblastic differentiation in human periodontal ligament cells. J. Periodontal Res. *46*, 712–721.

Leppard, J.B., Dong, Z., Mackey, Z.B., and Tomkinson, A.E. (2003). Physical and Functional Interaction between DNA Ligase III α and Poly(ADP-Ribose) Polymerase 1 in DNA Single-Strand Break Repair. Mol. Cell. Biol. *23*, 5919–5927.

Li, E. (2002). Chromatin modification and epigenetic reprogramming in mammalian development. Nat. Rev. Genet. *3*, 662–673.

Li, Y., Wu, D., Chen, B., Ingram, A., He, L., Liu, L., Zhu, D., Kapoor, A., and Tang, D. (2004). ATM activity contributes to the tumor-suppressing functions of p14ARF. Oncogene *23*, 7355–7365.

Li, Z., Hou, J., Sun, L., Wen, T., Wang, L., Zhao, X., Xie, Q., and Zhang, S.Q. (2012). NMI mediates transcription-independent ARF regulation in response to cellular stresses. Mol. Biol. Cell *23*, 4635–4646.

Lin, a W., and Lowe, S.W. (2001). Oncogenic ras activates the ARF-p53 pathway to suppress epithelial cell transformation. Proc. Natl. Acad. Sci. U. S. A. *98*, 5025–5030.

Lindahl, T. (1974). An N-Glycosidase from Escherichia coli That Releases Free Uracil from DNA Containing Deaminated Cytosine Residues. Proc. Natl. Acad. Sci. U. S. A. *71*, 3649–3653.

Lindahl, T. (1993). Instability and decay of the primary structure of DNA. Nature *362*, 709–715.

Lindahl, T., and Barnes, D.E. (2000). Repair of Endogenous DNA Damage. Cold Spring Harb. Symp. Quant. Biol. *65*, 127–134.

Lindahl, T., and Karlström, O. (1973). Heat-induced depyrimidination of deoxyribonucleic acid in neutral solution. Biochemistry *12*, 5151–5154.

Lindahl, T., and Nyberg, B. (1972). Rate of depurination of native deoxyribonucleic acid. Biochemistry *11*, 3610–3618.

Lindahl, T., and Nyberg, B. (1974). Heat-induced deamination of cytosine residues in deoxyribonucleic acid. Biochemistry *13*, 3405–3410.

Liu, D., Gharavi, R., Pitta, M., Gleichmann, M., and Mattson, M.P. (2009). Nicotinamide prevents NAD+ depletion and protects neurons against excitotoxicity and cerebral ischemia: NAD+ consumption by SIRT1 may endanger energetically compromised neurons. Neuromolecular Med. *11*, 28–42.

Liu, Q., Guntuku, S., Cui, X., Matsuoka, S., Cortez, D., Tamai, K., Luo, G., Carattini-rivera, S., Demayo, F., Bradley, A., et al. (2000). Chk1 is an essential kinase that is regulated by Atr and required for the G 2 / M DNA damage checkpoint. Genes Dev. *14*, 1448–1459.

Llanos, S., Clark, P. a, Rowe, J., and Peters, G. (2001). Stabilization of p53 by p14ARF without relocation of MDM2 to the nucleolus. Nat. Cell Biol. *3*, 445–452.

Locasale, J.W. (2013). Serine, glycine and one-carbon units: cancer metabolism in full circle. Nat. Rev. Cancer *13*, 572–583.

Loizou, J.I., El-khamisy, S.F., Zlatanou, A., Moore, D.J., Chan, D.W., Qin, J., Sarno, S., Meggio, F., Pinna, L.A., and Caldecott, K.W. (2004). The Protein Kinase CK2 Facilitates Repair of Chromosomal DNA Single-Strand Breaks. Cell *117*, 17–28.

Lomazzi, M., Moroni, M.C., Jensen, M.R., Frittoli, E., and Helin, K. (2002). Suppression of the p53- or pRB-mediated G1 checkpoint is required for E2F-induced S-phase entry. Nat. Genet. *31*, 190–194.

Van Loon, B., and Hübscher, U. (2009). An 8-oxo-guanine repair pathway coordinated by MUTYH glycosylase and DNA polymerase lambda. Proc. Natl. Acad. Sci. U. S. A. *106*, 18201–18206.

Lord, C.J., and Ashworth, A. (2012). The DNA damage response and cancer therapy. Nature *481*, 287–294.

Luna, A., Aladjem, M.I., and Kohn, K.W. (2013). SIRT1/PARP1 crosstalk: connecting DNA damage and metabolism. Genome Integr. *4*, 6.

Luo, X., and Kraus, W.L. (2012). On PAR with PARP: cellular stress signaling through poly(ADP-ribose) and PARP-1. Genes Dev. *26*, 417–432.

Mallette, F. a, Gaumont-Leclerc, M.-F., and Ferbeyre, G. (2007a). The DNA damage signaling pathway is a critical mediator of oncogene-induced senescence. Genes Dev. *21*, 43–48.

Mallette, F. a, Gaumont-Leclerc, M.-F., and Ferbeyre, G. (2007b). The DNA damage signaling pathway is a critical mediator of oncogene-induced senescence. Genes Dev. *21*, 43–48.

Mantha, A.K., Sarkar, B., and Tell, G. (2013). A short review on the implications of base excision repair pathway for neurons: Relevance to neurodegenerative diseases. Mitochondrion.

Mao, L., Merlo, A., Bedi, G., Shapiro, G.I., Edwards, C.D., Rollins, B.J., and Sidransky, D. (1995). A Novel pl6INK4A Transcript. Cancer Res. *55*, 2995–2997.

Marcon, G., Tell, G., Perrone, L., Garbelli, R., Quadrifoglio, F., Tagliavini, F., and Giaccone, G. (2009). APE1/Ref-1 in Alzheimer's disease: an immunohistochemical study. Neurosci. Lett. *466*, 124–127.

Maréchal, A., and Zou, L. (2013). DNA damage sensing by the ATM and ATR kinases. Cold Spring Harb. Perspect. Biol. *5*, 1–17.

Marintchev, a, Robertson, a, Dimitriadis, E.K., Prasad, R., Wilson, S.H., and Mullen, G.P. (2000). Domain specific interaction in the XRCC1-DNA polymerase beta complex. Nucleic Acids Res. *28*, 2049–2059.

Maso, V. Di, Avellini, C., Crocè, L.S., Rosso, N., Quadrifoglio, F., Cesaratto, L., Codarin, E., Bedogni, G., Beltrami, C.A., and Tell, G. (2007). Subcellular Localization of APE1/Ref-1 in Human Hepatocellular Carcinoma: Possible Prognostic Significance. Mol. Med. *13*, 89–96.

Masson, M., Niedergang, C., Schreiber, V., Murcia, J.M., Murcia, G. De, Schreiber, R.I.E., and Muller, S. (1998). XRCC1 Is Specifically Associated with Poly(ADP-Ribose) Polymerase and Negatively Regulates Its Activity following DNA Damage. Mol. Cell. Biol. *16*, 3563–3571.

Masutani, M., Nozaki, T., Nakamoto, K., Nakagama, H., Suzuki, H., Kusuoka, O., Tsutsumi, M., and Sugimura, T. (2000). The response of Parp knockout mice against DNA damaging agents. Mutat. Res. *462*, 159–166.

Matsuoka, S., Huang, M., and Elledge, S.J. (1998a). Linkage of ATM to Cell Cycle Regulation by the Chk2 Protein Kinase. Science (80-.). *282*, 1893–1897.

Matsuoka, S., Huang, M., and Elledge, S.J. (1998b). Linkage of ATM to Cell Cycle Regulation by the Chk2 Protein Kinase. Science (80-.). *282*, 1893–1897.

Maynard, S., Schurman, S.H., Harboe, C., de Souza-Pinto, N.C., and Bohr, V. a (2009). Base excision repair of oxidative DNA damage and association with cancer and aging. Carcinogenesis *30*, 2–10.

Meek, D.W. (2009). Tumour suppression by p53: a role for the DNA damage response? Nat. Rev. Cancer *9*, 714–723.

Meisenberg, C., Tait, P.S., Dianova, I.I., Wright, K., Edelmann, M.J., Ternette, N., Tasaki, T., Kessler, B.M., Parsons, J.L., Kwon, Y.T., et al. (2012). Ubiquitin ligase UBR3 regulates cellular levels of the essential DNA repair protein APE1 and is required for genome stability. Nucleic Acids Res. *40*, 701–711.

Michan, S., and Sinclair, D. (2007). Sirtuins in mammals: insights into their biological function. Biochem. J. *404*, 1–13.

Milojkovic, A., Hemmati, P.G., Müer, A., Overkamp, T., Chumduri, C., Jänicke, R.U., Gillissen, B., and Daniel, P.T. (2013). p14ARF induces apoptosis via an entirely caspase-3-dependent mitochondrial amplification loop. Int. J. Cancer *133*, 2551–2562.

Mol, C.D., Arvai, a S., Slupphaug, G., Kavli, B., Alseth, I., Krokan, H.E., and Tainer, J. a (1995). Crystal structure and mutational analysis of human uracil-DNA glycosylase: structural basis for specificity and catalysis. Cell *80*, 869–878.

Moll, U.M., Wolff, S., Speidel, D., and Deppert, W. (2005). Transcription-independent pro-apoptotic functions of p53. Curr. Opin. Cell Biol. *17*, 631–636.

Monasor, A., Murga, M., Lopez-Contreras, A.J., Navas, C., Gomez, G., Pisano, D.G., and Fernandez-Capetillo, O. (2013). INK4a/ARF limits the expansion of cells suffering from replication stress. Cell Cycle *12*, 1948–1954.

Montero, J., Dutta, C., van Bodegom, D., Weinstock, D., and Letai, a (2013). p53 regulates a non-apoptotic death induced by ROS. Cell Death Differ. *20*, 1465–1474.

Moore, D.H., Michael, H., Tritt, R., Parsons, S.H., and Kelley, M.R. (2000). Alterations in the Expression of the DNA Repair/Redox Enzyme APE/ref-1 in Epithelial Ovarian Cancers. Clin. Cancer Res. *6*, 602–609.

Moreira, M.C., Barbot, C., Tachi, N., Kozuka, N., Uchida, E., Gibson, T., Mendonça, P., Costa, M., Barros, J., Yanagisawa, T., et al. (2001). The gene mutated in ataxia-ocular apraxia 1 encodes the new HIT/Zn-finger protein aprataxin. Nat. Genet. *29*, 189–193.

De Murcia, J.M., Niedergang, C., Trucco, C., Ricoul, M., Dutrillaux, B., Mark, M., Oliver, F.J., Masson, M., Dierich, a, LeMeur, M., et al. (1997). Requirement of poly(ADP-ribose) polymerase in recovery from DNA damage in mice and in cells. Proc. Natl. Acad. Sci. U. S. A. *94*, 7303–7307.

Murphy, M.P. (2009). How mitochondria produce reactive oxygen species. Biochem. J. *417*, 1–13.

Nakamura, J., Asakura, S., Hester, S.D., de Murcia, G., Caldecott, K.W., and Swenberg, J. A (2003). Quantitation of intracellular NAD(P)H can monitor an imbalance of DNA single strand break repair in base excision repair deficient cells in real time. Nucleic Acids Res. *31*, 104e–104.

Normand, G., Hemmati, P.G., Verdoodt, B., von Haefen, C., Wendt, J., Güner, D., May, E., Dörken, B., and Daniel, P.T. (2005). p14ARF induces G2 cell cycle arrest in p53- and p21-deficient cells by down-regulating p34cdc2 kinase activity. J. Biol. Chem. *280*, 7118–7130.

Ohta, M., Inoue, H., Cotticelli, M.G., Kastury, K., Baffa, R., Palazzo, J., Siprashvili, Z., Mori, M., McCue, P., Druck, T., et al. (1996). The FHIT gene, spanning the chromosome 3p14.2 fragile site and renal carcinoma-associated t(3;8) breakpoint, is abnormal in digestive tract cancers. Cell *84*, 587–597.

Ohtani, N., Zebedee, Z., Huot, T.J.G., Stinson, J.A., Sugimoto, M., Ohashi, Y., Sharrocks, A.D., Peters, G., and Hara, E. (2001). Opposing effects of Ets and Id proteins on p16 INK4a expression during cellular senescence. Nature *409*, 1067–1070.

Okano, S., Lan, L., Caldecott, K.W., Mori, T., and Yasui, A. (2003). Spatial and Temporal Cellular Responses to Single-Strand Breaks in Human Cells. Mol. Cell. Biol. *23*, 3974–3981.

Ozaki, T., Okoshi, R., Sang, M., Kubo, N., and Nakagawara, A. (2009). Acetylation status of E2F-1 has an important role in the regulation of E2F-1-mediated transactivation of tumor suppressor p73. Biochem. Biophys. Res. Commun. *386*, 207–211.

Ozenne, P., Eymin, B., Brambilla, E., and Gazzeri, S. (2010). The ARF tumor suppressor: structure, functions and status in cancer. Int. J. Cancer *127*, 2239–2247.

Palmero, I., Pantoja, C., and Serrano, M. (1998). p19ARF links the tumour suppressor p53 to Ras. Nature *395*, 125–126.

Pang, J.H., and Chen, K.Y. (1994). Global change of gene expression at late G1/S boundary may occur in human IMR-90 diploid fibroblasts during senescence. J. Cell. Physiol. *160*, 531–538.

Pang, J., Gong, H., Xi, C., Fan, W., Dai, Y., and Zhang, T.-M. (2011). Poly(ADP-ribose) polymerase 1 is involved in glucose toxicity through SIRT1 modulation in HepG2 hepatocytes. J. Cell. Biochem. *112*, 299–306.

Parikh, S.S., Mol, C.D., Slupphaug, G., Bharati, S., Krokan, H.E., and Tainer, J. a (1998). Base excision repair initiation revealed by crystal structures and binding kinetics of human uracil-DNA glycosylase with DNA. EMBO J. *17*, 5214–5226.

Parker, J.B., Bianchet, M. a, Krosky, D.J., Friedman, J.I., Amzel, L.M., and Stivers, J.T. (2007). Enzymatic capture of an extrahelical thymine in the search for uracil in DNA. Nature *449*, 433–437.

Parsons, J.L., Dianova, I.I., and Dianov, G.L. (2004). APE1 is the major 3'-phosphoglycolate activity in human cell extracts. Nucleic Acids Res. *32*, 3531–3536.

Parsons, J.L., Dianova, I.I., Allinson, S.L., and Dianov, G.L. (2005). Poly(ADP-ribose) polymerase-1 protects excessive DNA strand breaks from deterioration during repair in human cell extracts. FEBS J. *272*, 2012–2021.

Parsons, J.L., Tait, P.S., Finch, D., Dianova, I.I., Allinson, S.L., and Dianov, G.L. (2008). CHIP-mediated degradation and DNA damage-dependent stabilization regulate base excision repair proteins. Mol. Cell *29*, 477–487.

Parsons, J.L., Tait, P.S., Finch, D., Dianova, I.I., Edelmann, M.J., Khoronenkova, S. V, Kessler, B.M., Sharma, R. a, McKenna, W.G., and Dianov, G.L. (2009). Ubiquitin ligase ARF-BP1/Mule modulates base excision repair. EMBO J. *28*, 3207–3215.

Parsons, J.L., Dianova, I.I., Finch, D., Tait, P.S., Ström, C.E., Helleday, T., and Dianov, G.L. (2010). XRCC1 phosphorylation by CK2 is required for its stability and efficient DNA repair. DNA Repair (Amst). *9*, 835–841.

Parsons, J.L., Dianova, I.I., Khoronenkova, S. V, Edelmann, M.J., Kessler, B.M., and Dianov, G.L. (2011). USP47 is a deubiquitylating enzyme that regulates base excision repair by controlling steady-state levels of DNA polymerase β. Mol. Cell *41*, 609–615.

Pascucci, B., Stucki, M., Jónsson, O., Dogliotti, E., Chem, J.B., Jo, O., and Hu, U. (1999). Long Patch Base Excision Repair with Purified Human Proteins: DNA LIGASE I AS PATCH SIZE MEDIATOR FOR DNA POLYMERASES δ AND ε. J. Biol. Chem. *274*, 33696–33702.

Peck, B., Chen, C.-Y., Ho, K.-K., Di Fruscia, P., Myatt, S.S., Coombes, R.C., Fuchter, M.J., Hsiao, C.-D., and Lam, E.W.-F. (2010). SIRT inhibitors induce cell death and p53 acetylation through targeting both SIRT1 and SIRT2. Mol. Cancer Ther. *9*, 844–855.

Pediconi, N., Guerrieri, F., Vossio, S., Bruno, T., Belloni, L., Schinzari, V., Scisciani, C., Fanciulli, M., and Levrero, M. (2009). hSirT1-dependent regulation of the PCAF-E2F1-p73 apoptotic pathway in response to DNA damage. Mol. Cell. Biol. *29*, 1989–1998.

Plo, I., Liao, Z., Barcelo, J., Kohlhagen, G., Caldecott, K., Weinfeld, M., and Pommier, Y. (2003). Association of XRCC1 and tyrosyl DNA phosphodiesterase (Tdp1) for the repair of topoisomerase I-mediated DNA lesions. DNA Repair (Amst). *2*, 1087–1100.

Pomerantz, J., Schreiber-Agus, N., Liégeois, N.J., Silverman, a, Alland, L., Chin, L., Potes, J., Chen, K., Orlow, I., Lee, H.W., et al. (1998). The Ink4a tumor suppressor gene product, p19Arf, interacts with MDM2 and neutralizes MDM2's inhibition of p53. Cell *92*, 713–723.

Pouliot, J.J., Yao, K.C., Robertson, C.A., and Nash, H.A. (1999). Yeast Gene for a Tyr-DNA Phosphodiesterase that Repairs Topoisomerase I Complexes. Science (80-.). *286*, 552–555.

Prasad, R., Dianov, G.L., Bohr, A., and Wilson, S.H. (2000). FEN1 Stimulation of DNA Polymerase β Mediates an Excision Step in Mammalian Long. J. Biol. Chem. *275*, 4460–4466.

Puebla-osorio, N., Lacey, D.B., Alt, F.W., and Zhu, C. (2006). Early Embryonic Lethality Due to Targeted Inactivation of DNA Ligase III. Mol. Cell. Biol. *26*, 3935–3941.

Quelle, D.E., Zindy, F., Ashmun, R. a, and Sherr, C.J. (1995). Alternative reading frames of the INK4a tumor suppressor gene encode two unrelated proteins capable of inducing cell cycle arrest. Cell *83*, 993–1000.

Radfar, a, Unnikrishnan, I., Lee, H.W., DePinho, R. a, and Rosenberg, N. (1998). p19(Arf) induces p53-dependent apoptosis during abelson virus-mediated pre-B cell transformation. Proc. Natl. Acad. Sci. U. S. A. *95*, 13194–13199.

El Ramy, R., Magroun, N., Messadecq, N., Gauthier, L.R., Boussin, F.D., Kolthur-Seetharam, U., Schreiber, V., McBurney, M.W., Sassone-Corsi, P., and Dantzer, F. (2009). Functional interplay between Parp-1 and SirT1 in genome integrity and chromatin-based processes. Cell. Mol. Life Sci. *66*, 3219–3234.

Resnick-Silverman, L., St. Clair, S., Maurer, M., Zhao, K., and Manfredi, J.J. (1998). Identification of a novel class of genomic DNA-binding sites suggests a mechanism for selectivity in target gene activation by the tumor suppressor protein p53. Genes Dev. *12*, 2102–2107.

Revollo, J.R., Grimm, A. a, and Imai, S. (2004). The NAD biosynthesis pathway mediated by nicotinamide phosphoribosyltransferase regulates Sir2 activity in mammalian cells. J. Biol. Chem. *279*, 50754–50763.

Reynolds, J.J., Walker, A.K., Gilmore, E.C., Walsh, C. a, and Caldecott, K.W. (2012). Impact of PNKP mutations associated with microcephaly, seizures and developmental delay on enzyme activity and DNA strand break repair. Nucleic Acids Res. *40*, 6608–6619.

Riley, P. a (1994). Free radicals in biology: oxidative stress and the effects of ionizing radiation. Int. J. Radiat. Biol. *65*, 27–33.

Riley, T., Sontag, E., Chen, P., and Levine, A. (2008). Transcriptional control of human p53-regulated genes. Nat. Rev. Mol. Cell Biol. *9*, 402–412.

Robertson, K.D., and Jones, P.A. (1998). The Human ARF Cell Cycle Regulatory Gene Promoter Is a CpG Island Which Can Be Silenced by DNA Methylation and Down-Regulated by Wild-Type p53. Mol. Cell. Biochem. *18*, 6457–6473.

Rocha, S., Garrett, M.D., Campbell, K.J., Schumm, K., and Perkins, N.D. (2005). Regulation of NF-kappaB and p53 through activation of ATR and Chk1 by the ARF tumour suppressor. EMBO J. *24*, 1157–1169.

Roche (1996). http://www.roche-applied-science.com/shop/CategoryDisplay?catalogId=10001&tab=&identifier=Universal+Probe+Library&langId=-1&storeId=15006#tab-0.

Rodier, F., Coppé, J.-P., Patil, C.K., Hoeijmakers, W. a M., Muñoz, D.P., Raza, S.R., Freund, A., Campeau, E., Davalos, A.R., and Campisi, J. (2009). Persistent DNA damage signalling triggers senescence-associated inflammatory cytokine secretion. Nat. Cell Biol. *11*, 973–979.

Rouleau, M., Patel, A., Hendzel, M.J., Kaufmann, S.H., and Poirier, G.G. (2010). PARP inhibition: PARP1 and beyond. Nat. Rev. Cancer *10*, 293–301.

Rulten, S.L., Fisher, A.E.O., Robert, I., Zuma, M.C., Rouleau, M., Ju, L., Poirier, G., Reina-San-Martin, B., and Caldecott, K.W. (2011). PARP-3 and APLF function together to accelerate nonhomologous end-joining. Mol. Cell *41*, 33–45.

Ryan, a J., Squires, S., Strutt, H.L., Evans, a, and Johnson, R.T. (1994). Different fates of camptothecin-induced replication fork-associated double-strand DNA breaks in mammalian cells. Carcinogenesis *15*, 823–828.

Sabisz, M., Wesierska-Gadek, J., and Skladanowski, A. (2010). Increased cytotoxicity of an unusual DNA topoisomerase II inhibitor compound C-1305 toward HeLa cells with downregulated PARP-1 activity results from re-activation of the p53 pathway and modulation of mitotic checkpoints. Biochem. Pharmacol. *79*, 1387–1397.

Sage, E., and Harrison, L. (2011). Clustered DNA lesion repair in eukaryotes: relevance to mutagenesis and cell survival. Mutat. Res. *711*, 123–133.

Saldivar, J.C., Miuma, S., Bene, J., Hosseini, S.A., Shibata, H., Sun, J., Wheeler, L.J., Mathews, C.K., and Huebner, K. (2012). Initiation of genome instability and preneoplastic processes through loss of Fhit expression. PLoS Genet. *8*, e1003077.

Saleh-gohari, N., Bryant, H.E., Schultz, N., Parker, K.M., Cassel, T.N., and Helleday, T. (2005). Spontaneous Homologous Recombination Is Induced by Collapsed Replication Forks That Are Caused by Endogenous DNA Single-Strand Breaks. Mol. Cell. Biol. *25*, 7158–7169.

Scharffetter-Kochanek, K., Wlaschek, M., Brenneisen, P., Schauen, M., Blaudschun, R., and Wenk, J. (1997). UV-induced reactive oxygen species in photocarcinogenesis and photoaging. Biol. Chem. *378*, 1247–1257.

Scheffner, M., Huibregtse, J.M., Vierstra, R.D., and Howley, P.M. (1993). The HPV-16 E6 and E6-AP complex functions as a ubiquitin-protein ligase in the ubiquitination of p53. Cell *75*, 495–505.

Schulze, A., and Harris, A.L. (2012). How cancer metabolism is tuned for proliferation and vulnerable to disruption. Nature *491*, 364–373.

Sedelnikova, O. a, Horikawa, I., Zimonjic, D.B., Popescu, N.C., Bonner, W.M., and Barrett, J.C. (2004). Senescing human cells and ageing mice accumulate DNA lesions with unrepairable double-strand breaks. Nat. Cell Biol. *6*, 168–170.

Serrano, M., Lin, A.W., Mccurrach, M.E., Beach, D., and Lowe, S.W. (1997). Oncogenic ras Provokes Premature Cell Senescence Associated with Accumulation of p53 and p16 INK4a. Cell *88*, 593–602.

Shen, J., Gilmore, E.C., Marshall, C. a, Haddadin, M., Reynolds, J.J., Eyaid, W., Bodell, A., Barry, B., Gleason, D., Allen, K., et al. (2010). Mutations in PNKP cause microcephaly, seizures and defects in DNA repair. Nat. Genet. *42*, 245–249.

Shen, M.R., Zdzienicka, M.Z., Mohrenweiser, H., Thompson, L.H., and Thelen, M.P. (1998). Mutations in hamster single-strand break repair gene XRCC1 causing defective DNA repair. Nucleic Acids Res. *26*, 1032–1037.

Sherr, C.J. (2006). Divorcing ARF and p53: an unsettled case. Nat. Rev. Cancer *6*, 663–673.

Sherr, C.J., and McCormick, F. (2002). The RB and p53 pathways in cancer. Cancer Cell *2*, 103–112.

Shiloh, Y., and Ziv, Y. (2013). The ATM protein kinase: regulating the cellular response to genotoxic stress, and more. Nat. Rev. Mol. Cell Biol. *14*, 197–210.

Silva, J., Domínguez, G., Silva, J.M., García, J.M., Gallego, I., Corbacho, C., Provencio, M., España, P., and Bonilla, F. (2001). Analysis of genetic and epigenetic processes that influence p14ARF expression in breast cancer. Oncogene *20*, 4586–4590.

Singh, N., Poirier, G., and Cerutti, P. (1985). Tumor promoter phorbol-12-myristate-13-acetate induces poly(ADP)-ribosylation in fibroblasts. Embo J. *4*, 1491–1494.

Singh, N., Mccoy, T., Tice, R., and Schneider, E.L. (1988). A simple Technique for Quantitation Damage of Low Levels of DNA damage in individual Cells '. Exp. Cell Res. *175*, 184–191.

Sleeth, K.M., Robson, R.L., and Dianov, G.L. (2004). Exchangeability of mammalian DNA ligases between base excision repair pathways. Biochemistry *43*, 12924–12930.

Sobol, R.W., Prasad, R., Evenski, a, Baker, a, Yang, X.P., Horton, J.K., and Wilson, S.H. (2000). The lyase activity of the DNA repair protein beta-polymerase protects from DNA-damage-induced cytotoxicity. Nature *405*, 807–810.

Sobol, R.W., Watson, D.E., Nakamura, J., Yakes, F.M., Hou, E., Horton, J.K., Ladapo, J., Van Houten, B., Swenberg, J. a, Tindall, K.R., et al. (2002). Mutations associated with base excision repair deficiency and methylation-induced genotoxic stress. Proc. Natl. Acad. Sci. U. S. A. *99*, 6860–6865.

Sossou, M., Flohr-Beckhaus, C., Schulz, I., Daboussi, F., Epe, B., and Radicella, J.P. (2005). APE1 overexpression in XRCC1-deficient cells complements the defective repair of oxidative single strand breaks but increases genomic instability. Nucleic Acids Res. *33*, 298–306.

Sozzi, G., Veronese, M.L., Negrini, M., Baffa, R., Cotticelli, M.G., Inoue, H., Tornielli, S., Pilotti, S., De Gregorio, L., Pastorino, U., et al. (1996). The FHIT gene 3p14.2 is abnormal in lung cancer. Cell *85*, 17–26.

Stanelle, J., Stiewe, T., Theseling, C.C., Peter, M., and Pützer, B.M. (2002). Gene expression changes in response to E2F1 activation. Nucleic Acids Res. *30*, 1859–1867.

Stott, F.J., Bates, S., James, M.C., McConnell, B.B., Starborg, M., Brookes, S., Palmero, I., Ryan, K., Hara, E., Vousden, K.H., et al. (1998). The alternative product from the human CDKN2A locus, p14(ARF), participates in a regulatory feedback loop with p53 and MDM2. EMBO J. *17*, 5001–5014.

Strosznajder, J.B., Czapski, G. a, Adamczyk, A., and Strosznajder, R.P. (2012). Poly(ADP-ribose) polymerase-1 in amyloid beta toxicity and Alzheimer's disease. Mol. Neurobiol. *46*, 78–84.

Stucki, M., Pascucci, B., Parlanti, E., Fortini, P., Wilson, S.H., Hübscher, U., and Dogliotti, E. (1998). Mammalian base excision repair by DNA polymerases delta and epsilon. Oncogene *17*, 835–843.

Sugimura, H., Kohno, T., Wakai, K., Nagura, K., Genka, K., Igarashi, H., Morris, B.J., Baba, S., Ohno, Y., Gao, C., et al. (1999). hOGG1 Ser326Cys polymorphism and lung cancer susceptibility. Cancer Epidemiol. Biomarkers Prev. *8*, 669–674.

Sugo, N., Aratani, Y., Nagashima, Y., Kubota, Y., and Koyama, H. (2000). Neonatal lethality with abnormal neurogenesis in mice deficient in DNA polymerase beta. EMBO J. *19*, 1397–1404.

Sykora, P., Wilson, D.M., and Bohr, V. a (2013). Base excision repair in the mammalian brain: implication for age related neurodegeneration. Mech. Ageing Dev. *134*, 440–448.

Takashima, H., Boerkoel, C.F., John, J., Saifi, G.M., Salih, M. a M., Armstrong, D., Mao, Y., Quiocho, F. a, Roa, B.B., Nakagawa, M., et al. (2002). Mutation of TDP1, encoding a topoisomerase I-dependent DNA damage repair enzyme, in spinocerebellar ataxia with axonal neuropathy. Nat. Genet. *32*, 267–272.

Tanaka, M., Lai, J.S., and Herr, W. (1992). Promoter-selective activation domains in Oct-1 and Oct-2 direct differential activation of an snRNA and mRNA promoter. Cell *68*, 755–767.

Tano, K., Nakamura, J., Asagoshi, K., Arakawa, H., Sonoda, E., Braithwaite, E.K., Prasad, R., Buerstedde, J.-M., Takeda, S., Watanabe, M., et al. (2007). Interplay between DNA polymerases beta and lambda in repair of oxidation DNA damage in chicken DT40 cells. DNA Repair (Amst). *6*, 869–875.

Tebbs, R.S., Flannery, M.L., Meneses, J.J., Hartmann, a, Tucker, J.D., Thompson, L.H., Cleaver, J.E., and Pedersen, R. a (1999). Requirement for the Xrcc1 DNA base excision repair gene during early mouse development. Dev. Biol. *208*, 513–529.

Tell, G., Quadrifoglio, F., Tiribelli, C., and Kelley, M.R. (2009). The many functions of APE1/Ref-1: not only a DNA repair enzyme. Antioxid. Redox Signal. *11*, 601–620.

Thakur, B.K., Dittrich, T., Chandra, P., Becker, A., Lippka, Y., Selvakumar, D., Klusmann, J.-H., Reinhardt, D., and Welte, K. (2012). Inhibition of NAMPT pathway by FK866 activates the function of p53 in HEK293T cells. Biochem. Biophys. Res. Commun. *424*, 371–377.

Thompson, L.H., Brookman, K.W., Dillehay, L.E., Carrano, a V, Mazrimas, J. a, Mooney, C.L., and Minkler, J.L. (1982). A CHO-cell strain having hypersensitivity to mutagens, a defect in DNA strand-break repair, and an extraordinary baseline frequency of sister-chromatid exchange. Mutat. Res. *95*, 427–440.

Thornborrow, E.C., and Manfredi, J.J. (2001). The Tumor Suppressor Protein p53 Requires a Cofactor to Activate Transcriptionally the Human BAX Promoter. J. Biol. Chem. *276*, 15598–15608.

Tokarsky-Amiel, R., Azazmeh, N., Helman, A., Stein, Y., Hassan, A., Maly, A., and Ben-Porath, I. (2013). Dynamics of senescent cell formation and retention revealed by p14ARF induction in the epidermis. Cancer Res. *73*, 2829–2839.

Tom, S., Henricksen, L.A., and Bambara, R.A. (2000). Mechanism Whereby Proliferating Cell Nuclear Antigen Stimulates Flap Endonuclease 1. J. Biol. Chem. *275*, 10498–10505.

Tomkinson, A.E., and Sallmyr, A. (2013). Structure and function of the DNA ligases encoded by the mammalian LIG3 gene. Gene *531*, 150–157.

Trucco, C., Oliver, F.J., de Murcia, G., and Ménissier-de Murcia, J. (1998). DNA repair defect in poly(ADP-ribose) polymerase-deficient cell lines. Nucleic Acids Res. *26*, 2644–2649.

Uziel, T., Lerenthal, Y., Moyal, L., Andegeko, Y., Mittelman, L., and Shiloh, Y. (2003). Requirement of the MRN complex for ATM activation by DNA damage. EMBO J. *22*, 5612–5621.

Valenzuela, M.T., Guerrero, R., Nu, M.I., Sarker, M., Murcia, G. De, and Oliver, F.J. (2002). PARP-1 modifies the efectiveness of p53-mediated DNA damage response. Oncogene *21*, 1108–1116.

Vaquero, A., Scher, M., Lee, D., Erdjument-Bromage, H., Tempst, P., and Reinberg, D. (2004). Human SirT1 interacts with histone H1 and promotes formation of facultative heterochromatin. Mol. Cell *16*, 93–105.

Velimezi, G., Liontos, M., Vougas, K., Roumeliotis, T., Bartkova, J., Sideridou, M., Dereli-Oz, A., Kocylowski, M., Pateras, I.S., Evangelou, K., et al. (2013). Functional interplay between the DNA-damage-response kinase ATM and ARF tumour suppressor protein in human cancer. Nat. Cell Biol. *15*, 967–977.

Vidal, a E., Boiteux, S., Hickson, I.D., and Radicella, J.P. (2001). XRCC1 coordinates the initial and late stages of DNA abasic site repair through protein-protein interactions. EMBO J. *20*, 6530–6539.

Wang, J.C. (2002). Cellular roles of DNA topoisomerases: a molecular perspective. Nat. Rev. Mol. Cell Biol. *3*, 430–440.

Wang, C., Chen, L., Hou, X., Li, Z., Kabra, N., Ma, Y., Nemoto, S., Finkel, T., Gu, W., Cress, W.D., et al. (2006). Interactions between E2F1 and SirT1 regulate apoptotic response to DNA damage. Nat. Cell Biol. *8*, 1025–1031.

Wang, F., Chan, C.-H., Chen, K., Guan, X., Lin, H.-K., and Tong, Q. (2012). Deacetylation of FOXO3 by SIRT1 or SIRT2 leads to Skp2-mediated FOXO3 ubiquitination and degradation. Oncogene *31*, 1546–1557.

Wang, X., Zha, M., Zhao, X., Jiang, P., Du, W., Tam, A.Y.H., Mei, Y., and Wu, M. (2013). Siva1 inhibits p53 function by acting as an ARF E3 ubiquitin ligase. Nat. Commun. *4*, 1551.

Wang, Y., Kim, N.S., Haince, J.-F., Kang, H.C., David, K.K., Andrabi, S. a, Poirier, G.G., Dawson, V.L., and Dawson, T.M. (2011). Poly(ADP-ribose) (PAR) binding to apoptosis-inducing factor is critical for PAR polymerase-1-dependent cell death (parthanatos). Sci. Signal. *4*, ra20.

Ward, J.F. (1990). The yield of DNA double-strand breaks produced intracellularly by ionizing radiation: a review. Int. J. Radiat. Biol. *57*, 1141–1150.

Watson, J.D., and Crick, F.H.C. (1953). the Structure of Dna. Cold Spring Harb. Symp. Quant. Biol. *18*, 123–131.

Watson, J. D., Crick, F.H.C. (1953). Molecular structure of nucleic acids. Nature 737–738.

Weber, H.O., Samuel, T., Rauch, P., and Funk, J.O. (2002). Human p14 ARF -mediated cell cycle arrest strictly depends on intact p53 signaling pathways. Oncogene *21*, 3207–3212.

Wei, W., Hemmer, R.M., and Sedivy, J.M. (2001). Role of p14 ARF in Replicative and Induced Senescence of Human Fibroblasts. Mol. Cell. Biol. *21*, 6748–6757.

Weissman, L., Jo, D.-G., Sørensen, M.M., de Souza-Pinto, N.C., Markesbery, W.R., Mattson, M.P., and Bohr, V. a (2007). Defective DNA base excision repair in brain from individuals with Alzheimer's disease and amnestic mild cognitive impairment. Nucleic Acids Res. *35*, 5545–5555.

Whitehouse, C.J., Taylor, R.M., Thistlethwaite, a, Zhang, H., Karimi-Busheri, F., Lasko, D.D., Weinfeld, M., and Caldecott, K.W. (2001). XRCC1 stimulates human polynucleotide kinase activity at damaged DNA termini and accelerates DNA single-strand break repair. Cell *104*, 107–117.

Wieler, S., Gagné, J.-P., Vaziri, H., Poirier, G.G., and Benchimol, S. (2003). Poly(ADP-ribose) polymerase-1 is a positive regulator of the p53-mediated G1 arrest response following ionizing radiation. J. Biol. Chem. *278*, 18914–18921.

Wilson, D.M., and Barsky, D. (2001). The major human abasic endonuclease: formation, consequences and repair of abasic lesions in DNA. Mutat. Res. *485*, 283–307.

Winters, T. a, Henner, W.D., Russell, P.S., McCullough, a, and Jorgensen, T.J. (1994). Removal of 3'-phosphoglycolate from DNA strand-break damage in an oligonucleotide substrate by recombinant human apurinic/apyrimidinic endonuclease 1. Nucleic Acids Res. *22*, 1866–1873.

Woodhouse, B.C., and Dianov, G.L. (2008). Poly ADP-ribose polymerase-1: an international molecule of mystery. DNA Repair (Amst). *7*, 1077–1086.

Woodhouse, B.C., Dianova, I.I., Parsons, J.L., and Dianov, G.L. (2008). Poly(ADP-ribose) polymerase-1 modulates DNA repair capacity and prevents formation of DNA double strand breaks. DNA Repair (Amst). *7*, 932–940.

Xanthoudakis, S., Smeyne, R.J., Wallace, J.D., and Curran, T. (1996). The redox/DNA repair protein, Ref-1, is essential for early embryonic development in mice. Proc. Natl. Acad. Sci. U. S. A. *93*, 8919–8923.

Xu, X., Page, J.L., Surtees, J. a, Liu, H., Lagedrost, S., Lu, Y., Bronson, R., Alani, E., Nikitin, A.Y., and Weiss, R.S. (2008). Broad overexpression of ribonucleotide reductase genes in mice specifically induces lung neoplasms. Cancer Res. *68*, 2652–2660.

Yamamori, T., DeRicco, J., Naqvi, A., Hoffman, T. a, Mattagajasingh, I., Kasuno, K., Jung, S.-B., Kim, C.-S., and Irani, K. (2010). SIRT1 deacetylates APE1 and regulates cellular base excision repair. Nucleic Acids Res. *38*, 832–845.

Yang, S.W., Burgin, a B., Huizenga, B.N., Robertson, C. a, Yao, K.C., and Nash, H. a (1996). A eukaryotic enzyme that can disjoin dead-end covalent complexes between DNA and type I topoisomerases. Proc. Natl. Acad. Sci. U. S. A. *93*, 11534–11539.

Ying, S., Hamdy, F.C., and Helleday, T. (2012). Mre11-dependent degradation of stalled DNA replication forks is prevented by BRCA2 and PARP1. Cancer Res. *72*, 2814–2821.

Zeng, Y., Kotake, Y., Pei, X., Smith, M.D., and Xiong, Y. (2011). p53 binds to and is required for the repression of Arf tumor suppressor by HDAC and polycomb. Cancer Res. *71*, 2781–2792.

Zhang, Y., and Xiong, Y. (1999). Mutations in human ARF exon 2 disrupt its nucleolar localization and impair its ability to block nuclear export of MDM2 and p53. Mol. Cell *3*, 579–591.

Zhang, T., Berrocal, J.G., Frizzell, K.M., Gamble, M.J., DuMond, M.E., Krishnakumar, R., Yang, T., Sauve, A. a, and Kraus, W.L. (2009). Enzymes in the NAD+ salvage pathway regulate SIRT1 activity at target gene promoters. J. Biol. Chem. *284*, 20408–20417.

Zhang, Y., Xiong, Y., and Yarbrough, W.G. (1998). ARF promotes MDM2 degradation and stabilizes p53: ARF-INK4a locus deletion impairs both the Rb and p53 tumor suppression pathways. Cell *92*, 725–734.

Zheng, S., Chen, P., McMillan, a, Lafuente, a, Lafuente, M.J., Ballesta, a, Trias, M., and Wiencke, J.K. (2000). Correlations of partial and extensive methylation at the p14(ARF) locus with reduced mRNA expression in colorectal cancer cell lines and clinicopathological features in primary tumors. Carcinogenesis *21*, 2057–2064.

Zhu, W., Chen, Y., and Dutta, A. (2004). Rereplication by Depletion of Geminin Is Seen Regardless of p53 Status and Activates a G 2 / M Checkpoint. *24*, 7140–7150.

Zilfou, J.T., and Lowe, S.W. (2009). Tumor suppressive functions of p53. Cold Spring Harb. Perspect. Biol. *1*.

Zindy, F., Eischen, C.M., Randle, D.H., Kamijo, T., Cleveland, J.L., Sherr, C.J., and Roussel, M.F. (1998). Myc signaling via the ARF tumor suppressor regulates p53-dependent apoptosis and immortalization. Genes Dev. *12*, 2424–2433.

Zou, L., and Elledge, S.J. (2003). Sensing DNA damage through ATRIP recognition of RPA-ssDNA complexes. Science *300*, 1542–1548.

Appendix I – List of materials and reagents

REAGENTS/MATERIALS	SUPPLIER
0.2 ml Thin-walled tubes	MOLECULAR BIO-PRODUCTS
1 ml syringes	BD
1.1 mm needles	BD
1.5 ml Eppendorf tube	GREINER BIO-ONE
10 cm dishes	GREINER BIO-ONE
15 ml falcon tubes	GREINER BIO-ONE
50 ml falcon tubes	GREINER BIO-ONE
50X TAE	BIO-RAD
75 cm^2 flasks	GREINER BIO-ONE
96-well flat bottom plates	CORNING
96-well PCR plates	THERMOSCIENTIFIC
ABsolute Blue SYBR Green ROX	THERMOSCIENTIFIC
Adhesive PCR films	THERMOSCIENTIFIC
Agarose	BIO-RAD
amicon ultra 0.5 ml tubes	MILLIPORE
Annexin V-FITC	ABCAM
AnnexinV binding buffer (10X)	ABCAM
Aprotinin	CALBIOCHEM
Bradford	BIO-RAD
Bromophenol blue powder	SIGMA
BSA	BIO-RAD
Buffer EB	QIAGEN
Buffer N3	QIAGEN
Buffer P1	QIAGEN
Buffer P2	QIAGEN
Buffer P3	QIAGEN
Buffer PE	QIAGEN
Buffer QBT	QIAGEN
Buffer QC	QIAGEN
CHX	SIGMA
Chymostatin	CALBIOCHEM
Cuvettes	FISHER
DEPC H_2O	AMBION
DMEM	GIBCO
DMSO	SIGMA

REAGENTS/MATERIALS	SUPPLIER
DNA gel cassettes	BIO-RAD
DNA gel tanks	BIO-RAD
dNTPs mix	BIOLINE
Dpn I restriction enzyme	NEB
DTT 0.1M	INVITROGEN
EDTA	BDH
Equipment for protein electrophoresis	NOVELL
Ethanol (100%)	FISHER
FBS	GIBCO
First strand buffer (5X)	INVITROGEN
FK866 powder	CALBIOCHEM
Gel Loading dye 6X, Blue	NEB
Glycerol	FLUKA
Gradient-mixer device	AMERSHAM
H_2O_2	SIGMA
Heating blocks	EPPENDORF
Immobilon-FL	MILLIPORE
Immobilon-FL PVDF	MILLIPORE
Isopropanol (100%)	FISHER
KCl	BDH
Leupeptin	CALBIOCHEM
Lipofectamine 2000	INVITROGEN
Methanol (100%)	FISHER
$MgCl_2$	SIGMA
MMS	ACROS
NAD cycling buffer mix	ABCAM
NAD cycling enzyme mix	ABCAM
NADH developer	ABCAM
NADH standard	ABCAM
NADH/NAD extraction buffer	ABCAM
NEM	SIGMA
Kanomycin	SIGMA
Nonidet P-40	SIGMA
NU1025 powder	CALBIOCHEM
Odyssey blocker buffer	LI-COR
PBS	SIGMA
Pepstatin	CALBIOCHEM
PfuTurbo buffer (10X)	AGILENT

REAGENTS/MATERIALS	SUPPLIER
PfuTurbo DNA polymerase	AGILENT
PMSF	SIGMA
Power suppliers	BIO-RAD
Pre-cast 4-20% Tris-glycine gels	NOVELL
Propidium Iodide	SIGMA
Protein LoBind 1.5 ml tubes	EPPENDORF
QIAfilter MaxiCartridge	QIAGEN
QIAGEN-tip 500	QIAGEN
QIAprep spin column	QIAGEN
RLT buffer	QIAGEN
RNAaseZAP detergent	SIGMA
RNAi max lipofectamine	INVITROGEN
RNase 100 mg/ml	QIAGEN
RNase H enzyme	NEB
RNase-free water	QIAGEN
RNaseOUT (40 U/µl)	INVITROGEN
RPE buffer	QIAGEN
RW1 buffer	QIAGEN
SDS	FISHER
Sponges for the WB transfer	NOVELL
SuperScript II RT enzyme	INVITROGEN
Tris/glycine buffer (10X)	BIO-RAD
Tris/glycine/SDS buffer (10X)	BIO-RAD
Triton-X 100	SIGMA
Trizma (Tris HCl)	SIGMA
Trypan blue	INVITROGEN
Trypsin-EDTA	GIBCO
TSA	CALBIOCHEM
Tube roller	STOVALL
Tube rotor	LABINCO
Western blot apparatus	NOVELL
XL1- blue competent bacterial cells	AGILENT
β-ME for bacterial transformation	AGILENT

Appendix II

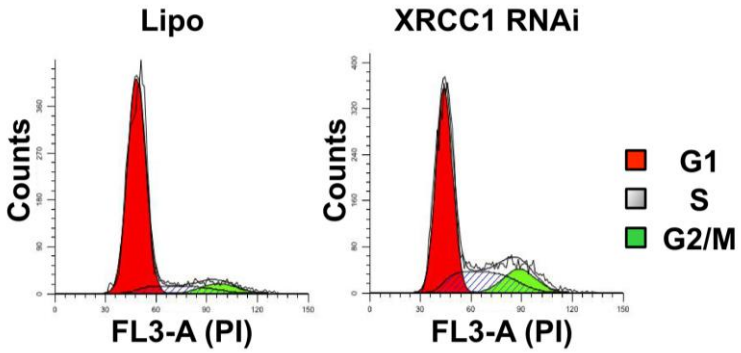

Appendix II: Cell cycle profiles of HeLa cells in response to XRCC1 knockdown obtained using Mod-Fit software.
HeLa cells were transfected with lipofectamine only (Lipo) or in combination with XRCC1 RNAi (200 pmol) for 72 h. Cells were collected, counted and $5x10^5$ cells were used for cell cycle analysis. Cells were fixed in ethanol and subsequently stained with PI. Sample acquisition was performed by using a FACSort machine and the cell cycle profile was analysed by Mod-Fit software. Images are representative of three independent experiments.

Appendix III

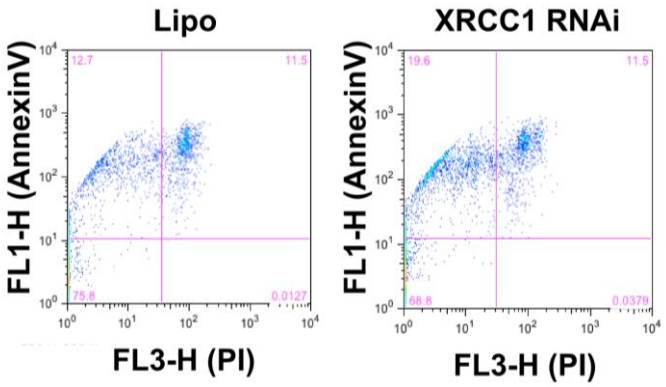

Appendix III: FlowJo dot plot data of HeLa cells in response to XRCC1 knockdown.
HeLa cells were transfected with lipofectamine only (Lipo) or in combination with XRCC1 RNAi (200 pmol) for 72 h. Cells were collected, counted and $2.5x10^5$ cells were used for cell cycle analysis. Cells were stained with PI and Annexin V for the apoptosis assay. Sample acquisition was performed using a FACSort machine and analysed by FlowJo software. Images are representative of three independent experiments.

Appendix IV

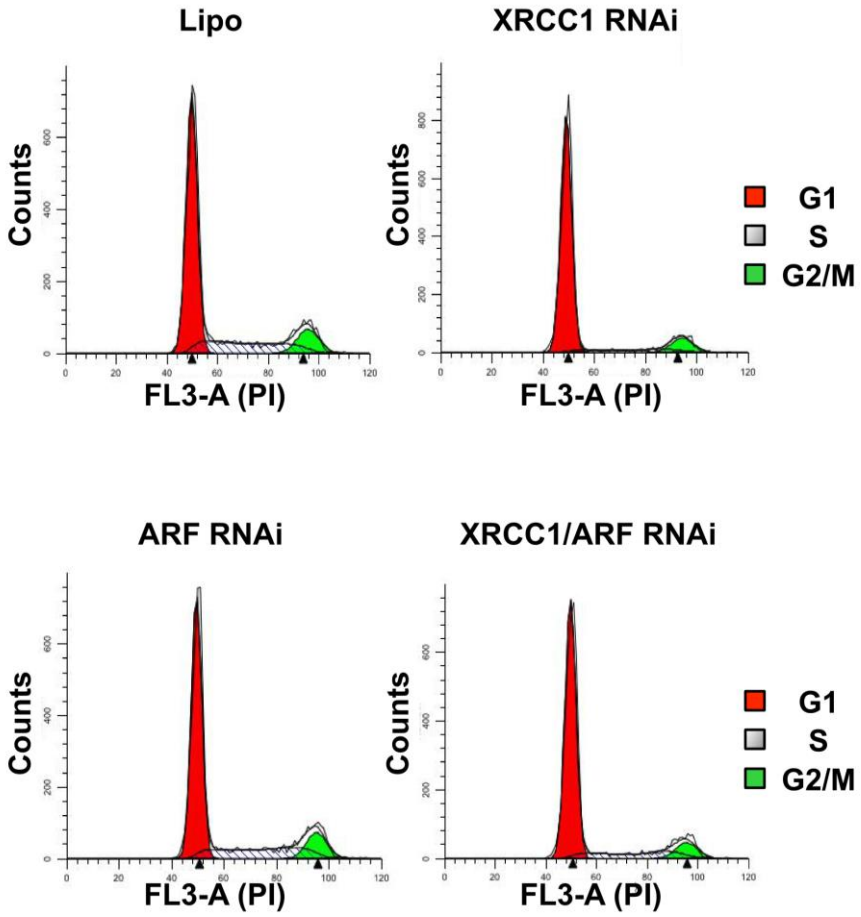

Appendix IV: Cell cycle profiles of TIG-1 cells in response to XRCC1 and ARF knockdowns obtained using Mod-Fit software.
TIG-1 cells were transfected with lipofectamine only (Lipo) or in combination with either XRCC1 RNAi or ARF RNAi (200 pmol), or a mixture of both for 48 h. Cells were harvested, counted, fixed in ethanol and subsequently stained with PI. Sample acquisition was performed using a FACSort machine and the cell cycle profile was analysed by Mod-Fit software. Images are representative of three independent experiments.

Appendix V – License agreement & Publications

The following article is reproduced with permission of The Royal Society of Chemistry:

Dianov G.L., Orlando G. and Parsons J.L. (2012). Tumour suppressor protein-mediated regulation of Base Excision Repair in response to DNA Damage. From the book: The Cellular Response to the Genotoxic Insult: The Question of Threshold for Genotoxic Carcinogens, Chapter 3.3, 174-183, *Toxicology No. 13*, The Royal Society of Chemistry 2012